Optimization and decision making under uncertainty for distributed generation technologies

By

Carlos Antonio Marino

A Dissertation
Submitted to the Faculty of
Mississippi State University
in Partial Fulfillment of the Requirements
for the Degree of Doctor of Philosophy
in Industrial and Systems Engineering
in the Department of Industrial and Systems Engineering

Mississippi State, Mississippi

December 2016

Optimization and decision making under uncertainty for distributed generation technologies

By

Carlos Antonio Marino

Approved:

Mohammad Marufuzzaman
(Major Professor)

Linkan Bian
(Committee Member)

Brian Smith
(Committee Member)

Pedro J. Mago
(Committee Member)

Stanley F. Bullington
(Graduate Coordinator)

Jason M. Keith
Dean
Bagley College of Engineering

Name: Carlos Antonio Marino

Date of Degree: December 09, 2016

Institution: Mississippi State University

Major Field: Industrial and Systems Engineering

Major Professor: Dr. Mohammad Marufuzzaman

Title of Study: Optimization and decision making under uncertainty for distributed generation technologies

Pages of Study: 107

Candidate for Degree of Doctor of Philosophy

This dissertation studies two important models in the field of the distributed generation technologies to provide resiliency to the electric power distribution system. In the first part of the dissertation, we study the impact of assessing a Combined Cooling Heating Power system (CCHP) on the optimization and management of an on-site energy system under stochastic settings. These mathematical models propose a scalable stochastic decision model for large-scale microgrid operation formulated as a two-stage stochastic linear programming model. The model is solved enhanced algorithm strategies for Benders decomposition are introduced to find an optimal solution for larger instances efficiently. Some observations are made with different capacities of the power grid, dynamic pricing mechanisms with various levels of uncertainty, and sizes of power generation units. In the second part of the dissertation, we study a mathematical model that designs a Microgrid (MG) that integrates conventional fuel based generating (FBG) units, renewable sources of energy, distributed energy storage (DES) units, and electricity demand response. Cur-

tailment of renewable resources generation during the MG operation affects the long-term revenues expected and increases the greenhouses emission. Considering the variability of renewable resources, researchers should pay more attention to scalable stochastic models for MG for multiple nodes. This study bridges the research gap by developing a scalable chance-constrained two-stage stochastic program to ensure that a significant portion of the renewable resource power output at each operating hour will be utilized. Finally, some managerial insights are drawn into the operation performance of the Combined Cooling Heating Power and a Microgrid.

Key words: Combined Cooling Heating Power, Microgrid, Renewable Energy, Power Outages, Benders decomposition, Chance-Constrained

DEDICATION

To my parents and my lovely wife Edit.

ACKNOWLEDGEMENTS

First and foremost I wish to thank my advisor, Dr. Mohammad Marufuzzaman. He has been supportive during my doctoral studies at Mississippi State University.His mentoring has been very valuable.

I would like to thank other members of my dissertation committee: Dr. Linkan Bian, Dr. Brian Smith and Dr. Pedro Mago for their valuable time, support and feedback that was invaluable to me. I also express my sincere gratitude to Dr. John M. Usher for his support, Dr. Kari Babski-Reeves for her valuable mentoring and Dr. Mengqi Hu from University of Illinois at Chicago.

Finally, my eternal thanks to my parents for their love, and affection. My last word is for my wife Edit for her love and perseverance. She is everything to me.

TABLE OF CONTENTS

LIST OF TABLES

LIST OF FIGURES

CHAPTER 1

INTRODUCTION

1.1 Introduction

In recent years, multiples environmental concerns have motivated different areas of research to find ways to reduce greenhouses emission. Since there is no a straightforward solution different approaches have emerged as promising technologies such as Combined Cooling Heating and Power Systems, and Microgrid. In this new landscape, the concept of this small scale of energy systems is defined as a configuration that uses Distributed Energy Resources (DER) and they have an autonomous capability from the traditional grid [69]. Integrating traditional power generation, and renewable generation satisfies more efficiently multiple types of customer's demand for cooling, heating, and electricity. Furthermore, their different configurations interact with the main power grid. [35]. Thus, researchers highlight network configurations composed of traditional fuel-based generators, Combined Heating, and Power, renewable sources, thermal and storage components [7].

Research done by Hanazadeh et.al [38] Jradi and Riffat [45] states as a broad definition of a CCHP that it can generate electricity, mechanical, cooling and thermal energy using the same source of power. Hence, CCHP is called trigeneration [115] [40], and it is an excellent alternative as a DER mode [87]. CCHP has several advantages. For instance, in efficiency, while in traditional generation systems, the average is 30-35% of energy con-

version, CHP and CCHP technologies achieve an average of 80% of energy conversion of fuel into energy [67] [96]. Furthermore, Lemar (2009) highlights the policies that promote Combined cooling, heating, and power (CCHP) on the cost saving impact on energy use and carbon emission reduction [44].

Ensuring that any power supply networks are cost effective is challenging due to the uncertainties of the environment. Investments in equipment and operational cost are significant for the long-term, and the major risk is that they are vulnerable to unexpected natural disasters, such as inclement weather, hurricanes, or human-made disasters [62]. Therefore, designing reliable power supply and distribution system to hedge against risks from unexpected natural disasters is important. In the operation of a CCHP system, uncertainty comes from different sources. The main sources of uncertainties are the weather conditions and the energy demand [123]. For instance, the forecast weather inaccuracy for the thermal load, government policies (i.e. tariffs), the nonlinearity of engines performance and power outages are critical factors of uncertainty analysis [97].Moreover, a CCHP-$Microgrid$ faces the random nature of the output power of renewable energy sources [64]. Finally, the most critical part is the computational time that increases drastically as soon the number of scenarios increase to consider the stochasticity of these complex systems.

These challenges have motivated researchers to identify decision models to help decision-makers in these micro-scale energy systems design and management decisions, so the aim of this paper is to build a model of these systems that guarantee an efficient and consistent performance under uncertainty. Following this stream of research, we use a case study to

demonstrate the role advanced mathematical optimization models we propose will have on reducing computational time, and provide an optimal power flow.

In Chapter 2, we present a two-stage stochastic mixed integer linear programming (SMILP) model to study the impact of the electricity demand uncertainty, and to obtain the optimal operation decisions strategies for the CCHP, the energy storage system (i.e. battery), and the thermal storage. The proposed model allow us to study the CCHP operation with an electric battery and thermal-storage under uncertainty and to minimize the operational. We solve this problem using enhanced techniques of generalized Benders decomposition algorithm and then integrate sample-averaged-approximation's algorithm with a Benders accelerated method. We develop a case study using data from the electric provider in Arizona, and by demand, simulation using the software Energy Plus. The results from the computational analysis show important observations about the impacts of changes in power grid capacities (including power outages), and different sizes of battery capacities, electricity generator units, and pricing mechanism.

Microgrid enables the integration of traditional generation sources, renewable sources of energy (e.g. solar or wind generation), distributed storage resources, and demand response. The efficiency and reliability of any power generator and distribution network capabilities are crucial aspects of the energy industry. Ensuring that these networks are cost-efficient is challenging due to the uncertainties of the environment. Furthermore, the curtailment of the power generation of renewable resources during the microgrid operation affects the long-term revenues expected and increases the emission of greenhouses gasses, and the reduction of renewable generation has grown notoriously in the last decade

of expansion of the renewable energy facilities. To address this need, Chapter 3 presents a chance-constrained two-stage stochastic programming model formulation for the microgrid operations under uncertain electricity demand. In the chance-constraint representation, we use three different policies to ensure that the utilization of renewable energy (i.e., solar) is high in microgrid operations. We develop a combined SAA algorithm to solve the chance-constrained two-stage stochastic programming model for the microgrid scheduling problem. The numerical analysis demonstrates that total system cost is mostly impacted by the distributed generation technologies. Also, the chance constraint model provides an efficient planning tool to allocate and dispatch renewable-generation power, and consequently, it reduces the risk to curtail during the microgrid operation.

In summary, our study provides models and algorithms for distributed generating technologies. We have conducted some real life experiments that will help the decision-makers to make sizing, pricing mechanism, and planning decisions to ensure long-term success regarding cost, and the resiliency for power outages.

CHAPTER 2

DEVELOPING A CCHP-$MICROGRID$ OPERATION DECISION MODEL UNDER UNCERTAINTY

2.1 Introduction

The US electricity demand which is, estimated by the US Energy Information Administration will grow by 29% (0.8%/year), from 3,826 billion kilowatt-hours (kWh) in 2012 to 4,954 billion kWh in 2040 [107]. To improve the energy efficiency in the U.S., the concept of micro-grid has attracted greater attentions during the past few years [119]. The micro-grid utilizes distributed generators, such as combined cooling, heating and power (CCHP) system and photovoltaic (PV) arrays, among others and distributed energy storage (DES), like batteries, to decentralize the current power system. The CCHP system has the capability to provide electric, cooling and heating energy simultaneously [35] and has the potential to reduce carbon emission and improve energy efficiency [67] [96] [44]. To this end, extensive research has been conducted in the past few years to develop efficient operation decisions for CCHP integrated micro-grid, termed as CCHP-microgrid in this research. The existing operation decision models can be classified into two groups: 1) deterministic model which does not consider uncertainties exist in operation environment and system configuration, 2) stochastic model which considers various sources of uncertainties.

The deterministic models mainly, focus on optimal dispatch to minimize the operation cost. For instance, a linear programming model is proposed in [125] to minimize the total system cost which includes operation and maintenance costs. Another deterministic approach handled forecasted demand and solar power generation [37]. Furthermore, deterministic linear programming has been applied for unit commitment problem for a Microgrid configuration [39].

Researchers have developed multiple deterministic approaches. A linear programming model introduced in (LP) [89] minimizes simultaneously the production and purchase costs of three energy components, and CO2 emissions costs, and overall cost of energy for the CCHP system in [51] .Non-linear programming model (NLP) to attain better operational efficiency, reduce the total cost, and improve environmental performance [58]. Literature shows mixed-integer programming model (MILP) to optimize operational efficiency and to analyze the economic and environmental impacts of distributed energy systems [79], and mixed integer nonlinear programming (MINLP) to find the optimal operation strategies under various load conditions [116]. As a note research work tended to focus on energy cost primary energy consumption (PEC), and carbon dioxide emission (CDE) reduction using different optimization and algorithm techniques [20] [53] [102] [111].

These studies emphasized in both on the CCHP architecture and the microgrid planning, operation and control. Furthermore, some studies have focused on multiple cogeneration units such as boilers, thermal storage, prime movers and refrigeration cycles [14].Later, the literature shows the addition to binary variables to including the start-up/shut down and the charging/discharging characteristic of some components CCHP sys-

tem (i.e. generator units and thermal storage respectively). Thus, MILP model was successfully introduced as a modeling technique to account those characteristics. Z. Zhou et al. (2013) developed a linearized model achieving better computational solution [122].

Another effort to study CCHP operation is the stochastic model which optimizes the performance of the CCHP system with uncertainties in energy demand [41] [123], and in the operation phase [29]. Researchers have proposed many stochastic optimization models for CCHP operation (i.e. unit commintment, economic dispatch, planning and control) [41] [118] [59], mostly for single units (e.g. residential homes) [18]. For instance, Sheng et.al (2015) studies a CCHP system developing a multi-objective chance-constrained model. It minimizes the total cost and minimize greenhouse emissions. They test the model in a hotel building improving the system efficiency [95]. Karimi et.al (2014) studied the stochasticity of the demand and its impact on the operation cost and performance. They studied a grid-connected home systems [46]. Furthermore, demand from different sizes of buildings are used to test a CCHP systems in [30]. The proposed model optimizes the size of the PGU and the CCHP operation systems as well. It founds mathematical relationships between the size of the building and the size of the PGU.

Additional efforts have done to reduce the computational burden has been done by Benam et.al in [11]. They developed a two-stage mixed-integer linear programming to determine the optimal number, and the size of the CCHP components. They tested the model for a large residential unit to measure the CCHP performance, but the study does not consider prices uncertainty, and the separation of the cooling and heating demand.

Although the existing deterministic and stochastic models are proven optimization techniques that improve the performance of CCHP in terms of energy efficiency, there are still numerous gaps and limitations in the literature such as the following:

1. The increase of complexity to integrate large scale of multiple energy systems with a large demand nodes under uncertainty is a challenge, and developing models to understand large complex energy systems is underdeveloped area of research.

2. Literature mention that computational complexity of stochastic models is significantly higher [59]. There is a huge gap in the literature to propose methodologies to reduce computational complexity to solve for large instances.

Given these gaps in the existing literature on the CCHP Operation models, to the best of our knowledge, our study contributes to fill the gap by modeling a complex energy system (a large CCHP, i.e $Microgrid$ type) considering its stochasticity with a large number of demand nodes.Thus, the main contributions in this research are summarized as follows: (1) Developing a scalable two-stage stochastic decision model for large scale micro-grid operation under uncertainty considering a larger number of scenarios which could make the CCHP operation strategy more reliable. (2) Proposing multiple enhanced algorithm strategies to obtain high quality optimal solutions to reduce significantly the computational time. (3) Providing a decision-making framework to establish better strategies to use energy efficiently under different uncertain parameters and scenarios (plan prices, demand level, etc.).

This paper is organized as follows: Section 2 describes the problem statement of the CCHP system proposed. Section 3 presents the two-stage stochastic linear programming mathematical model. Section 4 presents the proposed algorithms strategies; we explain the Sample Average Approximation (SAA), Benders decomposition algorithms. We introduce enhanced techniques of generalized Benders decomposition algorithm and finally, we integrate SAA with a Benders accelerated method. Section 5 presents the computational study, managerial insights, and conclusions of this paper.

2.2 Problem Description

In the following paragraphs, we will describe the Combined Cooling, Heating and Power system.

2.2.1 CCHP System Structure:

Network flows theory helps to set up linear programming models [5]. Network flows is used to visualizes the interactions among energy supplies, energy flows and loads [19]. Figure 2.1 shows an application of residential buildings clustered and integrated with a CCHP system. The dot-dashed line, solid line, and dashed line represent the primary energy flow, electricity flow, and thermal energy flow respectively. Buildings require electrical power and thermal energy. The CCHP has a power subsystem (power generation unit and boiler), a cooling/heating subsystem, and a heat recovery subsystem. The CCHP configuration depicted in this paper considers additionally an electrical battery that works as Energy Storage System (ESS), and an additional Thermal Storage system (TSS). From the figure, it is observed that the power generator unit (PGU), prime mover and generator,

is fuel-based, and it is suitable for a residential application. PGU provides the electricity required for the buildings (e.g. lights, computer, electrical appliances). Furthermore, when there is an excess of power (as shown in Figure 2.1), the CCHP has the capability of either storing power in the battery for future use or selling back the power excess to the grid. Regarding the thermal load requirement, waste heat recovered from the PGU and the boiler provides space for both cooling and heating. The electric battery buffers any fluctuations due to the stochasticity in the power grid or prime mover, and the thermal storage system absorbs any thermal excess, so both, battery and thermal storage, have an impact on the efficiency.

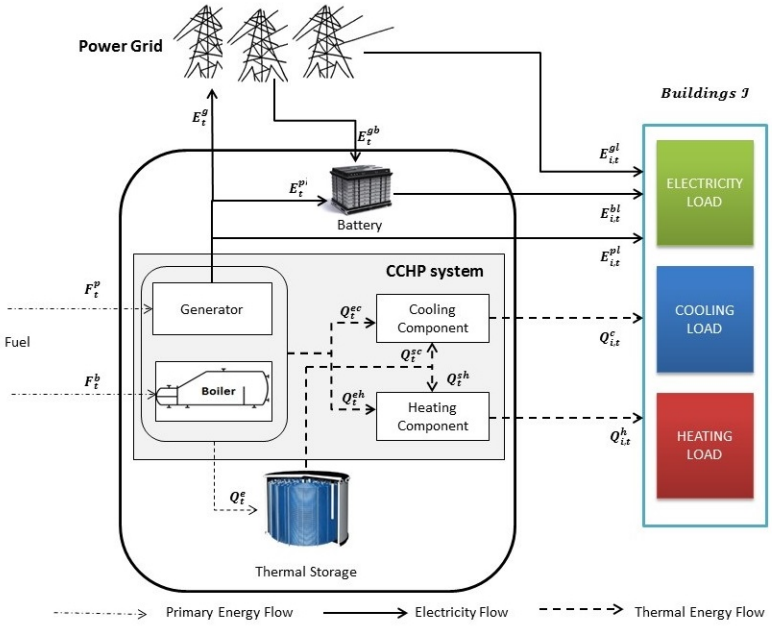

Figure 2.1

Schematic of the CCHP Integrated Energy System

There are two main operation modes strategies for analysis and optimization of CCHP systems [67] [66] [68]: (1) Following the electric load (FEL), and (2) following the thermal load (FTL). There are several studies that have studied both strategies under different conditions with electric and thermal demand styles. Although, both strategies will waste energy (i.e. not 100% efficiency) [61], studies shows that there are some advantages of FTL over FEL in operation cost (i.e. primary energy consumption) [66]. For the purpose of this paper, the CCHP configuration considers that it recovers the waste heat from the prime mover, and it satisfies the entire demand of the buildings' thermal energy (cooling and heating). If the prime mover is not enough, a boiler is added. Furthermore, the prime mover satisfies the electricity requirements of the buildings. If it is not sufficient, the power grid will provide the additional power. Thus, this paper considers that the CCHP operates under FTL strategy. Figure 1 shows a visual representation of the CCHP architecture under investigation.

This paper proposes a stochastic modeling formulation approach, and the next section will describe in detail the mathematical model.

2.3 Model Formulation:

In this section, we develop a stochastic mixed integer linear programming (SMILP) model to study the impact of the electricity demand uncertainty, and to obtain the optimal operation decisions strategies for the CCHP, the energy storage system (i.e. battery), and the thermal storage.

The model studied in this paper considers two kinds of variables. Binary variables for CCHPs on/off states, electric batterys charge/discharge states, and thermal storage systems charge/discharge states; and continuous variables for electrical and thermal energy flow. The CCHP will decide how its energy production is delivered to the buildings (users), or stored in the ESS or the TSS if a surplus of electricity or thermal energy occurs respectively. Decisions of the EES and TSS will decide their on/off sequence to charge/discharge, and how to deliver the discharged energy to each building. Furthermore, there exists a limitation for the battery and the thermal storage, they cannot charge/discharge simultaneously. Moreover, it is assumed that it is not possible buying and selling electricity simultaneously from/to local grid.

The model considers the following subscripts: i in $\mathcal{I}$ is the index for the buildings integrated to the CCHP system. The t in $\mathcal{T}$ is the index of the decision time interval, and ω in Ω for the generated scenario with its probability assigned.Each scenario generated will specify the electrical and thermal demand, the states of the generator, boiler, battery and the thermal storage. There are different scenario generation methods. For instance, Monte Carlo Sampling, Optimal quantization of probability distributions, and Quasi-Monte Carlo methods without nonanticipativity constraints.

These binary variables (i.e. 0/1), Z_t^p and Y_t^p describe the on/off status of the PGU, and S_t^p its limitation of the CCHP operation at partial loads.

$$Z_t^p = \begin{cases} 1 & \text{start-up state indicator for PGU at time } t \\ 0 & \text{otherwise;} \end{cases}$$

$$Y_t^p = \begin{cases} 1 & \text{shut-down state indicator for PGU at time } t \\ 0 & \text{otherwise;} \end{cases}$$

$$S_t^p = \begin{cases} 1 & \text{commitment state of PGU at time } t \\ 0 & \text{otherwise;} \end{cases}$$

The following binary variables, Z_t^e and Y_t^e describe the thermal storage on/off status, and S_t^{e+} and S_t^{e-} describe its limitation of simultaneous charge and discharge respectively.

$$Z_t^e = \begin{cases} 1 & \text{start-up state indicator for thermal storage at time } t \\ 0 & \text{otherwise;} \end{cases}$$

$$Y_t^e = \begin{cases} 1 & \text{shut-down state indicator for thermal storage at time } t \\ 0 & \text{otherwise;} \end{cases}$$

$$S_t^{e+} = \begin{cases} 1 & \text{charging state of thermal energy storage at time } t \\ 0 & \text{otherwise;} \end{cases}$$

$$S_t^{e-} = \begin{cases} 1 & \text{discharging state of thermal energy storage at time } t \\ 0 & \text{otherwise;} \end{cases}$$

Z_t^b and Y_t^b describe the battery on/off status and S_t^{b+} and S_t^{b-} its limitation of simultaneous charge and discharge respectively.

$$Z_t^b = \begin{cases} 1 & \text{start-up state indicator for battery at time } t \\ 0 & \text{otherwise;} \end{cases}$$

$$Y_t^b = \begin{cases} 1 & \text{shut-down state indicator for battery at time } t \\ 0 & \text{otherwise;} \end{cases}$$

$$S_t^{b+} = \begin{cases} 1 & \text{charging state of battery at time } t \\ 0 & \text{otherwise;} \end{cases}$$

$$S_t^{b-} = \begin{cases} 1 & \text{discharging state of battery at time } t \\ 0 & \text{otherwise;} \end{cases}$$

Table 2.1 lists all the variables for the stochastic model formulation.

The objective function is formulated as a two-stage stochastic mixed-integer linear programming. The first stage objective function is to minimize the startup cost of the PGU, the electrical battery and the thermal storage (on/off status). The second stage objective function is the minimization of the operation costs under the realization of scenarios (amount of energy generated by the PGU and boiler, amount of energy purchased/sold from/to the grid, states of the battery and thermal storage)where ρ_w is the probability of scenario ω in Ω.

$$\textbf{[CCHP]}\ Minimize \sum_{t\in\mathcal{T}}\Bigg(\psi_t^p Z_t^p + \psi_t^e Z_t^e + \psi_t^b Z_t^b + \sum_{\omega\in\Omega}\rho_w \Delta t\Big(\chi_t^+ E_{t\omega}^{gb} + \kappa_t^p F_{t\omega}^p + \kappa_t^b F_{t\omega}^b - \chi_t^- E_{t\omega}^g + \sum_{i\in\mathcal{I}}\chi_t^+ E_{it\omega}^{gl}\Big)\Bigg) \tag{2.1}$$

Subject to:

Table 2.1

Decision variables (DVs) used in stochastic

DVs	Description
$F^{p}_{t\omega}$	Fuel consumption of PGU at time t under scenario ω
$F^{b}_{t\omega}$	Fuel consumption of boiler at time t under scenario ω
$E^{gl}_{it\omega}$	Electricity purchased from grid for building i at time t under scenario ω
$E^{gb}_{t\omega}$	Electricity purchased from grid to charge battery at time t under scenario ω
$E^{g}_{t\omega}$	Electricity sold back to the grid at time t under scenario ω
$E^{pl}_{it\omega}$	Electricity generated by PGU for building i at time t under scenario ω
$E^{pb}_{t\omega}$	Electricity generated by PGU to charge battery at time t under scenario ω
$E^{bl}_{it\omega}$	Power discharged from battery for building i at time t under scenario ω
$E^{b+}_{t\omega}$	Power used to charge battery at time t under scenario ω
$E^{b-}_{t\omega}$	Power discharged from battery at time t under scenario ω
$E^{b}_{t\omega}$	Amount of electric energy stored in battery at time t under scenario ω
$Q^{ec}_{t\omega}$	Thermal energy to cooling component at time t under scenario ω
$Q^{eh}_{t\omega}$	Thermal energy to heating component at time t under scenario ω
$Q^{e}_{t\omega}$	Thermal energy to thermal energy storage at time t scenario ω
$Q^{e+}_{t\omega}$	Thermal energy used to charge storage at time t under scenario ω
$Q^{e-}_{t\omega}$	Thermal energy discharged from storage at time t under scenario ω
$Q^{s}_{t\omega}$	Amount of energy stored in the thermal energy storage at time t scenario ω
$Q^{sc}_{t\omega}$	Thermal energy from storage to cooling component at time t scenario ω
$Q^{sh}_{t\omega}$	Thermal energy from storage to heating component at time t scenario ω
$Q^{c}_{it\omega}$	Cooling energy from cooling component for building i at time t scenario ω
$Q^{h}_{it\omega}$	Heating energy from heating component for building i at time t scenario ω

The power purchased from the power grid is restricted by the capacity of the power grid as follows:

$$E^{gb}_{t\omega} + \sum_{i\in\mathcal{I}} E^{gl}_{it\omega} \quad \leq \quad \overline{e}^{p} \qquad\qquad \forall t \in \mathcal{T}, \omega \in \Omega \tag{2.2}$$

where $\overline{e}^{p}$ is the capacity of the power grid.

For PGU, the energy conservation should be observed, namely that the total electricity generated and offered to each building should be equal to the equivalent fuel consumption considering fuel-to-electric conversion parameters. Natural gas engine performance is modeled as

$$F^{p}_{t\omega} = \begin{cases} a\left(E^{pb}_{t\omega} + E^{g}_{t\omega} + \sum_{i\in\mathcal{I}} E^{pl}_{it\omega}\right) + b; \quad \forall t \in \mathcal{T}, \omega \in \Omega & \text{for PGU is operated} \\ 0 & \text{for PGU is off;} \end{cases}$$

where a and b are the two fuel-to-electric-energy conversion parameters for PGU, which equal to 2.97 and 11.66, respectively [19]. For equation (2), we introduce a binary variable S^{p}_{t} to denote the state of PGU at time interval t, which can simplify this constraint as following:

$$E^{pb}_{t\omega} + E^{g}_{t\omega} + \sum_{i\in\mathcal{I}} E^{pl}_{it\omega} - \frac{\left(F^{p}_{t\omega} - bS^{p}_{t}\right)}{a} \quad = \quad 0 \qquad \forall t \in \mathcal{T}, \omega \in \Omega \tag{2.3}$$

$$F^{p}_{t\omega} \quad \leq \quad MS^{p}_{t} \qquad \forall t \in \mathcal{T}, \omega \in \Omega \tag{2.4}$$

where M is a big number which is commonly used in the integer programming model.

For each building, the total electricity generated by PGU, from the battery, and the electricity purchased from the grid must cover the onsite electric demand load. The parameter $p^l_{it\omega}$ denotes the electric load at time t for building i at scenario ω.

$$E^{pl}_{it\omega} + E^{gl}_{it\omega} + E^{bl}_{it\omega} \geq p^l_{it\omega} \qquad \forall i \in \mathcal{I}, t \in \mathcal{T}, \omega \in \Omega \qquad (2.5)$$

$$S^p_{t-1} \geq Y^p_t \qquad \forall t \in \mathcal{T}, t > 1 \qquad (2.6)$$

$$1 - S^p_{t-1} \geq Z^p_t \qquad \forall t \in \mathcal{T}, t > 1 \qquad (2.7)$$

$$S^p_t - S^p_{t-1} = Z^p_t - Y^p_t \qquad \forall t \in \mathcal{T}, t > 1 \qquad (2.8)$$

$$0 \geq Y^p_1 \qquad (2.9)$$

$$1 \geq Z^p_1 \qquad (2.10)$$

$$S^p_1 = Z^p_1 - Y^p_1 \qquad (2.11)$$

The onsite heating and cooling demand must be fulfilled by a combination of the heat of the boiler, the recoverable heat of the PGU and the discharge from the thermal storage, so this is shown in equation 11.

$$Q^{ec}_{t\omega} + Q^{eh}_{t\omega} + Q^{e}_{t\omega} \leq \left(\eta^p F^p_{t\omega} + \eta^b F^b_{t\omega}\right) \qquad \forall t \in \mathcal{T}, \omega \in \Omega \quad (2.12)$$

$$\sum_{i \in \mathcal{I}} Q^c_{it\omega} = \eta^c \left(Q^{ec}_{t\omega} + Q^{sc}_{t\omega}\right) \qquad \forall t \in \mathcal{T}, \omega \in \Omega \quad (2.13)$$

$$\sum_{i \in \mathcal{I}} Q^h_{it\omega} = \eta^h \left(Q^{eh}_{t\omega} + Q^{sh}_{t\omega}\right) \qquad \forall t \in \mathcal{T}, \omega \in \Omega \quad (2.14)$$

$$Q^c_{it\omega} \geq p^c_{it} \qquad \forall i \in \mathcal{I}, t \in \mathcal{T}, \omega \in \Omega \quad (2.15)$$

$$Q^h_{it\omega} \geq p^h_{it} \qquad \forall i \in \mathcal{I}, t \in \mathcal{T}, \omega \in \Omega \quad (2.16)$$

where η^p is the fuel-to-thermal energy conversion efficiency of PGU, η^b, boiler thermal efficiency, η^c and η^h are the cooling and heating components thermal efficiency. They are equal to 0.51, 0.9, 0.7, and 0.85, respectively [19] [8]. Equations 12 and 13 are introduced for energy balance for meeting energy loads for building i at time t. Finally, Equations 14 and 15 display the constraint of p^c_{it} and p^h_{it} that are the cooling and heating loads of building i at time t respectively.

For storage operation, the thermal energy stored in the storage is restricted by its lower and upper limits as shown in equations (25)-(28). The charging (S^{e+}_t) and discharging rate (S^{e-}_t) is limited in the range of maximal $(\overline{q}^{e+}/\overline{q}^{e-})$ and minimal $(\underline{q}^{e+}/\underline{q}^{e-})$ charging /discharging rate. Then,

$$S^{e+}_t + S^{e-}_t \leq 1 \qquad \forall t \in \mathcal{T} \tag{2.17}$$

$$S^{e+}_{t-1} + S^{e-}_{t-1} \geq Y^e_t \qquad \forall t \in \mathcal{T}, t > 2 \tag{2.18}$$

$$1 - \left(S^{e+}_{t-1} + S^{e-}_{t-1}\right) \geq Z^e_t \qquad \forall t \in \mathcal{T}, t > 2 \tag{2.19}$$

$$\left(S^{e+}_t + S^{e-}_t\right) - \left(S^{e+}_{t-1} + S^{e-}_{t-1}\right) = Z^e_t - Y^e_t \qquad \forall t \in \mathcal{T}, t > 2 \tag{2.20}$$

$$0 \geq Y^e_t \tag{2.21}$$

$$1 \geq Z^e_t \tag{2.22}$$

$$S^{e+}_t + S^{e-}_t = Z^e_t - Y^e_t \tag{2.23}$$

$$Q^{e+}_{t\omega} \leq Q^e_{t\omega} \qquad \forall t \in \mathcal{T}, \omega \in \Omega \tag{2.24}$$

$$Q^{sc}_{t\omega} + Q^{sh}_{t\omega} = \eta^e Q^{e-}_{t\omega} \qquad \forall t \in \mathcal{T}, \omega \in \Omega \tag{2.25}$$

$$Q^{e+}_{t\omega} \leq \overline{q}^{e+} S^{e+}_t \qquad \forall t \in \mathcal{T}, \omega \in \Omega \tag{2.26}$$

$$Q_{t\omega}^{e+} \geq \underline{q}^{e+} S_t^{e+} \qquad \forall t \in \mathcal{T}, \omega \in \Omega \quad (2.27)$$

$$Q_{t\omega}^{e-} \leq \overline{q}^{e-} S_t^{e-} \qquad \forall t \in \mathcal{T}, \omega \in \Omega \quad (2.28)$$

$$Q_{t\omega}^{e-} \geq \underline{q}^{e-} S_t^{e-} \qquad \forall t \in \mathcal{T}, \omega \in \Omega \quad (2.29)$$

$$\left(Q_{t\omega}^{e+} - Q_{t\omega}^{e-}\right)\Delta t = \left(Q_{t\omega}^{s} - Q_{t-1,\omega}^{s}\right) \qquad \forall t \in \mathcal{T}, \omega \in \Omega \quad (2.30)$$

$$Q_{t\omega}^{s} \leq \overline{q}^{e} \qquad \forall t \in \mathcal{T}, \omega \in \Omega \quad (2.31)$$

$$Q_{t\omega}^{s} \geq \underline{q}^{e} \qquad \forall t \in \mathcal{T}, \omega \in \Omega \quad (2.32)$$

$$Q_{t\omega}^{sc} + Q_{t\omega}^{sh} \leq \eta^{e} Q_{t\omega}^{e} \qquad \forall t \in \mathcal{T}, \omega \in \Omega \quad (2.33)$$

where η^e is the thermal energy storage discharging efficiency, which equals to 0.95 [19] [31] [94]. Equation (24) is a energy balance for thermal energy discharged from storage $Q_{t\omega}^{e-}$ with the thermal energy transmitted from storage to cooling component $Q_{t\omega}^{sc}$ and heating component $Q_{t\omega}^{sh}$ at time t . For equation (29), $Q_{t\omega}^{s}$ is the amount of energy stored in the thermal energy storage at time, so $Q_{t-1\omega}^{s}$ is the amount of energy stored in the thermal energy storage at the time time interval t-1. Equations (31) and (32) limit $Q_{t\omega}^{s}$ by its maximum $\overline{q}^{e}$ and minimum $\underline{q}^{e}$ thermal energy storage capacity. Finally, equation (32) states that the thermal energy provided by the thermal storage cannot exceed the total amount of thermal energy transmitted to thermal energy storage, $Q_{t\omega}^{e}$, at time t.

For battery operation, the power stored in the battery cannot exceed its upper bound and be less than its lower bound. The charging/discharging rate is limited by the maximum and minimum charging/discharging rate. Therefore,

$$S_t^{b+} + S_t^{b-} \leq 1 \qquad \forall t \in \mathcal{T} \quad (2.34)$$

$$S_{t-1}^{b+} + S_{t-1}^{b-} \geq Y_t^b \qquad \forall t \in \mathcal{T}, t > 2 \quad (2.35)$$

$$1 - \left(S_{t-1}^{b+} + S_{t-1}^{b-}\right) \geq Z_t^b \qquad \forall t \in \mathcal{T}, t > 2 \quad (2.36)$$

$$\left(S_t^{b+} + S_t^{b-}\right) - \left(S_{t-1}^{b+} + S_{t-1}^{b-}\right) = Z_t^b - Y_t^b \qquad \forall t \in \mathcal{T}, t > 2 \quad (2.37)$$

$$0 \geq Y_t^b \quad (2.38)$$

$$1 \geq Z_t^b \quad (2.39)$$

$$S_t^{b+} + S_t^{b-} = Z_t^b - Y_t^b \quad (2.40)$$

$$E_{t\omega}^{b+}/\eta^{b+} + E_{t\omega}^{gb} = E_{t\omega}^{pb} \qquad \forall t \in \mathcal{T}, \omega \in \Omega \quad (2.41)$$

$$\sum_{i \in \mathcal{I}} E_{it\omega}^{bl} = \eta^{b-} E_{t\omega}^{b-} \qquad \forall t \in \mathcal{T}, \omega \in \Omega \quad (2.42)$$

$$E_{t\omega}^{b+} \leq \overline{q}^{b+} S_t^{b+} \qquad \forall t \in \mathcal{T}, \omega \in \Omega \quad (2.43)$$

$$E_{t\omega}^{b+} \geq \underline{q}^{b+} S_t^{b+} \qquad \forall t \in \mathcal{T}, \omega \in \Omega \quad (2.44)$$

$$E_{t\omega}^{b-} \leq \overline{q}^{b-} S_t^{b-} \qquad \forall t \in \mathcal{T}, \omega \in \Omega \quad (2.45)$$

$$E_{t\omega}^{b-} \geq \underline{q}^{b-} S_t^{b-} \qquad \forall t \in \mathcal{T}, \omega \in \Omega \quad (2.46)$$

$$\left(E_{t\omega}^{b+} - E_{t\omega}^{b-}\right)\Delta t = \left(E_{t\omega}^{b} - E_{t-1,\omega}^{b}\right) \qquad \forall t \in \mathcal{T}, \omega \in \Omega \quad (2.47)$$

$$E_{t\omega}^{b} \leq \overline{q}^{b} \qquad \forall t \in \mathcal{T}, \omega \in \Omega \quad (2.48)$$

$$E_{t\omega}^{b} \geq \underline{q}^{b} \qquad \forall t \in \mathcal{T}, \omega \in \Omega \quad (2.49)$$

where η^{b+} and η^{b-} are the battery charging and discharging efficiency, which equal to 0.9 and 0.9, respectively [19] [31] [94].

The Integrity and Non-negativity constraints are described as follows:

$$Z_t^p, S_t^p, Y_t^p, Z_t^e, Y_t^e, S_t^{e+}, S_t^{e-}, Z_t^b, S_t^{b+}, S_t^{b-}, Y_t^b \in \{0, 1\} \qquad \forall t \in \mathcal{T} \quad (2.50)$$

$$F_{t\omega}^p, F_{t\omega}^b, E_{it\omega}^{gl}, E_{t\omega}^{gb}, E_{t\omega}^g, E_{it\omega}^{pl}, E_{t\omega}^{pb}$$

$$, E^{bl}_{it\omega}, E^{b+}_{t\omega}, E^{b-}_{t\omega}, E^{b}_{t\omega}, Q^{ec}_{t\omega}, Q^{eh}_{t\omega}, Q^{e}_{t\omega},$$

$$Q^{e+}_{t\omega}, Q^{e-}_{t\omega}, Q^{s}_{t\omega}, Q^{sc}_{t\omega}, Q^{sh}_{t\omega}, Q^{c}_{it\omega}, Q^{h}_{it\omega} \quad \geq \quad 0 \qquad \forall t \in \mathcal{T}, \omega \in \Omega \quad (2.51)$$

In summary, the proposed model allow us to study the CCHP operation with an electric battery and thermal storage under uncertainty, and to minimize the operational costs. In the following section, solutions approaches are proposed to solve efficiently the model.

2.4 Solution Approaches

CCHP, as a typical power system, involves a high number of complexities that govern its operation. CCHP considers individual generators, transmission network, storage subsystems and load requirements. Thus, guaranteeing its reliability and robustness is an NP-hard problem, and testing CCHP systems over a large number of scenarios are the practice in the industry [1]. In addition, the problem stated in section 3, it is mixed-integer linear programming with discrete and continuous variables. Somma et.al [98] supports that although in a mixed-integer linear programming model for the operation Optimization of a Distributed Energy System (DES), the Branch-and-Cut is a powerful technique but the procedure of obtaining the convex hull (small set that contains all integer feasible solutions) is NP-hard. Hence, using commercial solvers (e.g. CPLEX) will not provide an efficient solution for large-scale problems.

In this part of this study, we will introduce various algorithm techniques to be applied to solve the stochastic CCHP problem. In sections 2.4.1, and 2.4.2, we will start describing the Sample Average Approximation (SAA), and Benders decomposition algorithms respectively. On section 2.4.3, we will introduce enhancement strategies for Benders de-

composition algorithm, and finally in section 2.4.4, we will integrate Sample Average Approximation approach with an accelerated Benders decomposition technique.

2.4.1 Scenario Generation for CCHP uncertainty:

Demand patterns, in the energy sector, are random in nature with a high degree of uncertainty. As a note, industry practices focus on the operational performance of an energy system (e.g. CCHP) to satisfy peaks energy demand either for summer and winter. However, the long-term planning requires incorporating the uncertainty [32]. The following figures support the statements. For instance, to forecast the demand for space cooling different approaches are needed. Traditionally, one approach is to forecast base on a simulation from aggregate historical data [27]. Another method is showed in Figure 2.2, it uses historical data to get the differences between cool and warmer days (e.g.hourly demand for a utility in Colorado in 2005) . Figure 2.3 shows this approach, it provides better understanding and provides expected trends (multiple scenarios) for various locations. Therefore, considering a large number of instances in modeling a CCHP systems is mandatory.

Therefore, to solve the two-stage stochastic linear programming model, a scenario analysis is an efficient method, and the probability description can be visualized using scenario tree [6]. Figure 2.4 shows the scenario tree where each scenario corresponds a particular outcome after the realization of the random variable. However, a reliable model requires generating a relatively small scenario set. Gamou et. al [32] supports that energy demand obeys to a normal probability distribution in which 95% of the whole area is within the

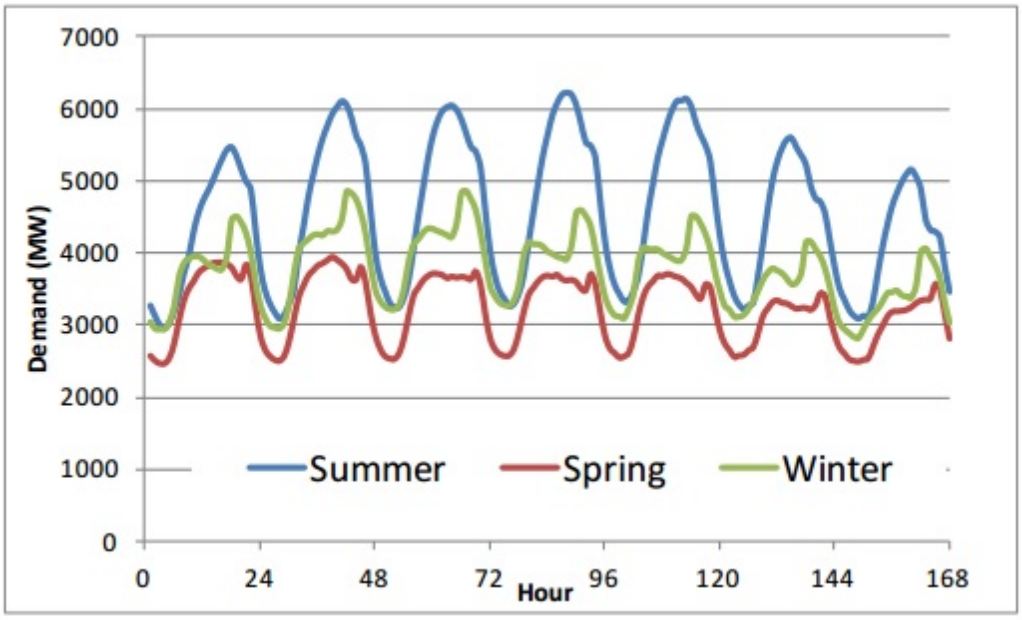

Figure 2.2

Seasonal demand patterns in Colorado

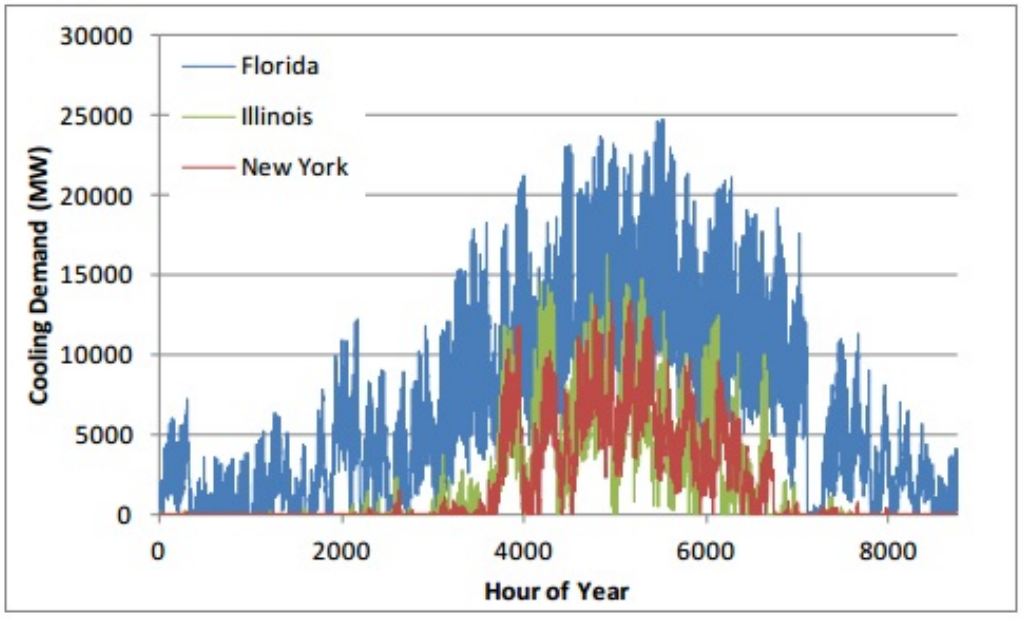

Figure 2.3

Estimated cooling load patterns for Florida, Illinois, and New York

range of 20% of the average energy demands. They worked with real data of more than 8700 hours of operation.

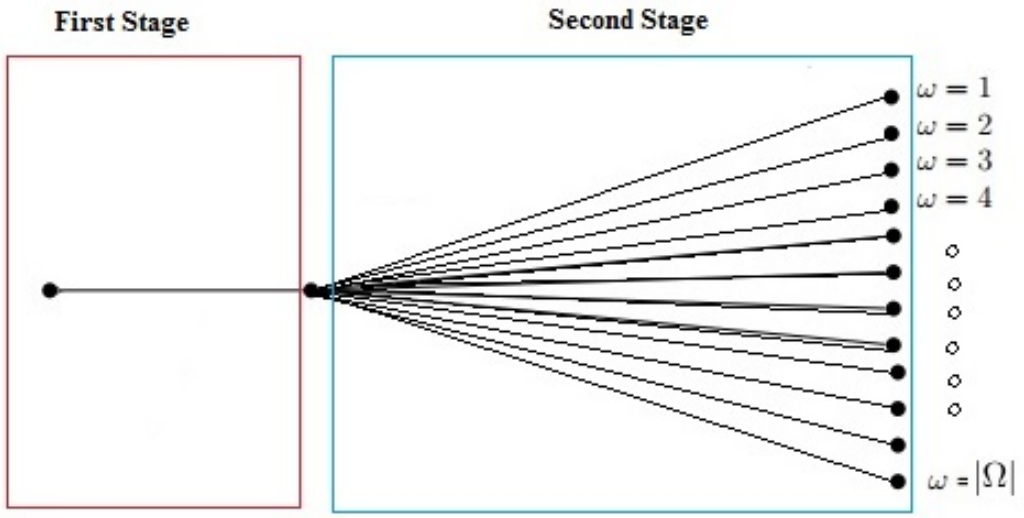

Figure 2.4

The scenario trees

Li et. al [56]adopted this assumption to do a sensitive analysis of energy demands on CCHP systems, and in proposing an optimization model for building cooling heating and power system with consideration of uncertainty of energy demands [57]. Zhou et.al [123] worked with normal distribution of energy demand in a two-stage stochastic programming for a distributed energy system (DER). We assumed that each type of energy demand obeys the normal distribution aforementioned, and the random number generator will be programmed accordingly with this assumption.

2.4.2 Sample Average Approximation:

The concept behind the Sample Average Approximation (SAA) is to generate random samples with $N < |\Omega|$ of realizations, and the expected value function is estimated (approximated) by the sample average function [49] [103]. A deterministic optimization technique solves the resulting sample average problem. The process is repeated with different samples generated to produce high-quality candidate solutions, and also statistical estimation of their optimality gaps [108] [78].

As mentioned above, we assume that all energy demand follows a normal distribution $\mathcal{N}(\mu; \sigma^2)$ for each location $i \in \mathcal{I}$ and time period $t \in \mathcal{T}$. The random number generates a large number of scenarios with equal probabilities $\frac{1}{N}$. Then, After the number of scenarios are generated (i.e. N scenarios),the SAA Algorithm is as follows:

$$Minimize \left\{ z^r_{\Omega'} := \sum_{t \in \mathcal{T}} \Big(\psi^p_t Z^p_t + \psi^e_t Z^e_t + \psi^b_t Z^b_t + \frac{1}{N} \sum_{n=1}^{N} \mathcal{Q} \left(Z^p Z^e Z^b, n \right) \Big) \right\} \quad (2.52)$$

Thus, as the sample size (i.e. the value of N) increases the optimal solution of the above equation converges with probability one to an optimal solution of the original problem **[CCHP]** [49]. On the other hand, assuming that the SAA-problem is solved within an absolute optimality gap $\delta \geq 0$, the size of N can be estimated to guarantee an ϵ-optimal solution with a probability at leat equal to $(1 - \alpha)$ as follows:

$$N \geq \frac{3\sigma^2_{max}}{(\epsilon - \delta)^2} \Big(|\mathcal{T}| \, (log 2) - log \alpha \Big) \quad (2.53)$$

where $\epsilon > \delta$, $\alpha \in (0,1)$, and σ^2_{max} is a maximal variance of certain function differences [49]. Thus, after choosing a sample size N, the solutions of the SAA algorithm provides lower and upper bounds for **[CCHP]**, and it terminates when the gap between the estimators falls below a pre-determined threshold value.

The steps to solve **[CCHP]** using the Sample Average Approximation (SAA) are as follows:

Step 1: Determine a sample size $|\Omega'|$ and number of replications $|R|$. Select a sample size $|\Omega''| \gg |\Omega'|$ to compute the estimated optimal objective solution of the SAA algorithm. Set, the probability of scenario ω equal to $\rho_\omega = 1/|\Omega'|; \forall \omega \in \Omega'$.

Step 2: For $r = 1 \rightarrow |R|$, apply the following steps:

2(a): Generate Ω' independent samples of size $|\Omega'|$ and solve the corresponding SAA. We denote the optimal objective function value by $z^r_{\Omega'}$ and the optimal solution denoted by $\mathcal{Z}^r$ (which consists of the vectors $\overline{\mathbf{Y}}$; $\overline{\mathbf{Z}}$ and $\overline{\mathbf{S}}$), of the replication r.

$$z^r_{\Omega'} = \sum_{t\in\mathcal{T}}\Bigg(\psi^p_t Z^p_t + \psi^e_t Z^e_t + \psi^b_t Z^b_t + \sum_{\omega\in\Omega'} \rho_w \Bigg(\chi^+_t E^{gb}_{t\omega} + \kappa^p_t F^p_{t\omega} + \kappa^b_t F^b_{t\omega} - \chi^-_t E^g_{t\omega} + \sum_{i\in\mathcal{I}} \chi^+_t E^{gl}_{it\omega}\Bigg)\Bigg) \tag{2.54}$$

2(b): Compute the average of all optimal objective function values from the SAA problems, $\hat{z}^r_{\Omega'}$ and their corresponding variance, $\sigma^2_{\hat{z}^r_{\Omega'}}$ as follows:

$$\hat{z}^r_{\Omega'} = \frac{1}{r}\sum_{i=1}^{r} z^i_{\Omega'} \tag{2.55}$$

$$\sigma^2_{\hat{z}^r_{\Omega'}} = \frac{1}{|R|(|R|-1)} \sum_{i=1}^{r} \Big(z^i_{\Omega'} - \hat{z}^r_{\Omega'} \Big)^2 \tag{2.56}$$

The average optimal function value $\hat{z}^r_{\Omega'}$ provides a statistical lower bound on the optimal objective function value for the original problem **[CCHP]**.

2(c): Generate a large sample size $|\Omega''|$. Use the solution $\mathcal{Z}^r$ to obtain an upper bound of the optimal solution on the generated sample size $|\Omega''|$, denoted by $z_{\Omega''}(\mathcal{Z}^r)$.

$$z_{\Omega''}(\mathcal{Z}^r) = \sum_{t \in \mathcal{T}} \Big(\psi^p_t Z^p_t + \psi^e_t Z^e_t + \psi^b_t Z^b_t + \sum_{\omega \in \Omega''} \rho_w \Big(\chi^+_t E^{gb}_{t\omega} + \kappa^p_t F^p_{t\omega} + \kappa^b_t F^b_{t\omega} - \chi^-_t E^g_{t\omega} + \sum_{i \in \mathcal{I}} \chi^+_t E^{gl}_{it\omega} \Big) \Big) \tag{2.57}$$

The variance of this estimated upper bound can be calculated as follows:

$$\sigma^2_{\Omega''} = \frac{1}{|\Omega''|(\Omega''-1)} \sum_{\omega \in \Omega''} \Big(A_\omega(\mathcal{Z}^r) - z_{\Omega''}(\mathcal{Z}^r) \Big)^2 \tag{2.58}$$

where

$$A_\omega(\mathcal{Z}^r) = \sum_{t \in \mathcal{T}} \Big(\psi^p_t Z^p_t + \psi^e_t Z^e_t + \psi^b_t Z^b_t + \chi^+_t E^{gb}_{t\omega} + \kappa^p_t F^p_{t\omega} + \kappa^b_t F^b_{t\omega} - \chi^-_t E^g_{t\omega} + \sum_{i \in \mathcal{I}} \chi^+_t E^{gl}_{it\omega} \Big) \tag{2.59}$$

2(d): Compute the SAA gap, $\epsilon^{SAA}(\Omega', \Omega'')$ and the variance of the gap $\sigma^2_{\epsilon^{SAA}(\Omega', \Omega'')}$ as follows:

$$\epsilon^{SAA}(\Omega', \Omega'') = z_{\Omega''}(\mathcal{Z}^r) - \hat{z}^r_{\Omega'} \tag{2.60}$$

$$\sigma^2_{\epsilon^{SAA}(\Omega', \Omega'')} = \sigma^2_{\Omega''} + \sigma^2_{\hat{z}^r_{\Omega'}} \tag{2.61}$$

The confidence interval of the optimality gap is then calculated as follows:

$$z_{\Omega''}(\mathcal{Z}^r) - \hat{z}^r_{\Omega'} + z_\alpha \left(\sigma^2_{\Omega''} + \sigma^2_{\hat{z}^r_{\Omega'}} \right)^{1/2} \tag{2.62}$$

with $z_\alpha := \Phi^{-1}(1-\alpha)$, where $\Phi(z)$ is the cumulative distribution function of the standard normal distribution.

Step 3: Choose the solution $\mathcal{Z}^r$ that gives the lowest upper bound $z_{\Omega''}(\mathcal{Z}^r)$ as the best solution.

2.4.3 Benders Decomposition:

[CCHP] has a mixed integer linear program structure, so Bender Decomposition method is a popular technique for optimization problems [90] [77]. Benders has been applied successfully for different problems in power systems [2]. The basic idea is to partition the original problem in two subproblems: (1) the master problem as integer programming, and (2) the subproblem as linear programing problem [12] We can refer the work of Geoffrion [34] for the proof of convergence properties of Benders. Thus, the Benders Decomposition reformulation for the model **[CCHP]** is as follows:

$$\begin{aligned} &\textbf{[CCHP]} Minimize \sum_{t \in \mathcal{T}} \left(\psi^p_t Z^p_t + \psi^e_t Z^e_t + \psi^b_t Z^b_t \right) \\ &+\textbf{[CCHP-SUB]}(E^{gb}, F^p, F^b, E^g, E^{gl} | \hat{Z}^p, \hat{Z}^e, \hat{Z}^b) \end{aligned} \tag{2.63}$$

Subject to $[2.2]$-$[2.50]$.

Thus, the Master Problem is

$$\textbf{[CCHP-M]}\ Minimize\ \sum_{t\in\mathcal{T}}\left(\psi_t^p Z_t^p + \psi_t^e Z_t^e + \psi_t^b Z_t^b\right) \tag{2.64}$$

Subject to

$$S_{t-1}^p \geq Y_t^p \qquad \forall t \in \mathcal{T}, t > 1 \tag{2.65}$$

$$1 - S_{t-1}^p \geq Z_t^p \qquad \forall t \in \mathcal{T}, t > 1 \tag{2.66}$$

$$S_t^p - S_{t-1}^p = Z_t^p - Y_t^p \qquad \forall t \in \mathcal{T}, t > 1 \tag{2.67}$$

$$0 \geq Y_t^p \tag{2.68}$$

$$S_t^p = Z_t^p - Y_t^p \qquad \forall t \in \mathcal{T} \tag{2.69}$$

$$S_t^{e+} + S_t^{e-} \leq 1 \qquad \forall t \in \mathcal{T} \tag{2.70}$$

$$S_{t-1}^{e+} + S_{t-1}^{e-} \geq Y_t^e \qquad \forall t \in \mathcal{T}, t > 2 \tag{2.71}$$

$$1 - \left(S_{t-1}^{e+} + S_{t-1}^{e-}\right) \geq Z_t^e \qquad \forall t \in \mathcal{T}, t > 2 \tag{2.72}$$

$$\left(S_t^{e+} + S_t^{e-}\right) - \left(S_{t-1}^{e+} + S_{t-1}^{e-}\right) = Z_t^e - Y_t^e \qquad \forall t \in \mathcal{T}, t > 2 \tag{2.73}$$

$$0 \geq Y_t^e \tag{2.74}$$

$$S_t^{e+} + S_t^{e-} = Z_t^e - Y_t^e \qquad \forall t \in \mathcal{T} \tag{2.75}$$

$$S_{t-1}^{b+} + S_{t-1}^{b-} \geq Y_t^b \qquad \forall t \in \mathcal{T}, t > 2 \tag{2.76}$$

$$S_t^{b+} + S_t^{b-} \leq 1 \qquad \forall t \in \mathcal{T} \tag{2.77}$$

$$1 - \left(S_{t-1}^{b+} + S_{t-1}^{b-}\right) \geq Z_t^b \qquad \forall t \in \mathcal{T}, t > 2 \tag{2.78}$$

$$\left(S_t^{b+} + S_t^{b-}\right) - \left(S_{t-1}^{b+} + S_{t-1}^{b-}\right) = Z_t^b - Y_t^b \qquad \forall t \in \mathcal{T}, t > 2 \tag{2.79}$$

$$0 \geq Y_t^b \tag{2.80}$$

$$S_t^{b+} + S_t^{b-} = Z_t^b - Y_t^b \qquad \forall t \in \mathcal{T} \tag{2.81}$$

$$1 \geq Z_t^p \tag{2.82}$$

$$1 \geq Z_t^e \tag{2.83}$$

$$1 \geq Z_t^b \tag{2.84}$$

$$Z_t^p, Z_t^e, Z_t^b, Y_t^p, Y_t^e, Y_t^b$$

$$, S_t^p, S_t^{e+}, S_t^{e-}, S_t^{b+}, S_t^{b-} \in \{0,1\} \qquad \forall t \in \mathcal{T} \tag{2.85}$$

and, **[CCHP-SUB]**($E^{gb}, F^p, F^b, E^g, E^{gl} | \hat{Z}^t, \hat{Z}^e, \hat{Z}^b$) represents the Bender subproblem.

For given values of the $\mathcal{Z}^p := Z^p_{t\in T}$, $\mathcal{Z}^p := Z^e_{t\in T}$,and $\mathcal{Z}^p := Z^b_{t\in T}$ variables that complies with the integrality conditions, the model **[CCHP]** reduces the below primal subproblem incorporating only the continuous variables $E^{gb}, F^p, F^b, E^g, E^{gl}$.

$$\textbf{[CCHP-SUB]}\ Minimize \sum_{t\in\mathcal{T}}\Big(\sum_{\omega\in\Omega}\rho_w\Delta t\Big(\chi_t^+ E_{t\omega}^{gb} + \kappa_t^p F_{t\omega}^p + \kappa_t^b F_{t\omega}^b - \chi_t^- E_{t\omega}^g + \sum_{i\in\mathcal{I}}\chi_t^+ E_{it\omega}^{gl}\Big)\Big) \tag{2.86}$$

Subject to:

$$E_{t\omega}^{gb} + \sum_{i\in\mathcal{I}} E_{it\omega}^{gl} \leq \overline{e}^p \qquad \forall t \in \mathcal{T}, \omega \in \Omega \tag{2.87}$$

$$E_{t\omega}^{pb} + E_{t\omega}^g + \sum_{i\in\mathcal{I}} E_{it\omega}^{pl} - \frac{\left(F_{t\omega}^p - b\hat{S}_t^p\right)}{a} = 0 \qquad \forall t \in \mathcal{T}, \omega \in \Omega \tag{2.88}$$

$$F_{t\omega}^p \leq M\hat{S}_t^p \qquad \forall t \in \mathcal{T}, \omega \in \Omega \tag{2.89}$$

$$E_{it\omega}^{pl} + E_{it\omega}^{gl} + E_{it\omega}^{bl} \geq p_{it\omega}^l \qquad \forall i \in \mathcal{I}, t \in \mathcal{T}, \omega \in \Omega \tag{2.90}$$

$$Q_{t\omega}^{ec} + Q_{t\omega}^{eh} + Q_{t\omega}^e \leq \left(\eta^p F_{t\omega}^p + \eta^b F_{t\omega}^b\right) \forall t \in \mathcal{T}, \omega \in \Omega \tag{2.91}$$

$$\sum_{i\in\mathcal{I}} Q_{it\omega}^c = \eta^c\left(Q_{t\omega}^{ec} + Q_{t\omega}^{sc}\right) \ \forall t \in \mathcal{T}, \omega \in \Omega \tag{2.92}$$

$$\sum_{i\in\mathcal{I}} Q^h_{it\omega} = \eta^h\Big(Q^{eh}_{t\omega} + Q^{sh}_{t\omega}\Big) \quad \forall t \in \mathcal{T}, \omega \in \Omega \quad (2.93)$$

$$Q^c_{it\omega} \geq p^c_{it} \qquad \forall i \in \mathcal{I}, t \in \mathcal{T}, \omega \in \Omega \quad (2.94)$$

$$Q^h_{it\omega} \geq p^h_{it} \qquad \forall i \in \mathcal{I}, t \in \mathcal{T}, \omega \in \Omega \quad (2.95)$$

$$Q^{e+}_{t\omega} \leq Q^e_{t\omega} \qquad \forall t \in \mathcal{T}, \omega \in \Omega \quad (2.96)$$

$$Q^{sc}_{t\omega} + Q^{sh}_{t\omega} = \eta^e Q^{e-}_{t\omega} \qquad \forall t \in \mathcal{T}, \omega \in \Omega \quad (2.97)$$

$$Q^{e+}_{t\omega} \leq \overline{q}^{e+}\hat{S}^{e+}_t \qquad \forall t \in \mathcal{T}, \omega \in \Omega \quad (2.98)$$

$$Q^{e+}_{t\omega} \geq \underline{q}^{e+}\hat{S}^{e+}_t \qquad \forall t \in \mathcal{T}, \omega \in \Omega \quad (2.99)$$

$$Q^{e-}_{t\omega} \leq \overline{q}^{e-}\hat{S}^{e-}_t \qquad \forall t \in \mathcal{T}, \omega \in \Omega \quad (2.100)$$

$$Q^{e-}_{t\omega} \geq \underline{q}^{e-}\hat{S}^{e-}_t \qquad \forall t \in \mathcal{T}, \omega \in \Omega \quad (2.101)$$

$$\Big(Q^{e+}_{t\omega} - Q^{e-}_{t\omega}\Big)\Delta t = \Big(Q^s_{t\omega} - Q^s_{t-1,\omega}\Big) \quad \forall t \in \mathcal{T}, \omega \in \Omega \quad (2.102)$$

$$Q^s_{t\omega} \leq \overline{q}^e \qquad \forall t \in \mathcal{T}, \omega \in \Omega \quad (2.103)$$

$$Q^s_{t\omega} \geq \underline{q}^e \qquad \forall t \in \mathcal{T}, \omega \in \Omega \quad (2.104)$$

$$Q^{sc}_{t\omega} + Q^{sh}_{t\omega} \leq \eta^e Q^e_{t\omega} \qquad \forall t \in \mathcal{T}, \omega \in \Omega \quad (2.105)$$

$$E^{b+}_{t\omega}/\eta^{b+} + E^{gb}_{t\omega} = E^{pb}_{t\omega} \qquad \forall t \in \mathcal{T}, \omega \in \Omega \quad (2.106)$$

$$\sum_{i\in\mathcal{I}} E^{bl}_{it\omega} = \eta^{b-} E^{b-}_{t\omega} \qquad \forall t \in \mathcal{T}, \omega \in \Omega \quad (2.107)$$

$$E^{b+}_{t\omega} \leq \overline{q}^{b+}\hat{S}^{b+}_t \qquad \forall t \in \mathcal{T}, \omega \in \Omega \quad (2.108)$$

$$E^{b+}_{t\omega} \geq \underline{q}^{b+}\hat{S}^{b+}_t \qquad \forall t \in \mathcal{T}, \omega \in \Omega \quad (2.109)$$

$$E^{b-}_{t\omega} \leq \overline{q}^{b-}\hat{S}^{b-}_t \qquad \forall t \in \mathcal{T}, \omega \in \Omega \quad (2.110)$$

$$E^{b-}_{t\omega} \geq \underline{q}^{b-}\hat{S}^{b-}_t \qquad \forall t \in \mathcal{T}, \omega \in \Omega \quad (2.111)$$

$$\Big(E^{b+}_{t\omega} - E^{b-}_{t\omega}\Big)\Delta t = \Big(E^b_{t\omega} - E^b_{t-1,\omega}\Big) \quad \forall t \in \mathcal{T}, \omega \in \Omega \quad (2.112)$$

$$E^b_{t\omega} \leq \overline{q}^b \qquad \forall t \in \mathcal{T}, \omega \in \Omega \qquad (2.113)$$

$$E^b_{t\omega} \geq \underline{q}^b \qquad \forall t \in \mathcal{T}, \omega \in \Omega \qquad (2.114)$$

$$\begin{aligned} F^p_{t\omega}, F^b_{t\omega}, E^{gl}_{it\omega}, E^{gb}_{t\omega}, E^g_{t\omega}, \\ E^{pl}_{it\omega}, E^{pb}_{t\omega}, E^{bl}_{it\omega}, E^{b+}_{t\omega}, E^{b-}_{t\omega}, E^b_{t\omega}, \\ Q^{ec}_{t\omega}, Q^{eh}_{t\omega}, Q^e_{t\omega}, Q^{e+}_{t\omega}, Q^{e-}_{t\omega}, \\ Q^s_{t\omega}, Q^{sc}_{t\omega}, Q^{sh}_{t\omega}, Q^c_{it\omega}, Q^h_{it\omega} \geq 0 \qquad \forall t \in \mathcal{T}, \omega \in \Omega \end{aligned} \qquad (2.115)$$

Let be the dual variables $\alpha^l = \{\alpha^l_{t\omega} \geq 0 | t \in \mathcal{T}; \omega \in \Omega\}$, l=1,2,3 for constraints $[2.87-2.89]$, $\beta = \{\beta_{it\omega} \geq 0 | i \in \mathcal{I}; t \in \mathcal{T}; \omega \in \Omega\}$, for constraint $[2.90]$, $\gamma^l = \{\gamma^l_{t\omega} \geq 0 | t \in \mathcal{T}; \omega \in \Omega\}$, l=1,2,3 for constraints $[2.91 - 2.93]$, $\delta^l = \{\delta^l_{t\omega} \geq 0 | i \in \mathcal{I}; t \in \mathcal{T}; \omega \in \Omega\}$, l=1,2 for constraints $[2.94-2.95]$, $\theta^l = \{\theta^l_{t\omega} \geq 0 | t \in \mathcal{T}; \omega \in \Omega\}$, l=1,...,10 for constraints $[2.96-2.105]$, $\lambda^l = \{\lambda^l_{t\omega} \geq 0 | t \in \mathcal{T}; \omega \in \Omega\}$ l=1,...,9 for constraints $[2.106 - 2.114]$, respectively.

The dual of the primal subproblem, **[CCHP-SUB(D)]** can be written as:

$$\begin{aligned} \textbf{[CCHP-SUB(D)]}\, Maximize \sum_{\forall t \in \mathcal{T} \omega \in \Omega} & -\overline{e}^p \alpha^1_{tw} - \frac{b}{a} \sum_{\forall t \in \mathcal{T} \omega \in \Omega} \hat{S}^p_t \alpha^2_{tw} \\ & - M \sum_{\forall t \in \mathcal{T} \omega \in \Omega} \hat{S}^p_t \alpha^3_{tw} + \sum_{\forall i \in \mathcal{I}, \forall t \in \mathcal{T} \omega \in \Omega} p^l_{it\omega} \beta_{itw} \\ & + \sum_{\forall i \in \mathcal{I}, \forall t \in \mathcal{T} \omega \in \Omega} p^c_{it\omega} \delta^1_{tw} + \sum_{\forall i \in \mathcal{I}, \forall t \in \mathcal{T} \omega \in \Omega} p^h_{it\omega} \delta^2_{tw} \\ - \sum_{\forall t \in \mathcal{T} \omega \in \Omega} & \overline{q}^{e+} \hat{S}^{e+}_t \theta^3_{tw} + \underline{q}^{e+} \sum_{\forall t \in \mathcal{T} \omega \in \Omega} \hat{S}^{e+}_t \theta^4_{tw} - \overline{q}^{e-} \sum_{\forall t \in \mathcal{T} \omega \in \Omega} \hat{S}^{e-}_t \theta^5_{tw} \\ & + \underline{q}^{e-} \sum_{\forall t \in \mathcal{T} \omega \in \Omega} \hat{S}^{e-}_t \theta^6_{tw} - \overline{q}^e \sum_{\forall t \in \mathcal{T} \omega \in \Omega} \theta^8_{tw} + \underline{q}^e \sum_{\forall t \in \mathcal{T} \omega \in \Omega} \theta^9_{tw} \\ - \overline{q}^{b+} \sum_{\forall t \in \mathcal{T} \omega \in \Omega} & \hat{S}^{b+}_t \lambda^3_{tw} + \underline{q}^{b+} \sum_{\forall t \in \mathcal{T} \omega \in \Omega} \hat{S}^{b+}_t \lambda^4_{tw} - \overline{q}^{b-} \sum_{\forall t \in \mathcal{T} \omega \in \Omega} \hat{S}^{b-}_t \lambda^5_{tw} \end{aligned}$$

$$+\underline{q}^{b-}\sum_{\forall t\in\mathcal{T}\omega\in\Omega}\hat{S}_t^{b-}\lambda_{tw}^6-\overline{q}^b\sum_{\forall t\in\mathcal{T}\omega\in\Omega}\lambda_{tw}^8+$$
$$\underline{q}^b\sum_{\forall t\in\mathcal{T}\omega\in\Omega}\lambda_{tw}^9 \tag{2.116}$$

Subject to:

$$-\alpha_{t\omega}^1+\lambda_{t\omega}^1 \leq \Delta t*\chi_t^+ \qquad \forall t\in\mathcal{T},\omega\in\Omega \tag{2.117}$$
$$-\frac{\alpha_{t\omega}^2}{a}-\alpha_{t\omega}^3+\eta^p\gamma_{t\omega}^1 \leq \Delta t*\kappa_t^p \qquad \forall t\in\mathcal{T},\omega\in\Omega \tag{2.118}$$
$$-\eta^b\gamma_{t\omega}^1 \leq \Delta t*\kappa_t^b \qquad \forall t\in\mathcal{T},\omega\in\Omega \tag{2.119}$$
$$\alpha_{t\omega}^2 \leq -\Delta t*\chi_t^- \qquad \forall t\in\mathcal{T},\omega\in\Omega \tag{2.120}$$
$$-\alpha_{t\omega}^1+\beta_{it\omega} \leq \Delta t*\chi_t^+ \qquad \forall t\in\mathcal{T},\omega\in\Omega \tag{2.121}$$
$$\alpha_{t\omega}^2-\lambda_{t\omega}^1 \leq 0 \qquad \forall t\in\mathcal{T},\omega\in\Omega \tag{2.122}$$
$$\alpha_{t\omega}^2+\beta_{it\omega} \leq 0 \qquad \forall t\in\mathcal{T},\omega\in\Omega \tag{2.123}$$
$$\beta_{it\omega}+\lambda_{t\omega}^2 \leq 0 \qquad \forall t\in\mathcal{T},\omega\in\Omega \tag{2.124}$$
$$\gamma_{t\omega}^1-\eta^c\gamma_{t\omega}^2 \leq 0 \qquad \forall t\in\mathcal{T},\omega\in\Omega \tag{2.125}$$
$$-\gamma_{t\omega}^1-\eta^h\gamma_{t\omega}^3 \leq 0 \qquad \forall t\in\mathcal{T},\omega\in\Omega \tag{2.126}$$
$$-\gamma_{t\omega}^1+\theta_{t\omega}^1-\eta^e\theta_{t\omega}^{10} \leq 0 \qquad \forall t\in\mathcal{T},\omega\in\Omega \tag{2.127}$$
$$\gamma_{t\omega}^2+\delta_{it\omega}^1 \leq 0 \qquad \forall i\in\mathcal{I}\forall t\in\mathcal{T},\omega\in\Omega \tag{2.128}$$
$$\gamma_{t\omega}^3+\delta_{it\omega}^2 \leq 0 \qquad \forall i\in\mathcal{I}\forall t\in\mathcal{T},\omega\in\Omega \tag{2.129}$$
$$-\eta^c\gamma_{t\omega}^2+\theta_{t\omega}^2-\theta_{t\omega}^{10} \leq 0 \qquad \forall t\in\mathcal{T},\omega\in\Omega \tag{2.130}$$
$$-\eta^h\gamma_{t\omega}^3+\theta_{t\omega}^2-\theta_{t\omega}^{10} \leq 0 \qquad \forall t\in\mathcal{T},\omega\in\Omega \tag{2.131}$$
$$-\theta_{t\omega}^1-\theta_{t\omega}^3+\theta_{t\omega}^4+\Delta t*\theta_{t\omega}^7 \leq 0 \qquad \forall t\in\mathcal{T},\omega\in\Omega \tag{2.132}$$
$$-\eta^e\theta_{t\omega}^2-\theta_{t\omega}^5+\theta_{t\omega}^6-\Delta t*\theta_{t\omega}^7 \leq 0 \qquad \forall t\in\mathcal{T},\omega\in\Omega \tag{2.133}$$

$$\frac{\lambda^1_{t\omega}}{\eta^{b+}} - \lambda^3_{t\omega} + \lambda^4_{t\omega} + \Delta t * \lambda^7_{t\omega} \leq 0 \qquad \forall t \in \mathcal{T}, \omega \in \Omega \quad (2.134)$$

$$-\theta^7_{t\omega} + \theta^7_{t+1,\omega} - \theta^8_{t\omega} + \theta^9_{t\omega} \leq 0 \qquad \forall t \in \mathcal{T}, \omega \in \Omega \quad (2.135)$$

$$-\eta^{b-}\lambda^2_{t\omega} - \lambda^5_{t\omega} + \lambda^6_{t\omega} - \Delta t * \lambda^7_{t\omega} \leq 0 \qquad \forall t \in \mathcal{T}, \omega \in \Omega \quad (2.136)$$

$$-\lambda^7_{t\omega} + \lambda^7_{t+1,\omega} - \lambda^8_{t\omega} + \lambda^9_{t\omega} \leq 0 \qquad \forall t \in \mathcal{T}, \omega \in \Omega \quad (2.137)$$

$$\alpha^1_t, \alpha^3_t, \beta_{it}, \delta^l_{it}, \theta^1_t,$$

$$\theta^3_t, \theta^4_t, \theta^5_t, \theta^6_t, \theta^8_t,$$

$$\theta^{10}_t, \lambda^3_t, \lambda^4_t, \lambda^5_t, \lambda^6_t \lambda^8_t, , \omega \in \mathcal{R}^+ \quad (2.138)$$

$$\alpha^2_t, \gamma^l_t, \theta^2_t, \theta^7_t, \lambda^1_t, \lambda^2_t \lambda^7_t, \in \mathcal{R} \quad (2.139)$$

By introducing an extra variable θ, the Benders reformulation can be equivalently written as the following Bender master problem **[CCHP-MP]**:

$$\textbf{[CCHP-MP]}\ Minimize \sum_{t\in\mathcal{T}}\left(\psi^p_t Z^p_t + \psi^e_t Z^e_t + \psi^b_t Z^b_t\right) + \theta \quad (2.140)$$

$$(2.141)$$

Subject to

Constraints (2.65) to (2.85).

$$\theta \geq 0 \quad (2.142)$$

$$\theta \geq \sum_{\forall t\in\mathcal{T}\omega\in\Omega} -\overline{e}^p \alpha^1_{tw} - \frac{b}{a}\sum_{\forall t\in\mathcal{T}\omega\in\Omega} \hat{S}^p_t \alpha^2_{tw} - M \sum_{\forall t\in\mathcal{T}\omega\in\Omega} \hat{S}^p_t \alpha^3_{tw}$$
$$+ \sum_{\forall i\in\mathcal{I},\forall t\in\mathcal{T}\omega\in\Omega} p^l_{it\omega}\beta_{itw} + \sum_{\forall i\in\mathcal{I},\forall t\in\mathcal{T}\omega\in\Omega} p^c_{it\omega}\delta^1_{tw} + \sum_{\forall i\in\mathcal{I},\forall t\in\mathcal{T}\omega\in\Omega} p^h_{it\omega}\delta^2_{tw}$$

$$
\begin{aligned}
&- \sum_{\forall t \in \mathcal{T} \omega \in \Omega} \overline{q}^{e+} \hat{S}_t^{e+} \theta_{tw}^3 + \sum_{\forall t \in \mathcal{T} \omega \in \Omega} \underline{q}^{e+} \hat{S}_t^{e+} \theta_{tw}^4 - \sum_{\forall t \in \mathcal{T} \omega \in \Omega} \overline{q}^{e-} \hat{S}_t^{e-} \theta_{tw}^5 \\
&\quad + \sum_{\forall t \in \mathcal{T} \omega \in \Omega} \underline{q}^{e-} \hat{S}_t^{e-} \theta_{tw}^6 - \sum_{\forall t \in \mathcal{T} \omega \in \Omega} \overline{q}^{e} \theta_{tw}^8 + \sum_{\forall t \in \mathcal{T} \omega \in \Omega} \underline{q}^{e} \theta_{tw}^9 \\
&- \sum_{\forall t \in \mathcal{T} \omega \in \Omega} \overline{q}^{b+} \hat{S}_t^{b+} \lambda_{tw}^3 + \sum_{\forall t \in \mathcal{T} \omega \in \Omega} \underline{q}^{b+} \hat{S}_t^{b+} \lambda_{tw}^4 - \sum_{\forall t \in \mathcal{T} \omega \in \Omega} \overline{q}^{b-} \hat{S}_t^{b-} \lambda_{tw}^5 \\
&\quad + \sum_{\forall t \in \mathcal{T} \omega \in \Omega} \underline{q}^{b-} \hat{S}_t^{b-} \lambda_{tw}^6 - \sum_{\forall t \in \mathcal{T} \omega \in \Omega} \overline{q}^{b} \lambda_{tw}^8 + \sum_{\forall t \in \mathcal{T} \omega \in \Omega} \underline{q}^{b} \lambda_{tw}^9 \\
&\qquad \forall (\alpha^l, \beta, \delta^l, \gamma l, \theta^l, \lambda^l) \in P_D
\end{aligned} \tag{2.143}
$$

These constraints are referred to as optimality cut constraints where P_D is the set of the extreme points in the feasible region of **[CCHP-SUB(D)]**. Thus, describing the Benders decomposition algorithm, let consider UB^n and LB^n as the upper and lower bound respectively of the original problem **[CCHP]** at iteration n. In each iteration, the solution of the master problem (z_{MP}^n) generates a lower bound for the original problem. Then, the following binary variables are fixed: $\hat{Z}_t^p, \hat{Z}_t^e, \hat{Z}_t^b, \hat{Y}_t^p, \hat{Y}_t^e, \hat{Y}_t^b, \hat{S}_t^p, \hat{S}_t^{e+}, \hat{S}_t^{e-}, \hat{S}_t^{b+}, \hat{S}_t^{b-}$ $\forall$ t in T obtained from the master problem **[CCHP-MP]**, and those values are used to solve the dual subproblem **[CCHP-SUB(D)]**. Lets denote the solution of the dual subproblem as (z_{SUB}^n). Thus, in iteration n, solving the dual subproblem **[CCHP-SUB(D)]** provides a new extreme point $p \in P_D$, and it is added to the master problem **[CCHP-MP]** by updating set P_D as $P_D^n = P_D^{n-1} \bigcup p$.

Let consider (z_{MAS}^n) = $\sum_{t \in \mathcal{T}} \left(\psi_t^p Z_t^p + \psi_t^e Z_t^e + \psi_t^b Z_t^b \right)$. Hence, the upper bound on the optimal solution value of the **[CCHP]** can be obtained from: UB^n = (z_{MAS}^n) + (z_{SUB}^n). At the end of each iteration, if the gap between the upper bound and the lower bound is below a given treshold value ϵ, the algorithm is terminated: otherwise P_D is updated by adding

an optimality cut in **[CCHP-MP]**. A pseudo-code of the general Benders decomposition is presented as follows in Table 2.2.

2.4.4 Enhancement Strategies for Benders Decomposition Algorithm

Computational efficiency for significant instances has an impact on the performance of the simple Benders decomposition algorithm, and its capability to converge in a reasonable amount of time [23]. Authors have proposed multiple techniques to improve the performance of the Benders decomposition algorithm [43]. This section will introduce some accelerating techniques to improve the computational performance in solving **[CCHP]**.

2.4.4.1 Simple Cuts:

1. For power generator unit, the number of times a PGU has started must be greater than or equal to the number of times that the PGU has shut down:

$$\sum_{\tau \leq t} Z_{\tau}^{p} \geq \sum_{\tau \leq t} Y_{\tau}^{p} \qquad \forall t \in \mathcal{T} \tag{2.144}$$

2. For thermal generation unit, the number of times the thermal storage unit has started must be greater than or equal to the number of times that the thermal storage unit has shut down:

$$\sum_{\tau \leq t} Z_{\tau}^{e} \geq \sum_{\tau \leq t} Y_{\tau}^{e} \qquad \forall t \in \mathcal{T} \tag{2.145}$$

3. For battery system, the number of times the battery system has started must be greater than or equal to the number of times that the battery system has shut down:

$$\sum_{\tau \leq t} Z_{\tau}^{b} \geq \sum_{\tau \leq t} Y_{\tau}^{b} \qquad \forall t \in \mathcal{T} \tag{2.146}$$

Table 2.2

Bender decomposition Algorithm

$UB^n \longleftarrow +\infty, LB^n \longleftarrow -\infty, n \longleftarrow 1, P_D \longleftarrow 0$
$terminate \longleftarrow$ **false**
while $(terminate =$ **false**$)$ **do**
Solve **[CCHP-MP]** to obtain $\{Z_t^p\}_{t\in T}, \{Z_t^e\}_{t\in T}, \left\{Z_t^b\right\}_{t\in T}, z_{MP}^n, z_{MAS}^n$
if $(z_{MP}^n > LB^n)$ **then**
$LB^n \longleftarrow z_{MP}^n$
end if
Set:
$\hat{Z}_t^p = Z_t^p : \forall t \in \mathcal{T}$
$\hat{Z}_t^e = Z_t^e : \forall t \in \mathcal{T}$
$\hat{Z}_t^b = Z_t^b : \forall t \in \mathcal{T}$
Solve **[CCHP-SUB(D)]** to obtain $(\alpha^l, \beta, \delta^l, \gamma l, \theta^l, \lambda^l) \in P_D$ and z_{SUB}^n
if $(z_{SUB}^n + z_{MAS}^n > UB^n)$ **then**
$UB^n \longleftarrow z_{SUB}^n + z_{MAS}^n$
end if
if $((UB^n - LB^n)/UB^n \leq \epsilon)$ **then**
$terminate \longleftarrow$ **true**
else
$P_D^{n+1} = P_D \bigcup \left\{\alpha^l, \beta, \delta^l, \gamma l, \theta^l, \lambda^l\right\}$
end if
$n \longleftarrow n + 1$
end while

4. It is impossible to discharge in thermal generation storage unit if no charging is previously made:

$$\sum_{\tau=1}^{t-1} S_{\tau}^{e+} \geq S_t^{e-} \qquad \forall t \in \mathcal{T} \tag{2.147}$$

5. It is impossible to discharge battery if no charging is previously made:

$$\sum_{\tau=1}^{t-1} S_{\tau}^{b+} \geq S_t^{b-} \qquad \forall t \in \mathcal{T} \tag{2.148}$$

The results of computational experiments showed that adding the above cuts reduced remarkably the number of iterations of the Benders algorithm. Furthermore, the numerical analysis showed that branching Z^p followed by Z^b and Z^e saves some CPU time in solving the problem.

2.4.4.2 Pareto-optimal cuts:

Cuts have significant impact in Benders decomposition algorithm. Stronger cuts influence in the convergence of the algorithm by reducing the number of iterations [65]. Pareto Optimal Cuts improves convergence of decomposition algorithm [71]. The pareto-optimal cut is obtained when the cut generated from an extreme point $(\alpha_1^l, \beta, \delta_1^l, \gamma l_1, \theta_1^l, \lambda_1^l)$ dominates the cut produced from another extreme point $(\alpha_2^l, \beta_2, \delta_2^l, \gamma l_2, \theta_2^l, \lambda_2^l)$, i.e.,

$$\begin{aligned}
&\sum_{\forall t\in\mathcal{T}\omega\in\Omega} -\overline{e}^p\alpha_{1tw}^1 - \frac{b}{a}\sum_{\forall t\in\mathcal{T}\omega\in\Omega} \hat{S}_t^p\alpha_{1tw}^2 - M\sum_{\forall t\in\mathcal{T}\omega\in\Omega} \hat{S}_t^p\alpha_{1tw}^3 \\
&+ \sum_{\forall i\in\mathcal{I},\forall t\in\mathcal{T}\omega\in\Omega} p_{it\omega}^l\beta_{1itw} + \sum_{\forall i\in\mathcal{I},\forall t\in\mathcal{T}\omega\in\Omega} p_{it\omega}^c\delta_{1tw}^1 + \sum_{\forall i\in\mathcal{I},\forall t\in\mathcal{T}\omega\in\Omega} p_{it\omega}^h\delta_{1tw}^2 \\
&- \sum_{\forall t\in\mathcal{T}\omega\in\Omega} \overline{q}^{e+}\hat{S}_t^{e+}\theta_{1tw}^3 + \sum_{\forall t\in\mathcal{T}\omega\in\Omega} \underline{q}^{e+}\hat{S}_t^{e+}\theta_{1tw}^4 - \sum_{\forall t\in\mathcal{T}\omega\in\Omega} \overline{q}^{e-}\hat{S}_t^{e-}\theta_{1tw}^5
\end{aligned}$$

$$
\begin{aligned}
&+\sum_{\forall t\in\mathcal{T}\omega\in\Omega}\underline{q}^{e-}\hat{S}_t^{e-}\theta_{1tw}^6-\sum_{\forall t\in\mathcal{T}\omega\in\Omega}\overline{q}^{e}\theta_{1tw}^8+\sum_{\forall t\in\mathcal{T}\omega\in\Omega}\underline{q}^{e}\theta_{1tw}^9\\
&-\sum_{\forall t\in\mathcal{T}\omega\in\Omega}\overline{q}^{b+}\hat{S}_t^{b+}\lambda_{1tw}^3+\sum_{\forall t\in\mathcal{T}\omega\in\Omega}\underline{q}^{b+}\hat{S}_t^{b+}\lambda_{1tw}^4-\sum_{\forall t\in\mathcal{T}\omega\in\Omega}\overline{q}^{b-}\hat{S}_t^{b-}\lambda_{1tw}^5\\
&+\sum_{\forall t\in\mathcal{T}\omega\in\Omega}\underline{q}^{b-}\hat{S}_t^{b-}\lambda_{1tw}^6-\sum_{\forall t\in\mathcal{T}\omega\in\Omega}\overline{q}^{b}\lambda_{1tw}^8+\sum_{\forall t\in\mathcal{T}\omega\in\Omega}\underline{q}^{b}\lambda_{1tw}^9\geq\sum_{\forall t\in\mathcal{T}\omega\in\Omega}\\
&-\overline{e}^{p}\alpha_{2tw}^1-\frac{b}{a}\sum_{\forall t\in\mathcal{T}\omega\in\Omega}\hat{S}_t^{p}\alpha_{2tw}^2-M\sum_{\forall t\in\mathcal{T}\omega\in\Omega}\hat{S}_t^{p}\alpha_{2tw}^3+\sum_{\forall i\in\mathcal{I},\forall t\in\mathcal{T}\omega\in\Omega}p_{it\omega}^{l}\beta_{2itw}\\
&+\sum_{\forall i\in\mathcal{I},\forall t\in\mathcal{T}\omega\in\Omega}p_{it\omega}^{c}\delta_{2tw}^1+\sum_{\forall i\in\mathcal{I},\forall t\in\mathcal{T}\omega\in\Omega}p_{it\omega}^{h}\delta_{2tw}^2-\sum_{\forall t\in\mathcal{T}\omega\in\Omega}\overline{q}^{e+}\hat{S}_t^{e+}\theta_{2tw}^3\\
&+\sum_{\forall t\in\mathcal{T}\omega\in\Omega}\underline{q}^{e+}\hat{S}_t^{e+}\theta_{2tw}^4-\sum_{\forall t\in\mathcal{T}\omega\in\Omega}\overline{q}^{e-}\hat{S}_t^{e-}\theta_{2tw}^5+\sum_{\forall t\in\mathcal{T}\omega\in\Omega}\underline{q}^{e-}\hat{S}_t^{e-}\theta_{2tw}^6\\
&-\sum_{\forall t\in\mathcal{T}\omega\in\Omega}\overline{q}^{e}\theta_{2tw}^8+\sum_{\forall t\in\mathcal{T}\omega\in\Omega}\underline{q}^{e}\theta_{2tw}^9-\sum_{\forall t\in\mathcal{T}\omega\in\Omega}\overline{q}^{b+}\hat{S}_t^{b+}\lambda_{2tw}^3\\
&+\sum_{\forall t\in\mathcal{T}\omega\in\Omega}\underline{q}^{b+}\hat{S}_t^{b+}\lambda_{2tw}^4-\sum_{\forall t\in\mathcal{T}\omega\in\Omega}\overline{q}^{b-}\hat{S}_t^{b-}\lambda_{2tw}^5+\sum_{\forall t\in\mathcal{T}\omega\in\Omega}\underline{q}^{b-}\hat{S}_t^{b-}\lambda_{2tw}^6\\
&-\sum_{\forall t\in\mathcal{T}\omega\in\Omega}\overline{q}^{b}\lambda_{2tw}^8+\sum_{\forall t\in\mathcal{T}\omega\in\Omega}\underline{q}^{b}\lambda_{2tw}^9
\end{aligned}
\tag{2.149}
$$

A pareto-optimal cut can be obtained by solving the following subproblem:

$$
\begin{aligned}
\textbf{[CCHP-SUB(D-MMW)]}\,Maximize\ &\sum_{\forall t\in\mathcal{T}\omega\in\Omega}-\overline{e}^{p}\alpha_{tw}^1-\frac{b}{a}\sum_{\forall t\in\mathcal{T}\omega\in\Omega}S_t^{p^0}\alpha_{tw}^2\\
&-M\sum_{\forall t\in\mathcal{T}\omega\in\Omega}S_t^{p^0}\alpha_{tw}^3+\sum_{\forall i\in\mathcal{I},\forall t\in\mathcal{T}\omega\in\Omega}p_{it\omega}^{l}\beta_{itw}+\sum_{\forall i\in\mathcal{I},\forall t\in\mathcal{T}\omega\in\Omega}p_{it\omega}^{c}\delta_{tw}^1\\
&+\sum_{\forall i\in\mathcal{I},\forall t\in\mathcal{T}\omega\in\Omega}p_{it\omega}^{h}\delta_{tw}^2-\sum_{\forall t\in\mathcal{T}\omega\in\Omega}\overline{q}^{e+}S_t^{e+^0}\theta_{tw}^3\\
&+\underline{q}^{e+}\sum_{\forall t\in\mathcal{T}\omega\in\Omega}S_t^{e+^0}\theta_{tw}^4-\overline{q}^{e-}\sum_{\forall t\in\mathcal{T}\omega\in\Omega}S_t^{e-^0}\theta_{tw}^5+\underline{q}^{e-}\sum_{\forall t\in\mathcal{T}\omega\in\Omega}S_t^{e-^0}\theta_{tw}^6\\
&-\overline{q}^{e}\sum_{\forall t\in\mathcal{T}\omega\in\Omega}\theta_{tw}^8+\underline{q}^{e}\sum_{\forall t\in\mathcal{T}\omega\in\Omega}\theta_{tw}^9-\overline{q}^{b+}\sum_{\forall t\in\mathcal{T}\omega\in\Omega}S_t^{b+^0}\lambda_{tw}^3\\
&+\underline{q}^{b+}\sum_{\forall t\in\mathcal{T}\omega\in\Omega}S_t^{b+^0}\lambda_{tw}^4-\overline{q}^{b-}\sum_{\forall t\in\mathcal{T}\omega\in\Omega}S_t^{b-^0}\lambda_{tw}^5+\underline{q}^{b-}\sum_{\forall t\in\mathcal{T}\omega\in\Omega}S_t^{b-^0}\lambda_{tw}^6\\
&-\overline{q}^{b}\sum_{\forall t\in\mathcal{T}\omega\in\Omega}\lambda_{tw}^8+\underline{q}^{b}\sum_{\forall t\in\mathcal{T}\omega\in\Omega}\lambda_{tw}^9
\end{aligned}
\tag{2.150}
$$

Subject to:

$$-\alpha^1_{t\omega} + \lambda^1_{t\omega} \leq \Delta t * \chi^+_t \qquad \forall t \in \mathcal{T}, \omega \in \Omega \quad (2.151)$$

$$-\frac{\alpha^2_{t\omega}}{a} - \alpha^3_{t\omega} + \eta^p \gamma^1_{t\omega} \leq \Delta t * \kappa^p_t \qquad \forall t \in \mathcal{T}, \omega \in \Omega \quad (2.152)$$

$$-\eta^b \gamma^1_{t\omega} \leq \Delta t * \kappa^b_t \qquad \forall t \in \mathcal{T}, \omega \in \Omega \quad (2.153)$$

$$\alpha^2_{t\omega} \leq -\Delta t * \chi^-_t \qquad \forall t \in \mathcal{T}, \omega \in \Omega \quad (2.154)$$

$$-\alpha^1_{t\omega} + \beta_{it\omega} \leq \Delta t * \chi^+_t \qquad \forall t \in \mathcal{T}, \omega \in \Omega \quad (2.155)$$

$$\alpha^2_{t\omega} - \lambda^1_{t\omega} \leq 0 \qquad \forall t \in \mathcal{T}, \omega \in \Omega \quad (2.156)$$

$$\alpha^2_{t\omega} + \beta_{it\omega} \leq 0 \qquad \forall t \in \mathcal{T}, \omega \in \Omega \quad (2.157)$$

$$\beta_{it\omega} + \lambda^2_{t\omega} \leq 0 \qquad \forall t \in \mathcal{T}, \omega \in \Omega \quad (2.158)$$

$$\gamma^1_{t\omega} - \eta^c \gamma^2_{t\omega} \leq 0 \qquad \forall t \in \mathcal{T}, \omega \in \Omega \quad (2.159)$$

$$-\gamma^1_{t\omega} - \eta^h \gamma^3_{t\omega} \leq 0 \qquad \forall t \in \mathcal{T}, \omega \in \Omega \quad (2.160)$$

$$-\gamma^1_{t\omega} + \theta^1_{t\omega} - \eta^e \theta^{10}_{t\omega} \leq 0 \qquad \forall t \in \mathcal{T}, \omega \in \Omega \quad (2.161)$$

$$\gamma^2_{t\omega} + \delta^1_{it\omega} \leq 0 \qquad \forall i \in \mathcal{I} \forall t \in \mathcal{T}, \omega \in \Omega \quad (2.162)$$

$$\gamma^3_{t\omega} + \delta^2_{it\omega} \leq 0 \qquad \forall i \in \mathcal{I} \forall t \in \mathcal{T}, \omega \in \Omega \quad (2.163)$$

$$-\eta^c \gamma^2_{t\omega} + \theta^2_{t\omega} - \theta^{10}_{t\omega} \leq 0 \qquad \forall t \in \mathcal{T}, \omega \in \Omega \quad (2.164)$$

$$-\eta^h \gamma^3_{t\omega} + \theta^2_{t\omega} - \theta^{10}_{t\omega} \leq 0 \qquad \forall t \in \mathcal{T}, \omega \in \Omega \quad (2.165)$$

$$-\theta^1_{t\omega} - \theta^3_{t\omega} + \theta^4_{t\omega} + \Delta t * \theta^7_{t\omega} \leq 0 \qquad \forall t \in \mathcal{T}, \omega \in \Omega \quad (2.166)$$

$$-\eta^e \theta^2_{t\omega} - \theta^5_{t\omega} + \theta^6_{t\omega} - \Delta t * \theta^7_{t\omega} \leq 0 \qquad \forall t \in \mathcal{T}, \omega \in \Omega \quad (2.167)$$

$$\frac{\lambda^1_{t\omega}}{\eta^{b+}} - \lambda^3_{t\omega} + \lambda^4_{t\omega} + \Delta t * \lambda^7_{t\omega} \leq 0 \qquad \forall t \in \mathcal{T}, \omega \in \Omega \quad (2.168)$$

$$-\theta^7_{t\omega} + \theta^7_{t+1,\omega} - \theta^8_{t\omega} + \theta^9_{t\omega} \leq 0 \qquad \forall t \in \mathcal{T}, \omega \in \Omega \qquad (2.169)$$

$$-\eta^{b-}\lambda^2_{t\omega} - \lambda^5_{t\omega} + \lambda^6_{t\omega} - \Delta t * \lambda^7_{t\omega} \leq 0 \qquad \forall t \in \mathcal{T}, \omega \in \Omega \qquad (2.170)$$

$$-\lambda^7_{t\omega} + \lambda^7_{t+1,\omega} - \lambda^8_{t\omega} + \lambda^9_{t\omega} \leq 0 \qquad \forall t \in \mathcal{T}, \omega \in \Omega \qquad (2.171)$$

$$\alpha^1_t, \alpha^3_t, \beta_{it}, \delta^l_{it}, \theta^1_t, \theta^3_t, \theta^4_t$$

$$, \theta^5_t, \theta^6_t, \theta^8_t, \theta^{10}_t, \lambda^3_t, \lambda^4_t, \lambda^5_t, \lambda^6_t \lambda^8_t, , \omega \in \mathcal{R}^+ \qquad (2.172)$$

$$\alpha^2_t, \gamma^l_t, \theta^2_t, \theta^7_t, \lambda^1_t, \lambda^2_t \lambda^7_t, \in \mathcal{R} \qquad (2.173)$$

In this formulation $S_t^{p^0}$, $S_t^{e+^0}$, $S_t^{e-^0}$, S^{b+^0}, and S^{b-^0} are core points (i.e. a point in the relative interior of the convex hull of a feasible region) used to generate a Pareto-optimal cut [65]. and the following equations were employed to generate approximate core points [84]:

$$\begin{aligned} S_t^{p^0} &= \tau S_t^{p^0} + (1-\tau)\hat{S}_t^p \\ S_t^{e+^0} &= \tau S_t^{e+^0} + (1-\tau)\hat{S}_t^{e+} \\ S_t^{e-^0} &= \tau S_t^{e-^0} + (1-\tau)\hat{S}_t^{e-} \\ S_t^{b+^0} &= \tau S_t^{b+^0} + (1-\tau)\hat{S}_t^{b+} \\ S_t^{b-^0} &= \tau S_t^{b-^0} + (1-\tau)\hat{S}_t^{b-} \end{aligned} \qquad (2.174)$$

$\forall t \in \mathcal{T}$. $\left\{\hat{S}_t^p\right\}_{t\in T}$, $\left\{\hat{S}_t^{e+}\right\}_{t\in T}$, $\left\{\hat{S}_t^{e-}\right\}_{t\in T}$, $\left\{\hat{S}_t^{b+}\right\}_{t\in T}$, $\left\{\hat{S}_t^{b-}\right\}_{t\in T}$ are generated from the master problem, and the best results are achieved by setting up τ = 0.5.

2.4.4.3 Multi-cuts:

Multicuts of Benders decomposition has been applied in different settings, the main idea is to cuts up the number of scenarios to be placed at once, so the master problem has to be modified [25, 105]. **[CCHP-SUB(D)]** can be descomposed into $|\Omega|$ independent dual problems (i.e. one subproblem for each scenario ω in Ω). Thus, it is added $|\Omega|$ numbers of cuts in each iteration of the Benders master problem **[CCHP-MP]**.

The revised master problem is as follows:

$$\textbf{[CCHP-MMP]}\ Minimize\ \sum_{t\in\mathcal{T}}\Big(\psi_t^p Z_t^p + \psi_t^e Z_t^e + \psi_t^b Z_t^b\Big) + \sum_{\omega\in\Omega}\rho_\omega\theta_\omega \tag{2.175}$$

Subject to

Constraints (53) to (73), and

$$\begin{aligned}\theta_\omega \geq \sum_{\omega\in\Omega} -\overline{e}^p\alpha_{tw}^1 - \frac{b}{a}\sum_{\omega\in\Omega}\hat{S}_t^p\alpha_{tw}^2 - M\sum_{\omega\in\Omega}\hat{S}_t^p\alpha_{tw}^3 + \sum_{\forall i\in\mathcal{I},\omega\in\Omega} p_{it\omega}^l\beta_{itw} \\ + \sum_{\forall i\in\mathcal{I},\omega\in\Omega} p_{it\omega}^c\delta_{tw}^1 + \sum_{\forall i\in\mathcal{I},\omega\in\Omega} p_{it\omega}^h\delta_{tw}^2 - \sum_{\omega\in\Omega}\overline{q}^{e+}\hat{S}_t^{e+}\theta_{tw}^3 + \sum_{\omega\in\Omega}\underline{q}^{e+}\hat{S}_t^{e+}\theta_{tw}^4 \\ - \sum_{\omega\in\Omega}\overline{q}^{e-}\hat{S}_t^{e-}\theta_{tw}^5 + \sum_{\omega\in\Omega}\underline{q}^{e-}\hat{S}_t^{e-}\theta_{tw}^6 - \sum_{\omega\in\Omega}\overline{q}^{e}\theta_{tw}^8 + \sum_{\omega\in\Omega}\underline{q}^{e}\theta_{tw}^9 \\ - \sum_{\omega\in\Omega}\overline{q}^{b+}\hat{S}_t^{b+}\lambda_{tw}^3 + \sum_{\omega\in\Omega}\underline{q}^{b+}\hat{S}_t^{b+}\lambda_{tw}^4 - \sum_{\omega\in\Omega}\overline{q}^{b-}\hat{S}_t^{b-}\lambda_{tw}^5 + \sum_{\omega\in\Omega}\underline{q}^{b-}\hat{S}_t^{b-}\lambda_{tw}^6 \\ - \sum_{\omega\in\Omega}\overline{q}^{b}\lambda_{tw}^8 + \sum_{\omega\in\Omega}\underline{q}^{b}\lambda_{tw}^9 \quad \forall t\in\mathcal{T}, \forall(\alpha^l,\beta,\delta^l,\gamma l,\theta^l,\lambda^l)\in P_D\end{aligned} \tag{2.176}$$

where P_D is the set of extreme points of the dual polyhedron P_D^ω associated with subproblem ω.

Then, **[CCHP-MMP]** considers multiple terms θ_ω, and cuts are defined for each scenario $\omega \in \Omega$. Thus, although with this strategy, it is expected fewer iterations to reach

optimality gap, it adds more variables and constraints, then, it potentially takes longer time to solve the problem [117].

2.5 Computational study and managerial insights:

In order to evaluate the performance of the proposed enhanced strategies for algorithms described in Section 3.4, a case study is developed and the data for the study is given in section 5.1 below. All the algorithms are coded with GAMS 24.4.6 [33] and run on a desktop computer with Intel Core i7-4790 @ 3.60 GHz processor and RAM 16.0 GB using an optimization solver ILOG CPLEX 12.6. In this section, we first describe in detail the data used. Then a computational study on model [CCHP] is conducted to evaluate the potential significant of the proposed enhanced strategies for algorithms and the corresponding results are depicted and managerial insights are drawn.

2.5.1 Data Description

Load demand of hourly electric and thermal energy for this section was obtained by a simulation using software Energy Plus. The premise is CCHP system shared by multi-building cluster. The step size of weights update and the decision time interval for this simulation are 0.01 and 1 hour respectively. Prices plan of electricity utilized in this research are taken from SRP (http://www.srpnet.com), a local electricity provider at Arizona. Other parameters values such as Fuel price ($/kWh) and Electricity sold back price ($/kWh) are 0.027 and 0.00367 respectively.

2.5.2 Experimental Results

We tested the model changing different capacities, pricing mechanisms, and levels of uncertainty.

2.5.2.1 Simulation under Different Power Grid Capacities

In this experiment, by setting the capacity of the power grid at 30kW, the model is run using data from summer and winter. The model finds optimal solutions, and the proposed CCHP system satisfies the demand. For different grid capacities in summer and winter, the comparison shows interesting managerial information via Figure 2.5, and Figure 2.6.

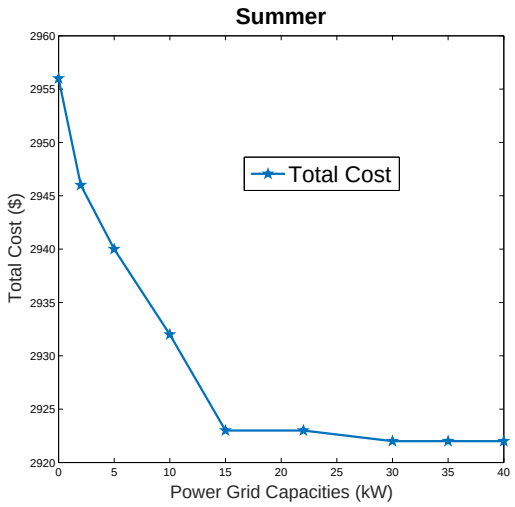

Figure 2.5

Total System Cost for different Power Grid Capacities

They reveal that when the power grid is disconnected (0 kW), the total cost of the system is high, and as soon as the power grid increases its capacity, the total cost drops as

expected. For summer data, the total cost decreases by 1% when the power grid capacity increases from 0Kw to 30Kw, while for winter, the total cost decreases by 3.8%.

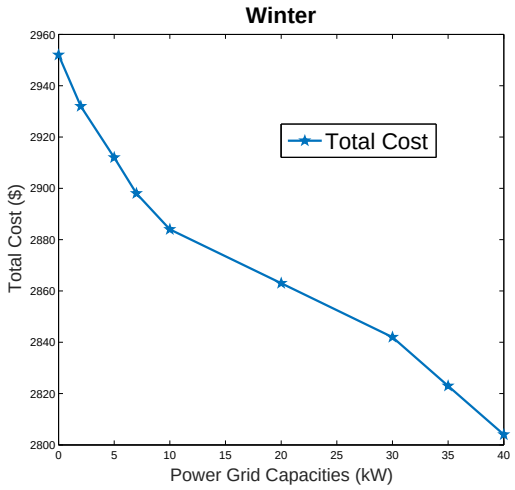

Figure 2.6

Total System Cost for different Power Grid Capacities

On the contrary, fig. 2.6 shows that with small power grid capacity, more fuel should be purchased to feed PGU to compensate for the shortfall of electricity which will result in the waste of excess thermal energy. It explains why the total cost of the system against the power grid capacities ranging from 0 KW to 5 KW did not fall drastically during winter.

2.5.2.2 Simulation under Different Storage Capacities

In order to investigate the performance of the CCHP model under different storage capacities (battery and thermal), the power grid size is set up at 15KW. The results are given in the following Figures and the decreasing trend in the total cost of the system is shown by line graphs in these figures.

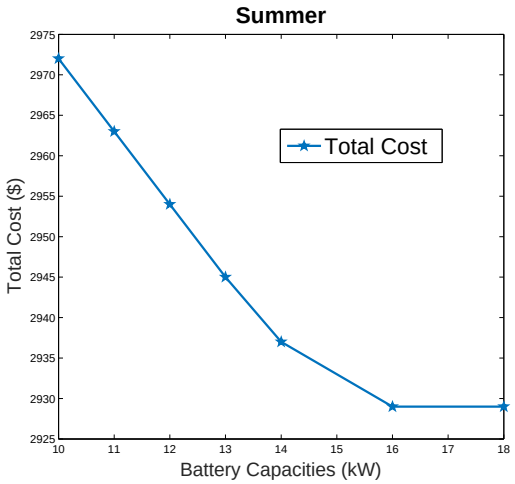

Figure 2.7

Data under different Battery Capacities

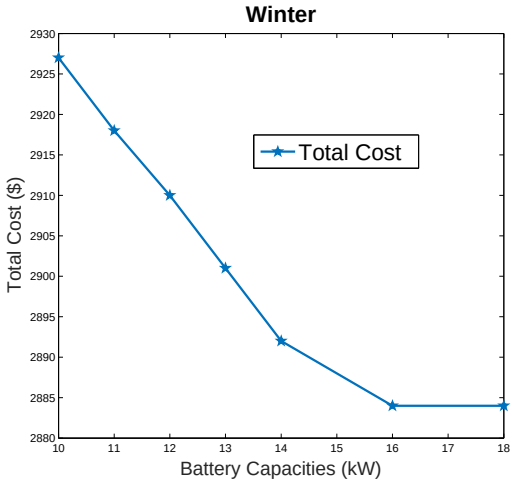

Figure 2.8

Data under different Battery Capacities

The line graphs in the Figure 2.9, Figure 2.10, Figure 2.9, and Figure 2.10 clearly show that the total cost of the system decreases as the storage capacity increases.

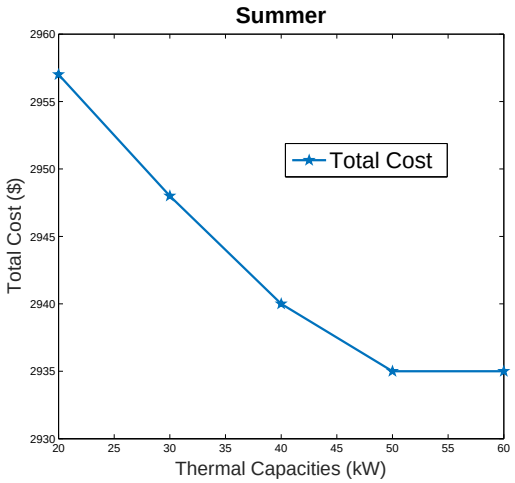

Figure 2.9

Data under different Thermal Capacities

Moreover, it can be observed that the total cost of the system does not vary as the battery capacity increases from 16KW to 18KW for both winter and summer data.

Figure 2.9, and Figure 2.10 shows that the total cost does not vary as the thermal capacity increases from 50KW to 60KW for summer data. For winter, while the thermal capacity reaches 40KW, the total cost keeps steady.

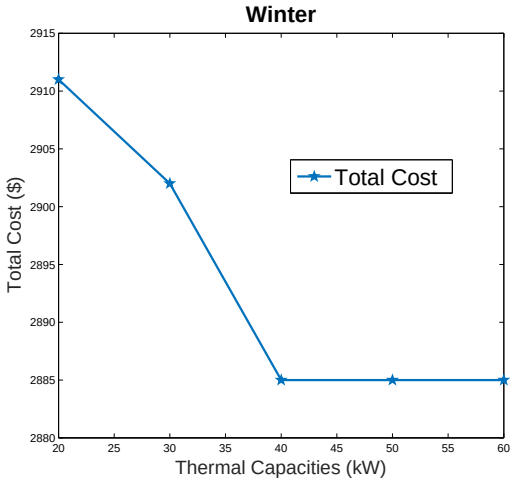

Figure 2.10

Data under different Thermal Capacities

2.5.2.3 Simulation under Different Pricing Mechanisms and Uncertainty Levels

The CCHP model evaluated under different pricing mechanisms and varying uncertainty levels are compared in this experiment. Different pricing mechanisms are used for electricity providers to motivate customers to use electricity in an eco-friendly way. Data used comes from a local electricity provider at Arizona [99]. It provides three plans: Basic, SRP EZ-3, and SRP Time of Use (TOU). The model assumes that decision makers choose plan price wisely.

Figure 2.11 shows that the SRP plan is more sensitive to uncertainty. Although the results can be considered intuitive, the model can assist the decision makers to choose the appropriate pricing mechanism for different levels of uncertainty.

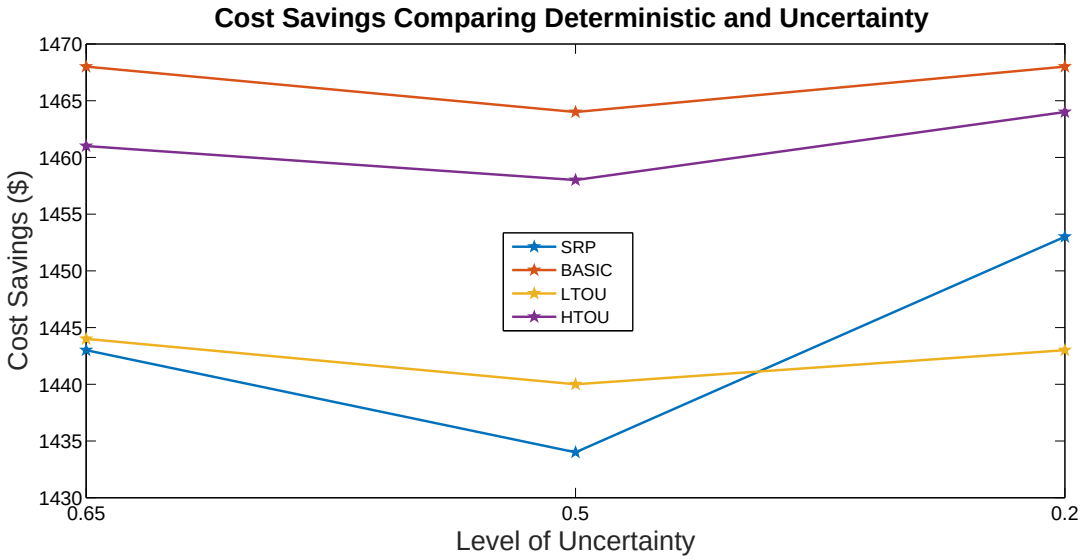

Figure 2.11

Different plan prices and Uncertainty Levels

2.5.2.4 Simulation under Different PGU Capacities

We aim to assess the model under different sizes of the PGU (PGU capacities). The following capacities 10Kw, 20Kw, 30Kw, 40Kw, and 50Kw are tested in this section. Figure 2.12, and Figure 2.13 show clearly that the total cost of the system decreases by 1.9% as the PGU capacity increases from 10KW to 30KW for winter data. In contrast, it is also consistent with summer data where the reduction in total cost is 1.14%.

Finally, it can be observed from Figure 2.12, and Figure 2.13 that the total cost of the system does not vary as the PGU capacity increases from 30KW to 50KW for both winter and summer data. That is, for both winter and summer, while the PGU capacity reaches 30KW, the total cost keeps steady. It provides managerial insights to decision-makers regarding sizing purposes for PGU capacity.

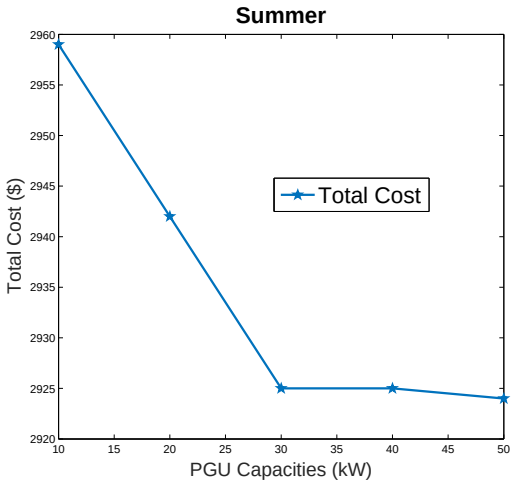

Figure 2.12

Data under different PGU capacities

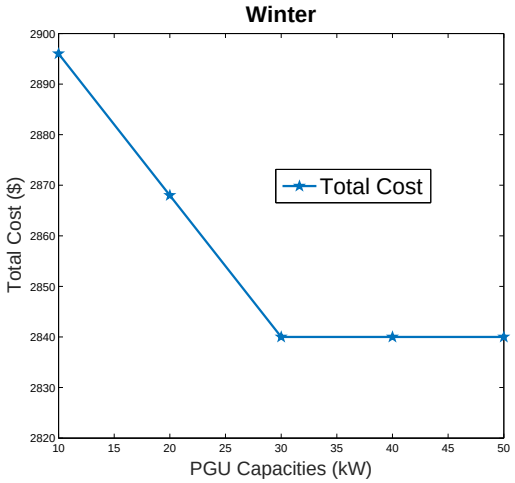

Figure 2.13

Data under different PGU capacities

2.5.3 Analyzing the Performance of Solution Algorithms

In order to evaluate the algorithms and proposed enhanced strategies, a computational study on the model **[CCHP]** is performed in this section. The following subsections describe the data set, present the results of the model **[CCHP]** under different parameters, and analyze the performance of the solution algorithms. This subsection explores the performance of the enhanced Benders strategies proposed. We choose the test with a number of buildings $\mathcal{I}$= $\{5, 10, 20\}$ for these experiments. The time is set up to $\mathcal{T}$= $\{288, 144\}$. Finally, the number of scenarios is set to Ω= $\{20, 30\}$. The enhanced algorithm strategies are set up to terminate when at least one of the following conditions is met: (a) the optimality gap (i.e., ϵ = —UB LB—/UB) falls below a threshold value ϵ = 0.01; or (b) the maximum time limit set up in 10,800 (in CPU seconds) is reached; or (c) the maximum number of iteration = 500 is reached. The size of the deterministic equivalent problem of model **[CCHP]** are presented in Table 2.3.

Table 2.3

Problem size of the test instances

Case	$\mathcal{I}$	$\mathcal{T}$	Binary Variables	Continuous Variables	Total Variables	No of Constraints
1	5	144	1584	4752	6336	6768
2	10	144	1584	6912	8496	6768
3	20	144	1584	11232	12816	13536
4	5	288	3168	9504	12672	13536
5	10	288	3168	13824	16992	13536
6	20	288	3168	22464	25632	13536

2.5.3.1 Performance of accelerated Benders techniques:

We examine the performance of three strategies: 1) [Benders + Pareto Cuts] described in 4.4.2 , 2) [Multi-cuts] describe in 4.4.3 , and 3) [All cuts] (pareto + muticuts). Table Table 2.4 and Table 2.5 report the performance of the proposed algorithms, and they shows that the "All cuts" and "Multi-cuts" strategies substantially improve the performance of the Benders decomposition algorithm. For instance, the average computational times for All cuts and Multi-cuts decrease by 95% and 70% respectively. It is observed that all the enhanced algorithms strategies solves problem instances in less 1% optimality gap within the specified time limit. Furthermore, algorithm strategy [All Cuts] drops the average optimality gap to 0.81% from 0.94% ($\mathcal{T} = 144$) and to 0.78% from 0.92% ($\mathcal{T} = 288$) provided by the [Benders + Pareto] algorithm.

Conversely, both the tables show clearly the impact of the number of scenarios coupled with the number of buildings. They lead to a significant increase in computational effort as ω and i increase. Hence the problem becomes larger and more challenge to solve it efficiently.

2.5.3.2 Enhancement Strategies for Sample Average Approximation (SAA) Algorithm

Evaluating **[CCHP-MP]** by the Sample Average Approximation (SAA), as a two-stage stochastic linear programming, the solution involves to define the number of scenarios Ω, and it is crucial. The problem has to consider a fair large number of scenarios. However, since the **[CCHP-MP]** problem considers to many components (i.e. battery, thermal stor-

Table 2.4

Comparison of Different accelerated Benders strategies T = 144

I	ω	**Benders + Pareto**			**Multicuts**			**All Cuts**		
		Gap (%)	CPU (sec)	Iter	Gap (%)	CPU (sec)	Iter	Gap (%)	CPU (sec)	Iter
5	20	0.93	747.00	48	0.90	75.5	49	0.60	**10.00**	29
	30	0.96	831.77	46	0.92	76.7	50	0.83	**15.00**	39
10	20	0.91	989.66	35	0.78	92.5	49	0.83	**39.52**	29
	30	0.93	1240.53	41	0.88	98.0	49	0.83	**54.20**	38
20	20	0.99	1258.90	148	0.99	91.3	69	0.83	**52.40**	31
	30	0.91	1358.60	147	0.97	94.7	74	0.83	**43.08**	49
Avergage		0.94	1071.07	77.5	0.91	88.17	56.7	0.81	**35.70**	36

Table 2.5

Comparison of Different accelerated Benders strategies T = 288

I	ω	**Benders + Pareto**			**Multicuts**			**All Cuts**		
		Gap (%)	CPU (sec)	Iter	Gap (%)	CPU (sec)	Iter	Gap (%)	CPU (sec)	Iter
5	20	0.91	290.19	293	0.90	106.27	121	0.71	**18.31**	21
	30	0.90	312.68	200	095	106.25	103	0.73	**16.55**	27
10	20	0.93	1398.10	298	0.95	370.51	145	0.82	**71.79**	33
	30	0.95	1871.90	293	0.90	419.37	167	0.80	**75.99**	40
20	20	0.90	1562.23	310	0.90	524.95	180	0.81	**78.67**	49
	30	0.93	1871.90	299	0.81	612.94	220	0.83	**83.02**	43
Avergage		0.92	1217.83	282	0.90	356.72	156	0.78	**57.39**	36

age, boiler) along with many constraints,the MILP problem becomes significant even by considering a fewer number of scenarios.

Critical observation in the **[CCHP-MP]** problem is that the subproblem of the SAA is amenable of being solved by an accelerated Benders decomposition algorithm. It achieves its optimal solution if the subproblem iteratively. adjusts its values. SMILP has achieved efficiency and robustness with large number of scenarios coupling SAA with Benders decomposition algorithm [23] [91].

2.5.3.3 Performance of SAA with accelerated Benders technique:

A Comparative study on the computational time (CPU time) for solving SAA using CPLEX MIP solver and the SAA with the accelerated Benders decomposition including all cuts are depicted by line graphs in Figure 2.14. It shows clearly how the SAA with the accelerated Benders outperforms consistently as the number of scenarios increase.

2.5.3.4 Quality of stochastic solutions

The difference between the stochastic programming model and a deterministic optimization problem is assessed in this sub-section. The solutions obtained from two approaches (deterministic and stochastic) are reported in Table 5. It is evident that the stochastic solution is more resilient to the variability of the problem parameters. It can easily be seen from Table 2.6 that as compared to deterministic approach, the stochastic approach finds much better or at least not worse solutions to the stochastic programming model. Indeed, the results show that stochastic model gets better optimality gap comparing to the deterministic approach.

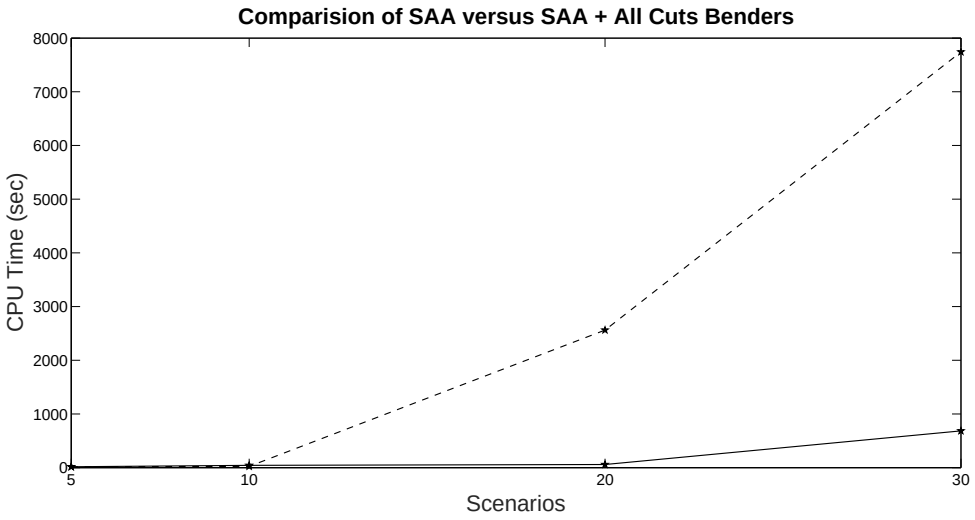

Figure 2.14

CPU seconds versus sample size

Table 2.6

Comparison Deterministic and Stochastic Approaches

I	T	**Deterministic Solution**		**Sample Averaged Algorithm**	
		Gap (%)	Total Cost ($)	Gap (%)	Total Cost ($)
5	288	1.07	3457.12	0.89	3458.12
10	288	1.59	4361.35	0.68	3460.24
20	288	1.72	6178.91	0.46	3463.46

2.6 Conclusions:

CCHP technology is part of the new landscape of emerging techniques of energy generation to achieve significant saving in costs and sustainability in our competitive world. CCHP provides an alternative path for decreasing the impact of power outages and also provides power reliability. In order to make a robust model, uncertainty considering a larger number of scenarios must be incorporated. However, to the best of our knowledge, limited literature exists on CCHP operation with enhanced methodologies to reduce computational complexity to solve large complex energy systems. In this paper, a two-stage stochastic programming model is proposed as an operational decision model to study a scalable stochastic decision model for a large scale micro-grid operation. In order to find an optimal solution for larger instances efficiently, the enhanced algorithm strategies for Benders decomposition are introduced. The experiments of operational strategy under different power grid capacities show a framework decision model for the decision-makers considering power grid fluctuations even power outages. The model with dynamic pricing mechanism with various levels of uncertainty can assist the decision makers to choose the appropriate pricing mechanism (i.e. an optimal pricing plan) for different levels of uncertainty. Assessment of the model under different sizes of the PGU (PGU capacities) provides managerial insights to decision-makers regarding sizing purposes for PGU capacity. Future research might be carried out in investigating the performance of the CCHP renewable energy technology, incorporating solar and wind energies to improve energy savings, and add electrical vehicles as an important component of multiple buildings. We intend to devote ourselves in this direction of future research.

CHAPTER 3

A CHANCE-CONSTRAINED STOCHASTIC MODEL FOR MICROGRID OPERATIONS UNDER UNCERTAINTY

3.1 Introduction

For several years, electricity has been produced and provided by a centralized power grid system, with a well-developed and complex network of power plants, transmission lines, big transformers, substations, and distribution lines. The U.S. Energy Information Administration (EIA) estimated a trend of electricity demand that grows by 29% (0.9%/year), from 3,826 billion kilowatt-hours (kWh) in 2012 to 4,954 billion kWh in 2040 [107]. Due to a number of recent incidents (e.g., 2003 U.S. Northeast blackout, 2005 Hurricane Katrina, 2008 China and 2009 Haiti Earthquakes) [75, 82, 110], it is evident that the power grid is vulnerable to a number of natural or human-made disasters. Thus, an alternative way to supply electricity has been a major concern for the last few decades. Efficiency and reliability of any power generator and distribution network are crucial for the energy industry. Further, ensuring that these networks are cost-efficient is a challenging task due to several factors. For instance, there is a significant long-term investment in operations and equipment. Therefore, new technologies, such as photo-voltaic arrays, micro-turbines, fuel cells, and combined heat and power (CHP), have created new forms of energy sources and thus provided a new landscape for electricity generation and distri-

bution network. Among them, microgrid is an excellent alternative to having local power grid with control capability that can be disconnected from the traditional grid and operate autonomously [54]. It also enables the integration of traditional generation sources, renewable sources of energy (e.g., solar or wind generation), distributed storage resources, and demand response.

Although a microgrid provides several advantages, its operation is challenging due to the interplay of multiple uncertainties (e.g., electricity demand and availability) and the unstable and uncertain renewable resource availability and its uncontrollable behavior. This adds more complexity in modeling renewable resources in microgrid. Indeed, part of its complexity is the fact that forcing to curtail renewable resources generation is becoming more widespread as the penetration of solar and wind energy alternative is expanding in the country [76]. This curtailment necessity generates two negative impacts. First, it affects the long-term revenues expected, and second, it might be increasing the greenhouse emission as results of compensating the curtailment with energy from fuel-based sources. Therefore, developing robust and reliable decision support models that can help decision makers of microgrid operators that deal with a broad range of scenarios, while considering the variability of renewable energy of microgrid is needed.

3.2 Literature Review

Microgrids have unique characteristics. Current literature defines a microgrid as a small cluster of distributed energy sources (close to the end users) such as distributed generators, solar power, wind power, storage components, and loads within a defined boundaries [100],

[48]. Microgrids operate controlled and coordinated fashion, either connected to the main power grid or in an islanded way [47]. They further have the capability to export electricity in the main grid. By having an on-site generation, microgrid operation mainly involves making *unit commitment* and *economic dispatch* decisions [60].

In recent years, research in microgrid has focused on optimization through minimizing the total system cost (economic and environmental) where the problem is formulated as a mixed-integer linear program (MILP) [73], [86], [80], [52], [104], [24], [10]. Essentially, focus is laid on three major categories: modeling, planning, and energy management. First, for modeling purposes, studies emphasize primary movers (e.g., steam turbines, fuel cells, combustion turbines), storage systems, renewable energy sources, and demand loads [21]. For instance, Buoro et al. [16] present a multi-objective optimization model considering a complex energy system composed of CHP units, solar thermal modules, and heating network. Second, for planning issues, studies focus on performance indicators such as energy savings and environmental impact. As an illustration, Bracco et al. [15] propose a mixed-integer linear programming model that focus on a system composed of buildings with different energy network configurations and aim to minimize a multi-objective function where capital and operating costs [85], as well as CO_2 emissions, are taken into consideration. Furthermore, the authors emphasize robust techniques for sizing the components of the microgrid. Finally, for energy management, studies include optimization techniques to optimally allocate the different energy resources to meet demand and operational objectives such as cost, performance, and emissions [36], [72]. For instance, Deng et al. [26] develop a 24-hour dispatching scheme for a microgrid as an off-line optimization model where the

objective is to minimize both economic and environmental costs. The model proposed by the authors consider various distributed resources in the microgrid while meeting the electricity and heat load of the customers. A multi-objective optimization model is presented where economic costs and emissions level are taken into consideration.

Due to the complexity in integrating renewable resources in microgrid operations (i.e., random and intermittent characteristics of renewable energies), researchers have assumed that there exists perfect knowledge of the net energy profile (i.e., known loads) [88]. To represent a more realistic case, stochastic nature of the renewable resources as well as their systematic integration to the microgrids need to be captured via developing a robust optimization model. Among many techniques, chance-constrained programming (CCP) can be employed to serve this purpose. Chance-constrained programming has been applied to approach many power system problems [70], [101]. For instance, Ozturk et al. [81] introduce chance-constrains to ensure that the load for an unit commitment problem is satisfied above a threshold value. Zhu et al. [124] add chance-constraints in an economic dispatch model to ensure that the utilization of wind power, which possess high variability, is utilized above a threshold value. Different from these studies, Wang et al. [113] and Zhao et al. [121] develop an optimization model that includes both the two-stage stochastic program and the chance-constrained stochastic program features. More specifically, Wang et al. [113] generate policies using two-stage chance-constraint to ensure reliable utilization of wind power output in an unit commitment problem. Zhao et al. [121] propose an expected value and chance-constrained stochastic optimization approach for the same unit commitment problem under uncertain wind power output. Our work, although related, is different from

the literatures discussed above in the sense that we develop a chance-constrained two-stage stochastic programming model that ensures system reliability by utilizing renewable resources above a threshold value while simultaneously minimizing microgrid operational cost under electricity demand uncertainty.

3.2.1 Research scope and contributions

The major contributions of this study to the literature are summarized as follows:

1. Propose a scalable chance-constrained two-stage stochastic programming model to ensure that, with high probability, a large portion of the renewable energy output at each operating hour will be utilized while simultaneously minimize the microgrid operational cost under electricity demand uncertainty. Three different policies are integrated into the two-stage stochastic programming model formulation through chance-constraints to ensure that the utilization of renewable energy (i.e., solar) is high in the microgrid operations.

2. Develop a combined Sample Average Approximation algorithm to provide high quality feasible solutions for solving the proposed chance-constrained two-stage stochastic programming model formulation in a reasonable amount of time.

3. Develop a real life case study using data from a *medium size medical college* in San Francisco. Investigate the impact of solar panels and the optimal energy sizing for fuel based generators and distributed energy storage on microgrid under different scenarios, including the failure of the main grid. Finally, the impact of different risk level is quantified on microgrid system performance.

The remainder of this paper is organized as follows. Section 3.3 describes the problem and introduces the chance-constraint two-stage stochastic programming model formulation. Section 3.4 introduces the combined Sample Average Approximation algorithm to solve the chance-constraint two-stage stochastic programming model formulation. Section 3.5 provides a detailed case study and compares the numerical results under various operational conditions. It provides an analysis the performance of the algorithm. Section 3.6 concludes this paper and discusses future research directions.

3.3 Problem Description and Model Formulation

The following subsections will describe the microgrid system structure and the model mathematical formulation.

3.3.1 Microgrid System Structure

We consider a microgrid that is composed of a set of conventional Fuel Based Generating (FBG) units ($\mathcal{I}$), Distributed Energy Storage (DES) facilities ($\mathcal{J}$), renewable energy resources ($\mathcal{L}$), and buildings ($\mathcal{K}$) with uncertain loads (see Figure 3.1). The microgrid is assumed to be operated in the grid-connected mode i.e., the microgrid can purchase electricity from the external utility grid when needed and sell in case of an electricity surplus. Let $\mathcal{T}$ be the set of time periods. We denote ψ_{it} and ζ_{it} be the startup and shutdown cost of turning a generator on and off at time period $t \in \mathcal{T}$. Furthermore, ϕ_{it} and a_i are the sunk cost of maintaining and running the generator $i \in \mathcal{I}$ at a minimum cost, respectively. For each generator $i \in \mathcal{I}$ with capacity c_{it}^{cap} in time period $t \in \mathcal{T}$, the maximum and minimum electricity output is denoted by $\overline{p}_i$ and $\underline{p}_i$, respectively.

The energy storage feature enables microgrid to operate based on a non-carbon-emitting resource and provide smooth intermittent power flow that allows distributed generation to synchronize with or without the presence of the external electricity grid. Furthermore, the integration of renewable energy resources not only provide an alternative energy sources for the microgrid system but also allow significant cost savings for the facilities. The energy deficiency, as well as the excess amount of energy of the local load, can be accommodated by trading with the main grid through the Point of Common Coupling (PCC) [106]. The microgrid is assumed to be a price-taker in the electricity market. During the time slots when the local power generation is surplus, the microgrid would sell its power to the main grid. We define c_t^- as the unit market selling price in time $t \in \mathcal{T}$. In contrast, if the local energy generation is not sufficient to meet its local load, the microgrid can import electricity from outside of the power grid for the unmet demand by paying an unit penalty cost π_t. We denote c_t^+ as the unit electricity purchasing cost in a given time period $t \in \mathcal{T}$.

The demand of the microgrid system is modeled as a random variable of which the probability distribution may not be known in advance. Accurate prediction of small-scale requirements is difficult to obtain due to the nature of the system components and the availability of resources on hand. To handle this uncertainty, we consider a fixed number of scenarios $|\Omega|$ where each scenario $\omega \in \Omega$ is associated with a positive probability ρ_ω ($\rho_\omega \geq 0$). We then define $d_{kt\omega}$ as the amount of electricity demand in building $k \in \mathcal{K}$ at time $t \in \mathcal{T}$ under scenario $\omega \in \Omega$. The next section summarizes all the necessary notation and our efforts in modeling a mathematical programming model for the microgrid operations subject to uncertain electricity demand.

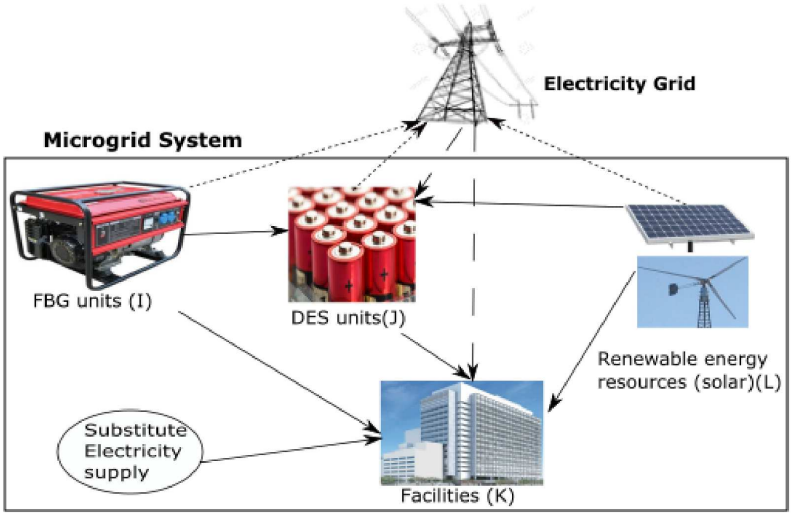

Figure 3.1

A network illustration of Microgrid system

3.3.2 Model Formulation

This section introduces a chance-constrained two-stage stochastic programming model formulation for the MG operations under uncertain electricity demand. The model considers an integrated scheduling scheme with multiple power supply sources a power grid, a number of conventional FBG units, several DES units, and renewable energy resources (i.e., solar PV panels) in order to satisfy the electricity demand. In order to discuss how we handle the model components, the following notation is introduced in Table 3.1 and Table 3.2:

We now introduce the following first and second-stage decision variables for our chance-constrained two-stage stochastic programming model formulation. The first-stage decision variables $\mathbf{U} := \{U_{it}\}_{i\in\mathcal{I},t\in\mathcal{T}}$, $\mathbf{Z} := \{Z_{it}\}_{i\in\mathcal{I},t\in\mathcal{T}}$, and $\mathbf{Y} := \{Y_{it}\}_{i\in\mathcal{I},t\in\mathcal{T}}$ determine timing

Table 3.1

Description of the sets and parameters

Symbol	Description
Sets	
$\mathcal{I}$	set of fuel based generating (FBG) units
$\mathcal{J}$	set of distributed energy storage (DES) units
$\mathcal{K}$	set of facility locations
$\mathcal{L}$	set of renewable energy resources (e.g., solar, wind)
$\mathcal{M}$	set of segment in linearized functions
$\mathcal{T}$	set of time periods
Ω	Set of scenarios
Parameters	
ψ_{it}	startup cost for FBG unit $i \in \mathcal{I}$ in time $t \in \mathcal{T}$
ζ_{it}	shutdown cost for FBG unit $i \in \mathcal{I}$ in time $t \in \mathcal{T}$
η_{im}	length of segment $m \in \mathcal{M}$ for FBG unit $i \in \mathcal{I}$
$\overline{p}_i$	maximum power generated by FBG unit $i \in \mathcal{I}$
$\underline{p}_i$	minimum power generated by FBG unit $i \in \mathcal{I}$
λ_{imt}	unit cost for segment $m \in \mathcal{M}$ of FBG unit $i \in \mathcal{I}$ in time $t \in \mathcal{T}$
c_{it}^{cap}	capacity of FBG unit $i \in \mathcal{I}$ in time $t \in \mathcal{T}$
β_{it}	initial power generation state for FBG unit $i \in \mathcal{I}$ in time $t \in \mathcal{T}$
ϕ_{it}	not load cost (fixed cost) for FBG unit $i \in \mathcal{I}$ in time $t \in \mathcal{T}$
α_i	cost of running at a minimum capacity of FBG unit $i \in \mathcal{I}$
$\overline{q}^{b+}$	maximum DES charging rate
$\underline{q}^{b+}$	minimum DES charging rate
$\overline{q}^{b-}$	maximum DES discharging rate
$\underline{q}^{b-}$	minimum DES discharging rate
$\overline{q}^{b}$	maximum DES stored energy
$\underline{q}^{b}$	minimum DES stored energy
s_t	availability of solar energy at time $t \in \mathcal{T}$
h_t	power availability in grid at time $t \in \mathcal{T}$
$d_{kt\omega}$	load for facility $k \in \mathcal{K}$ in time period $t \in \mathcal{T}$ under scenario $\omega \in \Omega$
c_t^+	unit electricity purchasing cost at time $t \in \mathcal{T}$
c_t^-	unit electricity selling cost at time $t \in \mathcal{T}$
π_t	penalty cost at time $t \in \mathcal{T}$

Table 3.2

Description of the Decision Variables

Symbol	Description
U_{it}	1 if commitment of FBG unit i is operational at time t; 0 otherwise
Z_{it}	1 if the startup state indicator for FBG unit i is on at time t; 0 otherwise
Y_{it}	1 if the shutdown state indicator for FBG unit i is on at time t; 0 otherwise
S^{+}_{jt}	0/1 denote the state of charging (on/off) for DES j in time t
S^{-}_{jt}	0/1 denote the state of discharging (on/off) for DES j time t
$P_{it\omega}$	amount of electricity generated from FBG unit i time t scenario ω
$\Delta_{imt\omega}$	amount of output on segment $m \in \mathcal{M}$ at FBG unit i time t scenario ω
$E^{+}_{jt\omega}$	amount of energy charged at DES j time t scenario ω
$E^{-}_{jt\omega}$	amount of energy discharging at DES j time t scenario ω
$X^{+}_{jt\omega}$	amount of energy from power grid to DES j time t scenario ω
$X_{kt\omega}$	amount of energy from power grid to facilities k time t scenario ω
$X_{ikt\omega}$	amount of energy from FBG i to facility k time $t \in \mathcal{T}$ scenario ω
$X_{it\omega}$	amount of energy from FBG i to power grid time t scenario ω
$X_{ijt\omega}$	amount of energy from FBG i to DES j time t scenario ω
$X^{-}_{jt\omega}$	amount of energy from DES j to power grid in time t scenario ω
$X_{jkt\omega}$	amount of energy from DES j to facility k in time $t \in \mathcal{T}$ scenario ω
$X_{lkt\omega}$	amount of energy from renewable resources to facility k time t scenario ω
$X_{lt\omega}$	amount of energy from renewable resources to power grid time t scenario ω
$X_{ljt\omega}$	amount of energy from renewable resources to DES j time t scenario ω
$Q_{jt\omega}$	amount of energy stored at DES j time t scenario ω
$V_{kt\omega}$	amount of energy unmet at facility k time $t \in \mathcal{T}$ scenario ω

for commitment of operational, startup and shutdown of FBG units in a given time period t, i.e.,

$$U_{it} = \begin{cases} 1 & \text{if commitment of FBG unit } i \text{ is operational at time period } t \\ 0 & \text{otherwise;} \end{cases}$$

$$Z_{it} = \begin{cases} 1 & \text{if the startup state indicator for FBG unit } i \text{ is on at time period } t \\ 0 & \text{otherwise;} \end{cases}$$

$$Y_{it} = \begin{cases} 1 & \text{if the shutdown state indicator for FBG unit } i \text{ is on at time period } t \\ 0 & \text{otherwise;} \end{cases}$$

The other first stage decision variables $\mathbf{S} := \{S^+_{jt}\}_{j\in\mathcal{J},t\in\mathcal{T}}$ and $\mathbf{S} := \{S^-_{jt}\}_{j\in\mathcal{J},t\in\mathcal{T}}$ determine timing for state of charging and discharging of DES units in a given time period t, i.e.,

$$S^+_{jt} = \begin{cases} 1 & \text{if the state of charging DES unit } j \text{ is on at time period } t \\ 0 & \text{otherwise;} \end{cases}$$

$$S^-_{jt} = \begin{cases} 1 & \text{if the state of discharging DES unit } j \text{ is on at time period } t \\ 0 & \text{otherwise;} \end{cases}$$

The second-stage decision variables determine: $X_{it\omega}$ the amount of power sold from FBG to the power grid in time $t \in \mathcal{T}$ and under scenario $\omega \in \Omega$; $X^-_{jt\omega}$ the amount of power delivered from DES $j \in \mathcal{J}$ to power grid in time $t \in \mathcal{T}$ under scenario $\omega \in \Omega$; $X_{lt\omega}$ the amount of renewable energy resource $l \in \mathcal{L}$ to power grid in time $t \in \mathcal{T}$ under scenario $\omega \in \Omega$; $X_{kt\omega}$ the amount of electricity purchased from the power grid to facility $k \in \mathcal{K}$

in time $t \in \mathcal{T}$ under scenario $\omega \in \Omega$; and $X^{+}_{jt\omega}$ the amount of electricity purchased from the power grid to the DES $j \in \mathcal{J}$ in time $t \in \mathcal{T}$ under scenario $\omega \in \Omega$. The amount of electricity generation at FBG unit $i \in \mathcal{I}$ at time period $t \in \mathcal{T}$ is denoted as $P_{it\omega}$ and amount of output on segment $m \in \mathcal{M}$ at FBG unit $i \in \mathcal{I}$ at time $t \in \mathcal{T}$ under scenario $\omega \in \Omega$ is denoted as $\Delta_{imt\omega}$. The amount of energy charged at DES unit $j \in \mathcal{J}$ at time $t \in \mathcal{T}$ denoted by $E^{+}_{jt\omega}$ and discharged at DES unit $j \in \mathcal{J}$ at time $t \in \mathcal{T}$ denoted by $E^{-}_{jt\omega}$. We further denote $X_{ikt\omega}$ as the amount of energy from FBG $i \in \mathcal{I}$ to facility $k \in \mathcal{K}$ in time period $t \in \mathcal{T}$ under scenario $\omega \in \Omega$; $X_{ijt\omega}$ as the amount of energy from FBG $i \in \mathcal{I}$ to DES unit $j \in \mathcal{J}$ in time period $t \in \mathcal{T}$ under scenario $\omega \in \Omega$; $X_{jkt\omega}$ as the amount of energy from DES $j \in \mathcal{J}$ to facility $k \in \mathcal{K}$ in time period $t \in \mathcal{T}$ under scenario $\omega \in \Omega$; $X_{lkt\omega}$ as the amount of energy from renewable energy resources $l \in \mathcal{L}$ to facility $k \in \mathcal{K}$ in time period $t \in \mathcal{T}$ under scenario $\omega \in \Omega$; $X_{ljt\omega}$ as the amount of energy from renewable energy resources $l \in \mathcal{L}$ to DES $j \in \mathcal{J}$ in time period $t \in \mathcal{T}$ under scenario $\omega \in \Omega$; $Q_{jt\omega}$ as the amount of energy stored at DES $j \in \mathcal{J}$ in time period $t \in \mathcal{T}$ under scenario $\omega \in \Omega$; and finally, $V_{kt\omega}$ as the amount of energy shortage at facility $k \in \mathcal{K}$ in time period $t \in \mathcal{T}$ under scenario $\omega \in \Omega$. For notational convenience, all the variables associated with X, E, V, P, and Q are denoted by set **X**, **E**, **V**, **P**, and **Q**, respectively.

Given that the electricity demand is uncertain, the model adds chance-constraints that force the usage of renewable energy resources to some extent. Furthermore, the variation of solar energy generation is high which impacts the design and operation of microgrid management. As discussed in Section 3.2, the amount of electricity can be adjusted without a significant loss in FBG, but any curtailment of solar generation during the operation

produce a great loss since its power generation cost is zero. This indicates that these resources should be utilized with the probability of at least $(1-\epsilon)$ where ϵ is a confidence parameter chosen by the decision maker, typically near zero e.g., ϵ=0.01 or 0.05.

The objective of our model is to minimize the first-stage and the expected value of the random second-stage costs. The decisions taken at the first stage correspond to the planning and scheduling time ahead of the energy generation from both the conventional electricity (i.e., from the grid) and distributed energy resources (e.g., startup, shutdown, and commitment statuses). These decisions must be made prior to the uncertainties, such as demand load and renewable resources, are realized. The recourse decisions include the power dispatch of all energy generating units, the real-time power delivery between the microgrid and the main grid at the second-stage. These depend on the first-stage decisions, and they are made after the uncertainties are unveiled and pertain to the real-time operation. With this, we are now ready to formulate the chance-constrained two-stage stochastic programming model **[MG]** as follows:

$$\begin{aligned}\textbf{[MG]}\ Minimize_{\mathbf{Z,Y,U,X,V}}\ & \sum_{t\in\mathcal{T}}\Big(\sum_{i\in\mathcal{I}}(\psi_{it}Z_{it}+\zeta_{it}Y_{it}+\phi_{it}U_{it})+\\ & \sum_{\omega\in\Omega}\rho_w\Delta t\Big(\sum_{i\in\mathcal{I},m\in\mathcal{M}}C\left(P_{it}\right)+\sum_{j\in\mathcal{J}}c_t^+X_{jt\omega}^+ +\sum_{k\in\mathcal{K}}c_t^+X_{kt\omega}\\ & -\sum_{i\in\mathcal{I}}c_t^-X_{it\omega}-\sum_{j\in\mathcal{J}}c_t^-X_{jt\omega}^- -\sum_{l\in\mathcal{L}}c_t^-X_{lt\omega}+\sum_{k\in\mathcal{K}}\pi_tV_{kt\omega}\Big)\Big)\end{aligned} \tag{3.1}$$

In **[MG]**, the first three terms of the objective function minimizes the total startup, shutdown, and no load cost of the FBG units. The fourth term represents the operation costs for the FBG units. The fifth and sixth term of the objective function represent the cost of pur-

chasing electricity from the external electricity grid. The following three terms represent the revenue obtained by selling electricity to the external grid from FBG units, DES unit, and renewable energy resources, respectively. The last term of the objective function is the penalty cost of electricity demand shortage. This penalty cost implies that if the cost of getting electricity from microgrid exceeds a threshold cost then the demand for electricity will be satisfied from other external sources.

The operation cost function are usually expressed as quadratic cost curves (QCCs). Thus, for each FBG unit $i \in \mathcal{I}$ and time period $t \in \mathcal{T}$, the function can be expressed as follows:

$$C\left(\mathbf{P}_{it}\right) = a_{it}U_{it} + b_{it}\mathbf{P}_{it} + c_{it}\mathbf{P}_{it}^{2} \tag{3.2}$$

where a_{it}, b_{it}, and c_{it} are the coefficients of the quadratic function. Equation (3.1) can be accurately approximated by a set of piecewise blocks $m \in \mathcal{M}$. If large number of segments $|\mathcal{M}|$ are used, then the nonlinear cost function (3.2) becomes equivalent to the following piecewise linear function [74], [17]:

$$C\left(\mathbf{P}_{it}\right) = \alpha_i U_{it} + \sum_{m\in\mathcal{M}} \lambda_{imt}\Delta_{imt\omega} \qquad \forall i \in \mathcal{I}, t \in \mathcal{T}, \omega \in \Omega \tag{3.3}$$

where α_i is the cost of running unit $i \in \mathcal{I}$ at its minimum power generation. With this, we can linearize the objective function **[MG]** to the following **[LMG]**:

$$\textbf{[LMG]}\ Minimize \sum_{t\in\mathcal{T}}\Big(\sum_{i\in\mathcal{I}}(\psi_{it}Z_{it} + \phi_{it}U_{it} + \zeta_{it}Y_{it} + \alpha_i U_{it}) + \sum_{\omega\in\Omega}\rho_w\Delta t\Big(\sum_{i\in\mathcal{I},m\in\mathcal{M}}\lambda_{imt}\Delta_{imt\omega} + \sum_{j\in\mathcal{J}}c_t^{+}X_{jt\omega}^{+} + \sum_{k\in\mathcal{K}}c_t^{+}X_{kt\omega}$$

$$-\sum_{i\in\mathcal{I}} c_t^- X_{it\omega} - \sum_{j\in\mathcal{J}} c_t^- X_{jt\omega}^- - \sum_{l\in\mathcal{L}} c_t^- X_{lt\omega} + \sum_{k\in\mathcal{K}} \pi_t V_{kt\omega}\Big)\Big)$$

In addition to the objective function above, the following sets of constraints constitute **[LMG]**.

Constraints (3.4) indicate that the uncertain on-site electricity demand ($d_{kt\omega}$) for each building $k \in \mathcal{K}$ in time period $t \in \mathcal{T}$ must be satisfied either from the electricity generated from FBG units, DES units, renewable energy resources, electricity purchased from the grid, or from any external energy sources. Constraints (3.5) represent the capacity constraints for the electricity grid.

$$X_{kt\omega} + \sum_{i\in\mathcal{I}} X_{ikt\omega} + \sum_{l\in\mathcal{L}} X_{lkt\omega} + \sum_{j\in\mathcal{J}} X_{jkt\omega} + V_{kt\omega} = d_{kt\omega} \forall k \in \mathcal{K}, t \in \mathcal{T}, \omega \in \Omega \quad (3.4)$$

$$\sum_{j\in\mathcal{J}} X_{jt\omega}^+ + \sum_{k\in\mathcal{K}} X_{kt\omega} \leq h_t \ \forall t \in \mathcal{T}, \omega \in \Omega \quad (3.5)$$

Constraint (3.6) ensure electricity flow balance at each DES $j \in \mathcal{J}$ in time period $t \in \mathcal{T}$ and under scenario $\omega \in \Omega$. Constraints (3.7-3.13) capture the limits on the charging and discharging power as well as the level of energy stored in each DES unit $j \in \mathcal{J}$. Constraint (3.14) assure that the DES cannot be charged and discharged simultaneously in a given time period $t \in \mathcal{T}$.

$$\begin{aligned} \sum_{i\in\mathcal{I}} X_{ijt\omega} + \sum_{l\in\mathcal{L}} X_{ljt\omega} + X_{jt\omega}^+ + E_{jt\omega}^- &= \sum_{k\in\mathcal{K}} X_{jkt\omega} + X_{jt\omega}^- + E_{jt\omega}^+ \ \forall j \in \mathcal{J}, \\ t \in \mathcal{T}, \omega \in \Omega & \quad (3.6) \\ Q_{jt\omega} &= Q_{j,t-1,\omega} + E_{jt\omega}^+ - E_{jt\omega}^- \ \forall j \in \mathcal{J}, \end{aligned}$$

$$t \in \mathcal{T}, \omega \in \Omega \tag{3.7}$$

$$Q_{jt\omega} \leq \overline{q}^{b} \qquad \forall j \in \mathcal{J}, t \in \mathcal{T}, \omega \in \Omega \tag{3.8}$$

$$\underline{q}^{b} \leq Q_{jt\omega} \quad \forall j \in \mathcal{J}, t \in \mathcal{T}, \omega \in \Omega \tag{3.9}$$

$$E^{+}_{jt\omega} \leq \overline{q}^{b+} S^{+}_{jt} \quad \forall j \in \mathcal{J}, t \in \mathcal{T}, \omega \in \Omega \tag{3.10}$$

$$E^{+}_{jt\omega} \geq \underline{q}^{b+} S^{+}_{jt} \quad \forall j \in \mathcal{J}, t \in \mathcal{T}, \omega \in \Omega \tag{3.11}$$

$$E^{-}_{jt\omega} \leq \overline{q}^{b-} S^{-}_{jt} \quad \forall j \in \mathcal{J}, t \in \mathcal{T}, \omega \in \Omega \tag{3.12}$$

$$E^{-}_{jt\omega} \geq \underline{q}^{b-} S^{-}_{jt} \quad \forall j \in \mathcal{J}, t \in \mathcal{T}, \omega \in \Omega \tag{3.13}$$

$$S^{+}_{jt} + S^{-}_{jt} \leq 1 \quad \forall j \in \mathcal{J}, t \in \mathcal{T} \tag{3.14}$$

Constraint (3.15) ensures that at each time slot $t \in \mathcal{T}$, the amount of energy transmitted from renewable energy resources must be limited by its available energy. Constraints (3.16) indicate that $\mathcal{H}(x, \xi) \leq 0$ should be satisfied with a probability of at least $(1-\epsilon)$. Constraint (3.16) is described in detail in the following subsection.

$$\sum_{l \in \mathcal{L}, k \in \mathcal{K}} X_{lkt\omega} + \sum_{l \in \mathcal{L}, j \in \mathcal{J}} X_{ljt\omega} + \sum_{l \in \mathcal{L}} X_{lt\omega} \leq s_t \qquad \forall t \in \mathcal{T}, \omega \in \Omega \tag{3.15}$$

$$\mathbf{Pr}\Big(H(x, \xi) \leq 0\Big) \geq 1 - \epsilon \tag{3.16}$$

Constraint (3.17) limits the amount of electricity generated, and constraint (3.18) enforces energy balance flow in each FBG unit. Constraints (3.19-3.22) limit the amount of output power generation, and constraints (3.23-3.29) show the relationship between the startup, shutdown, and unit commitment indicators (Z_{it}, Y_{it} and U_{it}) of the conventional FBG unit

i [9], [55], [112], [74], [17]. We refer the reader to [17] for more details on how the constraints are handled in FBG units.

$$\sum_{k\in\mathcal{K}} X_{ikt\omega} + \sum_{j\in\mathcal{J}} X_{ijt\omega} + X_{it\omega} \leq c_{it}^{cap} \quad \forall i \in \mathcal{I}, t \in \mathcal{T}, \omega \in \Omega \quad (3.17)$$

$$\sum_{k\in\mathcal{K}} X_{ikt\omega} + \sum_{j\in\mathcal{J}} X_{ijt\omega} + X_{it\omega} = P_{it\omega} \quad \forall i \in \mathcal{I}, t \in \mathcal{T}, \omega \in \Omega \quad (3.18)$$

$$P_{it\omega} = \underline{p}_i U_{it} + \sum_{m\in\mathcal{M}} \Delta_{imt\omega} \quad \forall i \in \mathcal{I}, t \in \mathcal{T}, \omega \in \Omega \quad (3.19)$$

$$\underline{p}_i U_{it} \leq P_{it\omega} \quad \forall i \in \mathcal{I}, t \in \mathcal{T}, \omega \in \Omega \quad (3.20)$$

$$P_{it\omega} \leq \overline{p}_i U_{it} \quad \forall i \in \mathcal{I}, t \in \mathcal{T}, \omega \in \Omega \quad (3.21)$$

$$\Delta_{imt\omega} \leq n_{im} \quad \forall i \in \mathcal{I}, m \in \mathcal{M}, t \in \mathcal{T}, \omega \in \Omega \quad (3.22)$$

$$U_{it} - U_{it-1} = Z_{it} - Y_{it} \quad \forall i \in \mathcal{I}, t \in \mathcal{T} \geq 2 \quad (3.23)$$

$$Y_{it} \leq U_{it-1} \quad \forall i \in \mathcal{I}, t \in \mathcal{T} \geq 2 \quad (3.24)$$

$$Z_{it} \leq 1 - U_{it-1} \quad \forall i \in \mathcal{I}, t \in \mathcal{T} \geq 2 \quad (3.25)$$

$$Z_{it} + Y_{it} \leq 1 \quad \forall i \in \mathcal{I}, t \in \mathcal{T} \quad (3.26)$$

$$Y_{i1} \leq \beta_{i1} \quad \forall i \in \mathcal{I} \quad (3.27)$$

$$Z_{i1} \leq 1 - \beta_{i1} \quad \forall i \in \mathcal{I} \quad (3.28)$$

$$U_{i1} - \beta_{i1} = Z_{i1} - Y_{i1} \quad \forall i \in \mathcal{I} \quad (3.29)$$

Constraints (3.30) are binary constraints and (3.31) are the non-negativity sign constraints on decision variables.

$$U_{it}, Z_{it}, Y_{it}, S_{jt}^{+}, S_{jt}^{-} \in \{0,1\} \quad \forall i \in \mathcal{I}, \forall j \in \mathcal{J}, \forall t \in \mathcal{T} \quad (3.30)$$

$$P_{it\omega}, \Delta_{imt\omega}, E^{+}_{jt\omega}, E^{-}_{jt\omega}, X^{+}_{jt\omega}, \tag{3.31}$$

$$X_{kt\omega}, X_{ikt\omega}, X_{it\omega}, X_{ijt\omega}, X^{-}_{jt\omega}, X_{jkt},$$

$$X_{lkt\omega}, X_{lt\omega}, X_{ljt\omega}, Q_{jt\omega}, V_{kt\omega} \quad \geq \quad 0 \qquad \forall i \in \mathcal{I}, j \in \mathcal{J}, l \in \mathcal{L},$$

$$k \in \mathcal{K}, m \in \mathcal{M}, t \in \mathcal{T}, \omega \in \Omega$$

3.3.3 Chance Constraint Representation

We use three different policies to ensure that the utilization of renewable energy (i.e., solar) is high in microgrid operations. Let $\mathcal{T}^1 \subseteq \mathcal{T}$ be the set of time periods when the solar energy is available (i.e., time periods from 9:00 A.M. to 5:00 P.M.). Since solar radiation is available only during day time, these policies are assumed to be effective from 9:00 A.M. to 5:00 P.M. Each policy corresponds to a type of chance-constraints where the restriction mapping in these three approaches is labeled as $\mathcal{H}^1$, $\mathcal{H}^2$, and $\mathcal{H}^3$, respectively. We assume that renewable energy sources will fulfill the $\gamma\%$ ($0 \leq \gamma \leq 100\%$) of the total electricity demand of facilities or larger with at least $(1 - \epsilon)$ chances.

First policy, $\mathcal{H}^1$: Constraint mapping $\mathcal{H}^1$ is for the entire time period $\mathcal{T}^1$ for which the solar energy is available (starting at 9:00 A.M. and ending at 5:00 P.M.). This guarantees that the utilization of renewable energy is larger than or equal to $\gamma\%$ of the total electricity demand with at least $(1 - \epsilon)$ chances.

$$\mathbf{Pr}(\gamma \sum_{k \in \mathcal{K}, t \in \{9..|\mathcal{T}|-7\}} d_{kt\omega} - \sum_{k \in \mathcal{K}, t \in \{9..|\mathcal{T}|-7\}} X_{lkt\omega} \leq 0) \geq 1 - \epsilon \tag{3.32}$$

Second policy, $\mathcal{H}^2$: Constraint mapping $\mathcal{H}^2$ is for each particular operating hour $t \in \mathcal{T}^1$. By this way, we assure that the utilization of renewable energy is larger than or equal to $\gamma\%$ of the total electricity demand with at least $(1-\epsilon)$ chances.

$$\mathbf{Pr}\Big(\gamma \sum_{k\in\mathcal{K}} d_{kt\omega} - \sum_{k\in\mathcal{K}} X_{lkt\omega} \leq 0\Big) \geq 1-\epsilon \qquad \forall t \in \{9..|\mathcal{T}|-7\} \tag{3.33}$$

Third policy, $\mathcal{H}^3$: Constraint mapping $\mathcal{H}^3$ ensures that the utilization of renewable energy is larger than or equal to $\gamma\%$ of the total electricity demand with at least $(1-\epsilon)$ chances for every operating hour $t \in \mathcal{T}^1$ in between 9:00 A.M. to 5:00 P.M.

$$\mathbf{Pr}\Big(\gamma \sum_{k\in\mathcal{K}} d_{k\omega} - \sum_{k\in\mathcal{K}} X_{lk\omega} \leq 0,\Big) \geq 1-\epsilon \tag{3.34}$$

where $d_{k\omega} = [d_{k1\omega}, d_{k2\omega}, ..., d_{k\mathcal{T}^1\omega}]^{\mathcal{T}^1}$, $X_{lk\omega} = [X_{lk1\omega}, X_{lk2\omega}, ..., X_{lk\mathcal{T}^1\omega}]^{\mathcal{T}^1}$, and 0 is a $\mathcal{T}$ dimensional vector of zeros. From the above three policies it can be observed that the third policy is more restrictive than the second, which is more restrictive than the first one. The third policy implies that at least $\gamma\%$ of electricity demand is fulfilled during each of the operating hours during the time period $t \in \mathcal{T}^1$ from 9:00 A.M. to 5:00 P.M.

3.3.4 Sorting Approach

Constraint (3.32) can easily be represented as a deterministic constraint by sorting the right-hand side values in descending order for each sample with size N and then locating the $\lceil$(1-ϵ) $* N\rceil$ right-hand-side value. Similarly, we can simplify (3.33) after taking samples, sorting the right-hand-side values in descending order of the constraints for each sample (i.e., solar power in each hour) and picking the $\lceil$(1-ϵ) $* N\rceil$ right-hand-side values. However, the sorting method does not work for constraint (3.34) since the sorting algorithm

cannot handle the joint chance-constraint. Therefore, reformulating it as an Mixed-integer Linear Programming (MILP) is required. In the next section, we convert (3.32) into an MILP formulation to consistently produce a high-quality solution in a reasonable amount of time.

3.4 Solution Approach

1 In this section, we develop a combined SAA algorithm to solve the chance-constrained two-stage stochastic programming model for the MG scheduling problem. It is challenging to solve two-stage stochastic program with chance-constraint because its feasibility region defined by chance-constraint is generally non-convex and requires multi-dimensional integration. Sample average approximation (SAA) has proved to be an efficient method for solving chance-constrained and two-stage stochastic problems. In SAA, the actual distribution is replaced by an empirical distribution corresponding to a random sample [114], [63], [83]. Conventional SAA is used in solving chance-constrained stochastic problems (e.g., [63], [83]) and two-stage stochastic programming problems (e.g., [50], [4], [109], [93], [92]). The concept behind the sample average approximation (SAA)is to generate random samples with $N < |\Omega|$ of realizations, and the expected value function is estimated (approximated) by the sample average function [50], [103]. A deterministic optimization technique solves the resulting sample average problem. The process is repeated with different samples generated to produce high-quality candidate solutions and also a statistical estimation of their optimality gaps [109]. Interested readers can find more details, where Wang et al. [113] and Zhao et al. [121] use the SAA method in solving a unit commitment

problem that contains both chance-constrained and two-stage stochastic program features. There are three major parts of our combined SAA framework: scenario generation, convergence analysis, and solution validation. We solve the resulting mixed-integer linear program (MILP) efficiently for each SAA problem. In the following sub-sections we will discuss in detail the combined SAA framework.

3.4.1 Scenario Generation

Gamou et al. [120] support that energy demand obeys a normal probability distribution in which 95% of the whole area is within the range of 20% of the average energy requirements. The authors worked with real data of more than 8,700 hours of operation. Based on this finding, we assume that the energy demand for each facility $k \in \mathcal{K}$ in time period $t \in \mathcal{T}$ follows a multivariate normal distribution $\mathcal{N}(\mu, \Sigma)$, where vector μ is chosen as the forecasted demand and matrix Σ describes its forecasting error. In the SAA framework, the regular distribution of the energy demand of the facility is replaced by an empirical distribution using computer simulation techniques. We use Monte Carlo simulation to generate scenarios for the energy demand in our tested region. It produces a large number of scenarios with equal probabilities $1/N$. After making N scenarios, the expected value function is estimated by a sample average function. The corresponding formulation is shown as follows:

$$Minimize_{\mathbf{Z,U,Y,X,V}} \sum_{t\in\mathcal{T}} \Big(\sum_{i\in\mathcal{I}} (\psi_{it} Z_{it} + \phi_{it} U_{it} + \zeta_{it} Y_{it} + \alpha_i U_{it})$$
$$+ \sum_{n=1}^{N} \frac{1}{N} \Big(\sum_{i\in\mathcal{I}, m\in\mathcal{M}} \lambda_{imt} \Delta_{imtn} + \sum_{j\in\mathcal{J}} c_t^+ X_{jtn}^+ + \sum_{k\in\mathcal{K}} c_t^+ X_{ktn} - \sum_{i\in\mathcal{I}} c_t^- X_{itn}$$

$$- \sum_{j \in \mathcal{J}} c_t^- X_{jtn}^- - \sum_{l \in \mathcal{L}} c_t^- X_{ltn} + \sum_{k \in \mathcal{K}} \pi_t V_{ktn} \Big) \Big) \tag{3.35}$$

Subject to: (3.6-3.15), (3.17-3.32), and the chance constraint (3.32) can be estimated by using the following indicator function:

$$\frac{1}{N} \sum_{n=1}^{N} \mathcal{I}_{(0,\infty)} \Big(\sum_{k \in \mathcal{K}} \gamma d_{ktn} - \sum_{l \in \mathcal{L}_s \bigcup \mathcal{L}_r k \in \mathcal{K}} X_{lktn} \, \forall t \in \{9..|\mathcal{T}| - 7\} \Big) \geq 1 - \epsilon \tag{3.36}$$

where $\mathcal{I}_{(0,\infty)}(.)$ is an indicator function. The value of the function is equal to one when $\Big(\sum_{k \in \mathcal{K}} \gamma d_{ktn} - \sum_{l \in \mathcal{L}, k \in \mathcal{K}} X_{lktn} \; \forall t \in \mathcal{T}^1 \Big) \in (0, \infty)$ or zero when $\Big(\sum_{k \in \mathcal{K}} \gamma d_{ktn} - \sum_{l \in \mathcal{L}, k \in \mathcal{K}} X_{lktn} \; \forall t \in \mathcal{T}^1 \Big) \leq 0$. Wang et at. [113] show that as the value of the sample size N approaches infinity (i.e., $N \to \infty$), the objective of the above formulation converges to corresponding true problem. The following subsection explains the detail for linearizing constraints (3.36).

3.4.2 Solution methods of the SAA Problem

Due to the presence of the non-convexity term in the constraint sets, the solution of the resulting indicator function (3.36) is still considered challenging. Thus, it requires using a mixed-integer linear program model to reformulate this sampled chance-constraint. To do so, we introduce a binary variable $\mathbf{R} := \{F_n\}_{\forall n \in \mathcal{N}}$, where $F_n = 0$ guarantees that the chance-constraint is satisfied in the corresponding scenario; otherwise, $F_n = 1$. Additionally, a big "M" is introduced to the model for the case when the chance-constraint is violated. The chance-constraint is equivalent to restrict the number of $F_n, 1 \leq n \leq N$, to be ones. Then, the chance-constraint can be represented as follows:

$$\gamma \sum_{k \in \mathcal{K}} d_{ktn} - \sum_{l \in \mathcal{L}_s \bigcup \mathcal{L}_r k \in \mathcal{K}} X_{lktn} \leq M \times F_n \quad \forall t \in \{9..|\mathcal{T}|-7\}, n \in N \quad (3.37)$$

$$\sum_{n=1}^{N} \mu_n F_n \leq \epsilon \quad (3.38)$$

$$F_n \in \{0,1\} \quad \forall n \in N \quad (3.39)$$

where μ_n are the probabilities associated with each scenario $n \in N$. Constraints (3.38) can be estimated by the following probabilistic constraint.

$$\sum_{n=1}^{N} \mu_n (1 - F_n) \geq 1 - \epsilon$$

We can set $\mu_n = 1/N; \forall n \in N$ in case of equal probabilities. Now, let $r = max\Big\{k : \sum_{n=1}^{k} 1/N \leq \epsilon\Big\} = \lfloor N\epsilon \rfloor$ and the knapsack constraint (3.38) becomes:

$$\sum_{n=1}^{N} F_n \leq N \times \epsilon \quad (3.40)$$

3.4.3 Solution Validation

The basic idea for the validation process is to apply statistical techniques to approximate the upper and lower bounds of the optimal objective value of the SAA problem. The optimality gap can be obtained through the validation process with a confidence level. We refer to Pagnoncelli et al. [83], and Ahmed and A. Shapiro [4] as a methodology for solution validation for the two-stage and chance-constrained problems. We assume that $\bar{\mathbf{z}}$, $\bar{\mathbf{u}}$, and $\bar{\mathbf{y}}$ are an optimal solution for the SAA problem, and $\bar{\mathbf{v}}$ is the corresponding objective

value. For a given candidate solution for the SAA problem, solution validation provides a scheme to validate its quality by obtaining upper and lower bounds for the corresponding optimal objective value. We construct the upper and lower bounds as follows:

1. Upper bound:

Let $\{\omega^1, \omega^2, ..., \omega^N\}$ be a sample of size N to generate an SAA problem. We start with the feasibility of the solution $\overline{\mathbf{y}}$ by estimating the true probability distribution of the chance-constraint: $\hat{q}\left(\overline{\mathbf{y}}\right) = \mathbf{Pr}\Big(\sum_{k\in\mathcal{K}} \gamma d_{kt}(\omega^n) - \sum_{l\in\mathcal{L},k\in\mathcal{K}} X_{lkt}(\omega^n) \geq 0 \,\forall t \in \mathcal{T}^1, n \in N\Big)$. As discussed in [3] and [83], the $(1-\tau)$ confidence interval on $q\left(\overline{\mathbf{y}}\right)$ will be as follows:

$$U\left(\overline{\mathbf{y}}\right) = \hat{q}_{N'}\left(\overline{\mathbf{y}}\right) + z_\tau \sqrt{\frac{\hat{q}_{N'}\left(\overline{\mathbf{y}}\right)\left(1-\hat{q}_{N'}\left(\overline{\mathbf{y}}\right)\right)}{N'}} \tag{3.41}$$

where N' denotes the sample size for the validation of the chance-constraint, and $\hat{q}_{N'}\left(\overline{\mathbf{y}}\right)$ is the estimated value of $q\left(\overline{\mathbf{y}}\right)$ for the given sample size N'. If this upper bound of $q\left(\overline{\mathbf{y}}\right)$ is less than the risk level ϵ, then $\overline{\mathbf{y}}$ is feasible with confidence level $(1-\tau)$. Thus, as studied by Ahmed et al. [4], we can evaluate the upper bound of the optimal value for the second stage in **[MG]** as follows:

$$U\left(\overline{\mathbf{v}}\right) = c^T\overline{\mathbf{y}} + \frac{1}{N'}\sum_{n=1}^{N'} \mathcal{Q}(\mathbf{y}, \omega^n) \tag{3.42}$$

2. Lower bound:

Now we need to find the lower bound for the combined SAA algorithm. For getting the lower bound of the objective value $\overline{\mathbf{v}}$, we take $\hat{\mathbf{S}}$ iterations. We run the N scenario SAA problem M times for each iteration $1 \leq s \leq \hat{\mathbf{S}}$. For these M runs, we pick the Lth smallest

optimal value denoted as $\bar{\mathbf{v}}_{L_s}$ as described in [3] and [83]. This is the approximated lower bound for the chance-constrained part with confidence level $(1-\tau)$, where L is calculated as described in [83]. Finally, the average of $\left\{\bar{\mathbf{v}}_{L_s}, 1 \leq s \leq \hat{\mathbf{S}}\right\}$ provides the lower bound for our **[MG]**.

3.4.4 Summary of the Combined SAA Algorithm

As inspired by Wang et al. [113], we developed the combined SAA algorithm to solve model **[MG]**. The proposed combined SAA algorithm for solving **[MG]** is discussed as follows:

1. *Initialize*: Υ, N, N', M, $\bar{\mathbf{v}} \leftarrow -\infty$, $\hat{\mathbf{w}} \leftarrow \infty$

   For $s = 1, 2, ..., \hat{S}$, repeat the following steps:

   (a) For $m = 1, 2, ..., M$, repeat the following steps:

   i. Solve the associated SAA problem with N scenarios. Denote the solution as $\bar{\mathbf{z}}_m$, $\bar{\mathbf{u}}_m$, and $\bar{\mathbf{y}}_m$ and, the optimal value as $\bar{\mathbf{v}}_m$

   ii. Generate scenarios $\{\xi^1, \xi^1, ..., \xi^{N'}\}$.
   Estimate the $q(\bar{\mathbf{z}}_m, \bar{\mathbf{u}}_m, \bar{\mathbf{y}}_m)$ by $\hat{q}_{N'}(\bar{\mathbf{z}}_m, \bar{\mathbf{u}}_m, \bar{\mathbf{y}}_m)$ and use (3.42)
   to get $U(\bar{\mathbf{z}}_m, \bar{\mathbf{u}}_m, \bar{\mathbf{y}}_m)$

   iii. If $U(\bar{z}_m, \bar{u}_m, \bar{y}_m) \leq \epsilon$, go to **Step (iv)**; else skip **Step (iv)** and go to the next iteration

   iv. Generate N' scenarios discussed in **Step (ii)** and estimate the corresponding upper bound for model **[MG]** using (3.43)

   (b) Pick the smallest upper bound obtained from **Step (1)** and denote $\hat{\mathbf{w}}^s$ as an approximated upper bound for model **[MG]**

   (c) Sort the M optimal values obtained from **Step (1)** in non-decreasing order, e.g., $\bar{\mathbf{v}}_1 \leq \bar{\mathbf{v}}_2 \leq ... \leq \bar{\mathbf{v}}_m$. Pick the Lth optimal value $\hat{\mathbf{v}}_L$ and denote it as $\hat{\mathbf{v}}_{L_s}$

2. By taking the average of $\bar{\mathbf{v}}_{L_1}$, $\bar{\mathbf{v}}_{L_2}$,..., $\bar{\mathbf{v}}_{L_s}$, we can obtain the lower bound for model **[MG]** as follows: $\bar{\mathbf{v}} = \frac{1}{\hat{S}} \sum_{s=1}^{\hat{S}} \hat{\mathbf{v}}_{L_s}$

3. By taking the minimum of $\hat{\mathbf{w}}^1$, $\hat{\mathbf{w}}^2$,...,$\hat{\mathbf{w}}^S$, we can obtain the upper bound for model **[MG]** as follows: $\hat{\mathbf{w}} = \min_{1 \leq s \leq S} \hat{\mathbf{w}}^s$

4. Compute the optimality gap (Υ) as follows: $\Upsilon = (\hat{\mathbf{w}} - \bar{\mathbf{v}})/\bar{\mathbf{v}} \times 100\%$. If the gap Υ falls below a pre-specified optimality gap, then **STOP** the algorithm. Otherwise, go to **Step (1)** to continue the steps.

3.5 Computational study and managerial insights

This section summarizes our efforts in solving model **[MG]** using the combined SAA approach and the managerial insights derived from a real life case study. Our algorithm is coded in Python 3.4.4 and executed on a desktop computer with Intel Core i7-4790 3.60 GHz processor and 16.0 GB RAM. GUROBI 6.5.1 (http://www.gurobi.com/) is used as an optimization solver.

We obtained the electricity price and plan information from *Electricity Local*, a public resource to obtain electricity rates [28]. Other parameters such as unit electricity purchasing (c_t^+) and selling price (c_t^-) are set to be equal to \$0.072/kWh and \$0.0037/kWh, respectively. Electricity demand load data belong to a *Medium Size Medical College* in San Francisco. Solar energy data belong to Distributed Energy Resources Customer Adoption Model (DER-CAM) developed by Berkeley Laboratory [13]. The model objective is to minimize the cost of operating on-site generation and combined heat and power (CHP) systems and provide historical load data, weather, and tariffs.

3.5.1 Experiments under different power grid (h_t), DES ($\overline{q}^b$), and FBG (c_{it}^{cap}) capacities:

The reliability of the proposed microgrid operational model depends on the capacity of the power grid h_t. Changes on it may lead to deviations from the desired operation quality and therefore must be quantified and carefully evaluated. Figure 3.2 shows the relationship between different capacity level of the power grid h_t and the total cost during a typical day in summer and winter. It is observed that the total cost increases significantly as the capacity of the power grid decreases from 300 kW until the power grid is disconnected, although the microgrid system still satisfies the electricity demand by other means (e.g., solar energy, DES, FBG). On the other hand, the numerical experiments show that the change in total cost is minimal when the total capacity is between 300 kW and 500 kW.

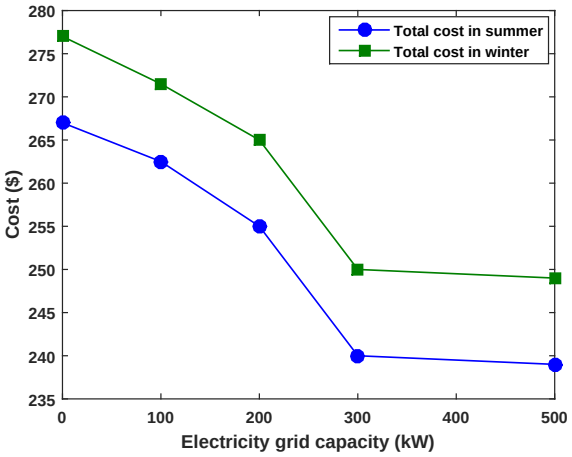

Figure 3.2

System cost under different capacities: h_t

We further assessed the impact of changes in total operational cost when the proposed microgrid system is exposed to different DES capacities ($\overline{q}^b$). Figure Figure 3.3 demonstrates the relationship between the operational cost of microgrid under different DES capacities. It is observed that the total operational cost of microgrid increases with a decrease in the DES capacities and become stabilized after the capacities researches to 400 kW.

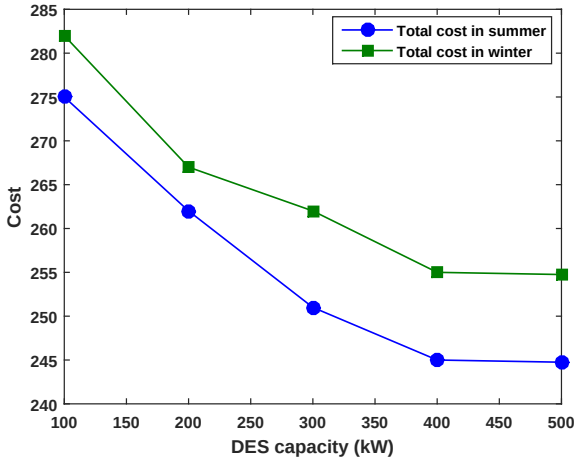

Figure 3.3

System cost under different capacities: $\overline{q}^b$ in a typical summer and winter day

Our final set of experiments illustrate the performance of the proposed microgrid operation under different FBG capacities (c_{it}^{cap}). Figure 3.4 shows how much the total cost increases as we decrease the FBG capacities to zero. It is observed that the total cost for the microgrid system operation remains almost steady after FBG capacities increases to 400 kW. We note that these observations can aid the decision makers to select capacity levels (e.g., h_t, $\overline{q}^b$, and c_{it}^{cap}) for different components of the microgrid system.

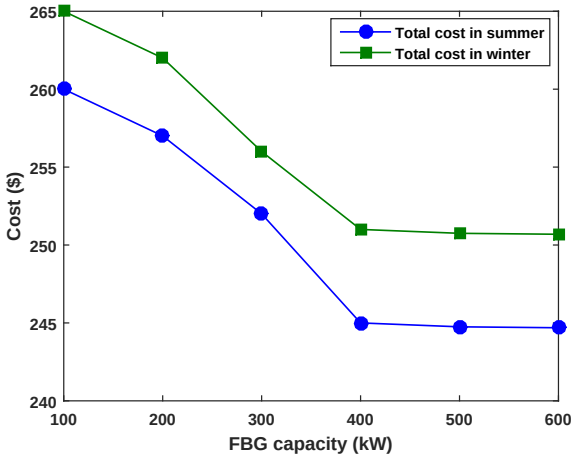

Figure 3.4

System cost under different capacities:c_{it}^{cap} in a typical summer and winter day

3.5.2 Allocation of Distributed Resources Generation

We note that the proposed chance-constrained model will allow the operator to request a portion of the solar power output to be utilized at a certain probability, and then plan an optimal dispatch. Furthermore, operators can adjust any curtailment. Figures Figure 3.5, and Figure 3.6 shows that following the policy $\mathcal{H}^3$ explained in Section 3.3.3, the operator can plan and allocate different power generator resources to meet the electricity demand. It can be seen that for summer, there is more time for solar energy to be dispatched as expected and the level of this type of energy need is quantified. Moreover, during a typical summer and winter day between 10:00 AM and 2:00 P.M., the electricity from grid reaches its minimum. Finally, there is more energy requested from FBG when the time is in between 4:00 AM and 8:00 AM in winter compared to the same period in summer which can be explained due to the nature of dark mornings in the winter. Our model does not only

assist the microgrid systems operator to set a service level but also serves as a planning tool to get the minimum cost operation and the best allocation of available resources.

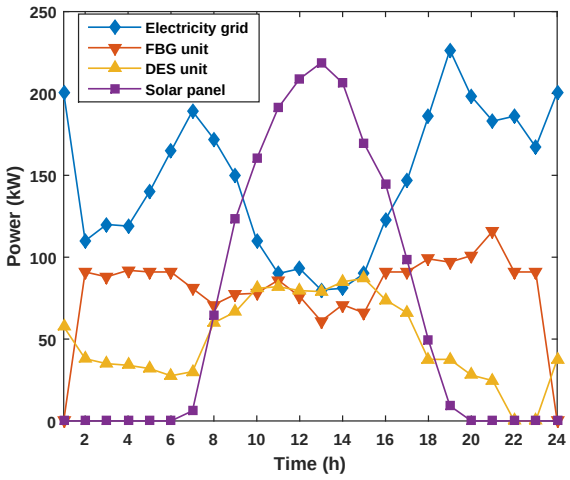

Figure 3.5

Sources for a summer typical day

3.5.3 Experimenting with FBG/DES units and solar panels under power outages

The power grid disruption database shows a noticeable increase in power outages from 2000 through the first half of 2014 [42]. Weather-related events (e.g., storms and severe weather, cold weather, ice storms, hurricanes and tropical storms, tornadoes, and combination of extreme heat events and wildfires) are the key reasons behind these power outages [22]. Therefore, we now experimenting with the performance of the microgrid under the case when a power outage is occurred. More specifically, we will emphasize any potential benefits of having solar panels under different FBG/DES units on fulfilling the required energy load during a power outage.

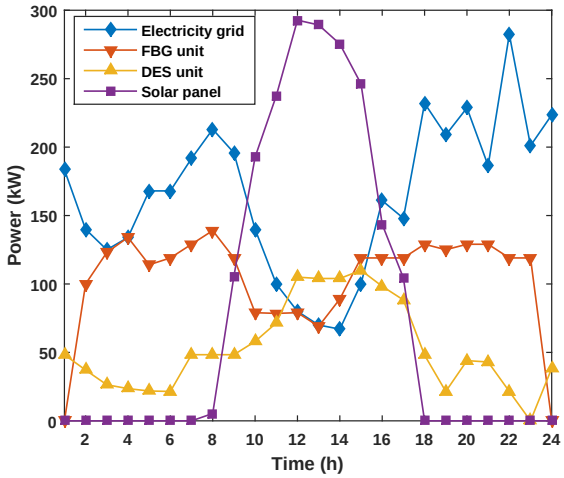

Figure 3.6

Sources for a winter typical day

The first set of experiment conducts sensitivity analysis on enabling and not enabling solar panels in the microgrid while varying the number of FBG units installed in the microgrid to compute the total cost of the operation under power outages (shown in Figure 3.7). We assume that the power outages occur in the California Medical College area [13] where the chance-constraint ensures that a certain percentage of the total electricity demand of load will be fulfilled from the solar panels with a predetermined probability. Figure 3.7 demonstrates the potential that exists to make use of FBG unit along with solar panels. It is evident from the results that having four FBG units with capacity 400 kWh provides the lowest total cost for both sets of experiments. Furthermore, it is important to note that the leftmost points in the two curves in Figure 3.7 denote the case where microgrid only uses external electricity with a penalty (without FBG units and solar panels) and thus, the total operation cost of the microgrid is very high. Our results show that FBG can bring a saving

of 8.74% to the system. Moreover, by comparing the two curves, we find out that the cost reduction achieved by solar panels is more than 7.51%. In summary, it is observed that the FBG units and renewable energy sources play a significant role in the microgrid system performance.

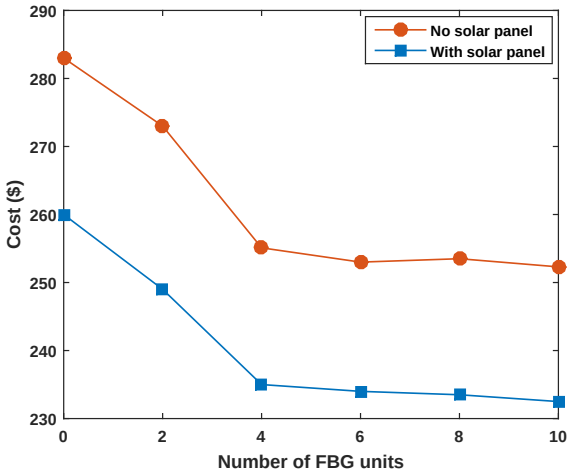

Figure 3.7

Cost reduction for different number of FBG units with and without solar panels

The second set of experiment conducts sensitivity analysis on enabling and not enabling solar panels in the microgrid while varying the number of DES units installed in the microgrid to compute the total cost of the operation under power outages (shown in Figure Figure 3.8). Similar to the first set of experiments, the chance-constraint ensures that a significant portion of solar power will be utilized at each operating hour with a high probability. Figure 3.8 demonstrates the potential that exists to make use of DES units along with solar panels. It is observed that having four DES with the full capacity of 400

kWh is sufficient to obtain the lowest total cost of the microgrid system. From Figure 3.8, it is seen that total cost of the microgrid system goes higher when microgrid only uses external electricity (without FBG units and solar panels). It is possible to reduce total cost by 9.49% to the system by using FBG. Furthermore, it is observed that by comparing the two curves a significant amount of cost reduction is achieved by solar panels (approximately 6.58%). These results are an indication of the prospective investment for microgrid system on satisfying the electricity demand on extreme events.

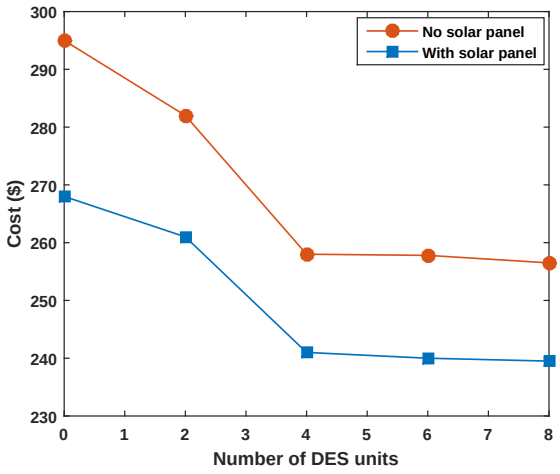

Figure 3.8

Cost reduction for different number of DES units with and without solar panels

3.5.4 Impact of different risk level ϵ on system performance

To understand the impact of risk level on MG system, we generate 200 scenarios to run a series of experiments on different risk levels. We investigate the impact of risk levels on the three policies discussed in Section 2.3. Table Table 3.3, Table 3.4, and Table 3.5

demonstrate the total cost, utilization and CPU times for various risk levels when the first, second and third policy is employed, respectively. In general, we conclude that the total cost is increased as the risk level increases from 10% to 100%. It is well expected since the increased utilization of solar energy sources decreases the total cost of the MG system. An extreme case is ϵ=100% when the chance constraint is neglected. In such a case, the optimal cost is higher than that at any other risk level. It implies that if the MG does not bound with the chance constraint then the total costs increase for all policies. Meanwhile, the solar energy utilization is at its lowest value as well (below 10%) for 100% risk level. More specifically, from the table Table 3.3- Table 3.5, we observe that third policy is the most restrictive among all policies. For the same given risk level and under same experimental setting, the solar utilization is the highest among all three policies.

Table 3.3

Computational results of the First policy for the MG system considering different risk levels

Risk Level ϵ	**Total cost ($)**	**Utilization**	**CPU Time (sec)**
10%	235	19.54%	212
20%	238	19.02%	210
40%	245	15.12%	190
80%	253	10.43%	225
100%	274	7.38%	160

Table 3.4

Computational results of the Second policy for the MG system considering different risk levels

Risk Level ϵ	**Total cost ($)**	**Utilization**	**CPU Time (sec)**
10%	232	21.27%	125
20%	231	20.19%	142
40%	241	17.46%	161
80%	249	11.29%	164
100%	274	7.38%	160

Table 3.5

Computational results of the Third policy for the MG system considering different risk levels

Risk Level ϵ	**Total cost ($)**	**Utilization**	**CPU Time (sec)**
10%	224	25.73%	285
20%	228	25.14%	309
40%	235	23.63%	328
80%	238	21.47%	357
100%	274	7.38%	160

3.5.5 Analyzing the performance of solution algorithms

This section presents our computational experience in solving model **[MG]** using a combined sample average approximation (SAA) algorithm proposed in Section 3.4. The algorithm is terminated when at least one of the following criteria is met: (a) the optimality gap (i.e., $\Upsilon = |UB - LB|/UB$) falls below a threshold value Υ = 0.01; or (b) the maximum time limit $time^{max}$ = 3,600.0 (in CPU seconds) is reached; or (c) the maximum number of iteration $iter^{max}$ = 100 is reached. The size of the deterministic equivalent problem of model **[MG]** for different input parameters is presented in Table 3.6.

Table 3.7 presents the computational performance of solving model **[MG]** using a combined SAA algorithm. We set $N' = 200, N = 20, M = 5$ to obtain the experimental results. The first column reports different problem sizes which are considered in the experiments. The risk level is given in the second column. The third and fourth column represent the Lower Bound (LB) and the Upper Bound (UB). The gap is expressed in the fifth column which is calculated by the $|UB - LB|/UB \times 100\%$ and finally the CPU time which is represented in the sixth column.

Results indicate that the combined SAA solves 20 out of 20 problem instances by obeying the termination criteria in a reasonable amount of time. The overall average of optimality gap for the combined SAA is reported as 0.65%. Moreover, it is observed that the optimality gap provided by combined SAA algorithm for case 5 is relatively high. It mandates developing additional techniques for solving the subproblems of the combined SAA algorithm efficiently.

Table 3.6

Problem size of the test instances

Case	$\|\mathcal{I}\|$	$\|\mathcal{J}\|$	$\|\mathcal{K}\|$	$\|\mathcal{L}\|$	$\|\mathcal{M}\|$	$\|\mathcal{T}\|$	**Binary Variable**	**Continuous Variable**	**Total Variables**	**No. of Constraints**
1 (Base)	4	4	1	8	1,000	24	288	9,580	9,868	389,952
2	4	4	5	8	1,000	24	288	20,840	21,128	390,336
3	4	4	10	8	1,000	24	288	33,470	33,758	390,816
4	4	4	20	8	1,000	24	288	57,330	57,618	393,816
5	4	4	40	8	1,000	24	288	105,700	105,988	397,696

Table 3.7

Computational performance of combined SAA algorithm

Case	**Risk Level** ϵ **(%)**	**UB**	**LB**	**Gap (%)**	**CPU (sec)**
4*1 (Base)	10	235	234	0.37	285.05
	25	240	239	0.45	311.24
	50	249	247	0.57	338.46
	100	274	273	0.39	160.69
4*2	10	1,179	1,173	0.52	521.37
	25	1,203	1,195	0.68	583.74
	50	1,241	1,233	0.59	648.63
	100	1,351	1,345	0.41	374.49
4*3	10	2,345	2,328	0.72	764.27
	25	2,436	2,418	0.74	857.58
	50	2,507	2,489	0.69	892.82
	100	2,857	2,839	0.61	415.64
4*4	10	4,721	4,690	0.66	805.17
	25	4,841	4,805	0.74	868.06
	50	4,956	4,912	0.88	985.34
	100	5,521	5,490	0.56	548.93
4*5	10	9,514	9,425	0.93	1,387.47
	25	9,625	9,539	0.89	1,436.13
	50	9,974	9,878	0.96	1,545.81
	100	10,854	10,781	0.67	889.24
Average		3,806	3,776	0.65	728.51

3.6 Conclusions

In this research, we propose a scalable quantitative modeling framework to evaluate the impacts of the variability on renewable resources in the microgrid operation. The energy and reserve dispatch decisions are obtained from a chance-constrained stochastic mixed integer linear programming model. We use three different policies to ensure that the utilization of renewable energy (i.e., solar) is high in microgrid operations. We observe that the third policy is more restrictive than the other two policies. A Sample Average Approximation algorithm is applied to provide high quality feasible solution for our proposed model in a reasonable amount of time. For the given data and parameter settings used in this research, the numerical analysis demonstrates the following conclusions: First, the measures at the system level, total system cost is mostly impacted by the distributed generation technologies (i.e., fuel-based generators, distributed energy storage, and renewable resources). Second, the chance-constrained model provides an efficient planning tool to allocate and dispatch solar-generation power efficiently. Third, the chance-constraints reduce the risk to curtail during the microgrid operation.

For future study, we will investigate the performance of the proposed approach considering solar and wind power generation and additional uncertainties in the load profile. To continue testing scalability of the proposed approach, a large scale power system which contains more types of storage systems, renewable energy sources, and heating/cooling demand load should be studied.

REFERENCES

[1] "IEEE Vision for Smart Grid Controls: 2030 and Beyond Reference Model," *IEEE Vision for Smart Grid Control: 2030 and Beyond Reference Model*, Sept 2013, pp. 1–10.

[2] H. R. Abdolmohammadi and A. Kazemi, "A Benders decomposition approach for a combined heat and power economic dispatch," *Energy Conversion and Management*, vol. 71, 2013, pp. 21 – 31.

[3] Ahmed S., Shapiro A., "Solving chance-constrained stochastic programs via sampling and integer programming.," *Tutorials in Operations Research*, vol. 10, 2008, pp. 261–270.

[4] Ahmed S., Shapiro A., Shapiro Er., "The sample average approximation method for stochastic programs with integer recourse.," *SIAM Journal of Optimization*, vol. 12, 2002, pp. 479–502.

[5] R. K. Ahuja, T. L. Magnanti, and J. B. Orlin, *Network Flows: Theory, Algorithms, and Applications*, Prentice-Hall, Inc., Upper Saddle River, NJ, USA, 1993.

[6] M. Alipour, B. Mohammadi-Ivatloo, and K. Zare, "Stochastic risk-constrained short-term scheduling of industrial cogeneration systems in the presence of demand response programs," *Applied Energy*, vol. 136, 2014, pp. 393 – 404.

[7] M. Ameri and Z. Besharati, "Optimal design and operation of district heating and cooling networks with {CCHP} systems in a residential complex," *Energy and Buildings*, vol. 110, 2016, pp. 135 – 148.

[8] P. ASHRAE, "heating and cooling, ASHRAE Handbook-HVAC Systems and Equipment, SI ed," *American Society of Heating Refrigerating and Air-Conditioning Engineers (ASHRAE) Atlanta, GA, US*, 2008.

[9] Bahramirad S., Reder W., Khodaei A., "Reliability-Constrained Optimal Sizing of Energy Storage System in a Microgrid.," *IEEE Transactions on Smart Grid*, vol. 3, no. 4, 2012, pp. 2056 – 2062.

[10] Basu A. K., Chowdhury S. P., Chowdhury S., Paul S., "Microgrids: Energy management by strategic deployment of DERsA comprehensive survey.," *Renewable and Sustainable Energy Reviews*, vol. 15, no. 9, 2011, pp. 4348–4356.

[11] M. R. Benam, S. S. Madani, S. M. Alavi, and M. Ehsan, "Optimal configuration of the CHP system using stochastic programming," *IEEE Transactions on Power Delivery*, vol. 30, no. 3, 2015, pp. 1048–1056.

[12] J. F. Benders, "Partitioning Procedures for Solving Mixed-variables Programming Problems," *Numer. Math.*, vol. 4, no. 1, Dec. 1962, pp. 238–252.

[13] Berkeley Lab, "Microgrid at Berkeley Lab.," Available from: https://building-microgrid.lbl.gov/projects/how-access-der-cam, 2015.

[14] A. Bischi, L. Taccari, E. Martelli, E. Amaldi, G. Manzolini, P. Silva, S. Campanari, and E. Macchi, "A detailed {MILP} optimization model for combined cooling, heat and power system operation planning," *Energy*, vol. 74, 2014, pp. 12 – 26.

[15] Bracco S., Dentici G., Siri S., "Economic and environmental optimization model for the design and the operation of a combined heat and power distributed generation system in an urban area.," *Energy*, vol. 55, 2013, pp. 1014–1024.

[16] Buoro D., Casisi M., Nardi A. D., Pinamonti P., Reini M., "Multicriteria optimization of a distributed energy supply system for an industrial area.," *Energy*, vol. 58, 2013, pp. 128 – 137.

[17] Carrion M., Arroyo J.M., "A computationally efficient mixed-integer linear formulation for the thermal unit commitment problem.," *IEEE Transactions on Power Systems*, vol. 21, no. 3, 2006, pp. 1371 – 1378.

[18] Z. Chen, L. Wu, and Y. Fu, "Real-time price-based demand response management for residential appliances via stochastic optimization and robust optimization," *Smart grid, IEEE transactions on*, vol. 3, no. 4, 2012, pp. 1822–1831.

[19] H. Cho, R. Luck, and L. M. Chamra, "Supervisory feed-forward control for real-time topping cycle CHP operation," *Journal of Energy Resources Technology*, vol. 132, no. 1, 2010, p. 012401.

[20] H. Cho, P. J. Mago, R. Luck, and L. M. Chamra, "Evaluation of {CCHP} systems performance based on operational cost, primary energy consumption, and carbon dioxide emission by utilizing an optimal operation scheme," *Applied Energy*, vol. 86, no. 12, 2009, pp. 2540 – 2549.

[21] Chung M., Park H. C., "Building energy demand patterns for department stores in Korea.," *Applied Energ*, vol. 90, no. 1, 2012, pp. 241 – 249.

[22] Climate Central, "Weather-related blackouts doubled since 2003: report," Available from: http://www.climatecentral.org/news/weather-related-blackouts-doubled-since-2003-report-17281/, 2016.

[23] I. Contreras, J.-F. Cordeau, and G. Laporte, "Stochastic uncapacitated hub location," *European Journal of Operational Research*, vol. 212, no. 3, 2011, pp. 518 – 528.

[24] Costa A., Fichera A., "A mixed-integer linear programming (MILP) model for the evaluation of CHP system in the context of hospital structures.," *Applied Thermal Engineering*, vol. 71, no. 2, 2014, pp. 921–929.

[25] R. S. de Camargo, G. de Miranda, Jr., and H. P. L. Luna, "Benders Decomposition for Hub Location Problems with Economies of Scale.," *Transportation Science*, vol. 43, no. 1, 2009, pp. 86 – 97.

[26] Deng Q., Gao X., Zhou H., Hu W., *Intelligent Control and Information Processing (ICICIP), 2011 2nd International Conference on.*, chapter System modeling and optimization of microgrid using genetic algorithm, 2011, pp. 540–544.

[27] M. Deru, K. Field, D. Studer, K. Benne, B. Griffith, P. Torcellini, B. Liu, M. Halverson, D. Winiarski, M. Rosenberg, et al., "US Department of Energy commercial reference building models of the national building stock," 2011.

[28] Electricity Local, "California Electricity Rates & Consumption.," Available from: http://www.electricitylocal.com/states/california/, 2015.

[29] I. Ersoz and U. Colak, "Combined cooling, heat and power planning under uncertainty," *Energy*, vol. 109, 2016, pp. 1016 – 1025.

[30] M. Farahnak, M. Farzaneh-Gord, M. Deymi-Dashtebayaz, and F. Dashti, "Optimal sizing of power generation unit capacity in ICE-driven {CCHP} systems for various residential building sizes," *Applied Energy*, vol. 158, 2015, pp. 203 – 219.

[31] E. C. D. G. for Research and O. for Official Publications of the European Communities, *Energy Storage: A Key Technology for Decentralised Power, Power Quality and Clean Transport*, EUR / European Commission. Office for Official Publications of the European Communities, 2001.

[32] S. Gamou, R. Yokoyama, and K. Ito, "Optimal unit sizing of cogeneration systems in consideration of uncertain energy demands as continuous random variables," *Energy Conversion and Management*, vol. 43, no. 912, 2002, pp. 1349 – 1361.

[33] General Algebraic Modeling System (GAMS), ," Available from: http://www.gams.com/, 2015.

[34] A. Geoffrion, "Generalized Benders decomposition," *Journal of Optimization Theory and Applications*, vol. 10, no. 4, 1972, pp. 237–260, cited By 0.

[35] W. Gu, Z. Wu, R. Bo, W. Liu, G. Zhou, W. Chen, and Z. Wu, "Modeling, planning and optimal energy management of combined cooling, heating and power microgrid: A review," *International Journal of Electrical Power Energy Systems*, vol. 54, 2014, pp. 26 – 37.

[36] Gu W., Wu Z., Bo R., Liu W., Zhou G., Chen W., Wu Z., "Modeling, planning and optimal energy management of combined cooling, heating and power microgrid: A review.," *International Journal of Electrical Power & Energy Systems*, vol. 54, 2014, pp. 26 – 37.

[37] X. Guan, Z. Xu, and Q.-S. Jia, "Energy-efficient buildings facilitated by microgrid," *Smart Grid, IEEE Transactions on*, vol. 1, no. 3, 2010, pp. 243–252.

[38] P. Hanafizadeh, J. Eshraghi, P. Ahmadi, and A. Sattari, "Evaluation and sizing of a {CCHP} system for a commercial and office buildings," *Journal of Building Engineering*, vol. 5, 2016, pp. 67 – 78.

[39] A. Hawkes and M. Leach, "Modelling high level system design and unit commitment for a microgrid," *Applied energy*, vol. 86, no. 7, 2009, pp. 1253–1265.

[40] J. Hernndez-Santoyo and A. Snchez-Cifuentes, "Trigeneration: an alternative for energy savings," *Applied Energy*, vol. 76, no. 13, 2003, pp. 219 – 227, Energex 2002 - Energy Policies and Economics and Rational Use of Energy of Energy Topics {VI} and {VII}.

[41] M. Hu and H. Cho, "A probability constrained multi-objective optimization model for {CCHP} system operation decision support," *Applied Energy*, vol. 116, 2014, pp. 230 – 242.

[42] Inside Energy, "Bringing energy reporting down to earth," Available from: http://insideenergy.org/2014/08/18/power-outages-on-the-rise-across-the-u-s/, 2014.

[43] M. Jeihoonian, M. K. Zanjani, and M. Gendreau, "Accelerating Benders decomposition for closed-loop supply chain network design: Case of used durable products with different quality levels," *European Journal of Operational Research*, vol. 251, no. 3, 2016, pp. 830 – 845.

[44] P. L. L. Jr., "The potential impact of policies to promote combined heat and power in {US} industry," *Energy Policy*, vol. 29, no. 14, 2001, pp. 1243 – 1254, Scenarios for a clean energy future.

[45] M. Jradi and S. Riffat, "Tri-generation systems: Energy policies, prime movers, cooling technologies, configurations and operation strategies," *Renewable and Sustainable Energy Reviews*, vol. 32, 2014, pp. 396 – 415.

[46] H. Karami, M. J. Sanjari, S. Hadavi, S. H. Hosseinian, and G. B. Gharehpetian, "Stochastic load effect on home energy system scheduling optimization," *International Transactions on Electrical Energy Systems*, vol. 25, no. 10, 2015, pp. 2412–2426.

[47] Katirae F., Iravani M. R., Lehn P. W., "Micro-grid autonomous operation during and subsequent to islanding process.," *IEEE Transactions on Power Delivery*, vol. 20, no. 1, 2005, pp. 248–257.

[48] Kim H. M., Kinoshita T., *Security-Enriched Urban Computing and Smart Grid.*, vol. 6, 2010, pp. 250–260.

[49] A. J. Kleywegt, A. Shapiro, and T. Homem-de Mello, "The sample average approximation method for stochastic discrete optimization," *SIAM Journal on Optimization*, vol. 12, no. 2, 2002, pp. 479–502.

[50] Kleywegt A.J., Shapiro A., Homem-De-Mello T., "The sample average approximation method for stochastic discrete optimization.," *SIAM Journal of Optimization*, vol. 12, 2001, pp. 479–502.

[51] X. Kong, R. Wang, and X. Huang, "Energy optimization model for a CCHP system with available gas turbines," *Applied Thermal Engineering*, vol. 25, no. 2-3, 2005, pp. 377–391, cited By 126.

[52] Kriett P. O., Salani M., "Optimal control of a residential microgrid.," *Energy*, vol. 42, no. 1, 2012, pp. 321–330.

[53] R. Lahdelma and H. Hakonen, "An efficient linear programming algorithm for combined heat and power production," *European Journal of Operational Research*, vol. 148, no. 1, 2003, pp. 141–151, cited By 65.

[54] Lasseter R. H., Paigi P., *Microgrid: a conceptual solution.*, vol. 6, chapter In: Handbook of Bioenergy , 2004, pp. 4285–4290.

[55] Lei W., Shahidehpour M., Tao L., "Stochastic Security-Constrained Unit Commitment.," *IEEE Transactions on Power Systems*, vol. 22, no. 2, 2007, pp. 800 – 811.

[56] C. Li, Y. Shi, and X. Huang, "Sensitivity analysis of energy demands on performance of {CCHP} system," *Energy Conversion and Management*, vol. 49, no. 12, 2008, pp. 3491 – 3497.

[57] C.-Z. Li, Y.-M. Shi, S. Liu, Z. ling Zheng, and Y. chen Liu, "Uncertain programming of building cooling heating and power (BCHP) system based on Monte-Carlo method," *Energy and Buildings*, vol. 42, no. 9, 2010, pp. 1369 – 1375.

[58] L. Li, H. Mu, W. Gao, and M. Li, "Optimization and analysis of CCHP system based on energy loads coupling of residential and office buildings," *Applied Energy*, vol. 136, 2014, pp. 206–216, cited By 9.

[59] H. Liang and W. Zhuang, "Stochastic modeling and optimization in a microgrid: A survey," *Energies*, vol. 7, no. 4, 2014, pp. 2027–2050.

[60] Liang H., Zhuang W., "Stochastic Modeling and Optimization in a Microgrid: A Survey.," *Energies*, vol. 7, no. 4, 2014, pp. 20–27.

[61] M. Liu, Y. Shi, and F. Fang, "A new operation strategy for {CCHP} systems with hybrid chillers," *Applied Energy*, vol. 95, 2012, pp. 164 – 173.

[62] M. Liu, Y. Shi, and F. Fang, "Combined cooling, heating and power systems: A survey," *Renewable and Sustainable Energy Reviews*, vol. 35, 2014, pp. 1 – 22.

[63] Luedtke J., Ahmed S., "A sample approximation approach for optimization with probabilistic constraints.," *SIAM Journal on Optimization*, vol. 19, no. 2, 2008, pp. 674–699.

[64] Z. Luo, Z. Wang, W. Gu, Y. Tang, and C. Xu, "A Two-Stage Energy Management Strategy for CCHP Microgrid considering house characteristics," *Power Energy Society General Meeting, 2015 IEEE*, July 2015, pp. 1–5.

[65] T. Magnanti and R. Wong, "ACCELERATING BENDERS DECOMPOSITION: ALGORITHMIC ENHANCEMENT AND MODEL SELECTION CRITERIA.," *Operations Research*, vol. 29, no. 3, 1981, pp. 464–484, cited By 150.

[66] P. Mago and L. Chamra, "Analysis and optimization of {CCHP} systems based on energy, economical, and environmental considerations," *Energy and Buildings*, vol. 41, no. 10, 2009, pp. 1099 – 1106.

[67] P. J. Mago, N. Fumo, and L. M. Chamra, "Performance analysis of CCHP and CHP systems operating following the thermal and electric load," *International Journal of Energy Research*, vol. 33, no. 9, 2009, pp. 852–864.

[68] P. J. Mago and A. K. Hueffed, "Evaluation of a turbine driven {CCHP} system for large office buildings under different operating strategies," *Energy and Buildings*, vol. 42, no. 10, 2010, pp. 1628 – 1636.

[69] C. Marnay and G. Venkataramanan, "Microgrids in the evolving electricity generation and delivery infrastructure," *Power Engineering Society General Meeting, 2006. IEEE*, 2006, pp. 5 pp.–.

[70] Martinez G., Gatsis N., Giannakis G., *Computational Advances in Multi-Sensor Adaptive Processing (CAMSAP), 2013 IEEE 5th International Workshop on.*, chapter Stochastic programming for energy planning in microgrids with renewables, 2013, pp. 472–475.

[71] M. Marufuzzaman, S. D. Eksioglu, X. Li, and J. Wang, "Transportation Research Part E," 2014.

[72] Milo A., Gaztañaga H., Etxeberria-Otadui I., Bilbao E., Rodríguez P., *PowerTech, 2009 IEEE Bucharest.*, chapter Optimization of an experimental hybrid microgrid operation: Reliability and economic issues, 2009, pp. 1–6.

[73] Morais H., Kadar P., Faria P., Vale Z. A., Khodr H.M., "Optimal scheduling of a renewable micro-grid in an isolated load area using mixed-integer linear programming.," *Renewable Energy*, vol. 35, no. 1, 2010, pp. 151–156.

[74] Morales J. M., Conejo A.J., Perez-Ruiz J., "Economic Valuation of Reserves in Power Systems With High Penetration of Wind Power.," *IEEE Transactions on Power Systems*, vol. 24, no. 2, 2009, pp. 900 – 910.

[75] National Oceanic and Atmospheric Administration., "Hurricane Katrina.," Available from: http://www1.ncdc.noaa.gov/pub/data/extremeevents/specialreports/Hurricane-Katrina.pdf, 2005.

[76] National Renewable Energy Laboratory, "Wind and solar energy curtailment: experience and practices in the United States," Available from: http://http://www.nrel.gov/docs/fy14osti/60983.pdf, 2014.

[77] S. S. Nielsen and S. A. Zenios, "Scalable parallel Benders decomposition for stochastic linear programming," *Parallel Computing*, vol. 23, no. 8, 1997, pp. 1069 – 1088.

[78] V. I. Norkin, G. C. Pflug, and A. Ruszczyński, "A branch and bound method for stochastic global optimization," *Mathematical programming*, vol. 83, no. 1-3, 1998, pp. 425–450.

[79] A. Omu, R. Choudhary, and A. Boies, "Distributed energy resource system optimisation using mixed integer linear programming," *Energy Policy*, vol. 61, 2013, pp. 249 – 266.

[80] Omu A., Choudhary R., Boies A., "Distributed energy resource system optimisation using mixed integer linear programming.," *Energy Policy*, vol. 61, 2013, pp. 249–266.

[81] Ozturk U. A., Mazumdar M., Norman B. A., "A solution to the stochastic unit commitment problem using chance constrained programming.," *IEEE Transactions on Power Systems*, vol. 19, no. 3, 2004, pp. 1589–1598.

[82] Pacific Northwest National Laboratory, "Looking back at the August 2003 blackout.," Available from: http:http://eioc.pnnl.gov/research/, 2013.

[83] Pagnoncelli B.K., Ahmed S., Shapiro A., "Sample average approximation method for chance constrained programming: Theory and applications.," *Journal of Optimization Theory and Applications*, vol. 142, no. 2, 2008, pp. 399–416.

[84] N. Papadakos, "Practical enhancements to the MagnantiWong method," *Operations Research Letters*, vol. 36, no. 4, 2008, pp. 444 – 449.

[85] Parisio A., Glielmo L., *Energy efficient microgrid management using model predictive control.*, 2011, pp. 5449–5454.

[86] Parisio A., Glielmo L., *Smart Grid Communications (SmartGridComm), 2011 IEEE International Conference on.*, vol. 6, 2011, pp. 505–510.

[87] Y. D. Qi, Z. G. Liu, and G. M. Song, "CCHP and Reliability of Electricity Supply," *Advanced Materials Research*. Trans Tech Publ, 2011, vol. 250, pp. 3173–3176.

[88] Rahbar K., Xu J., Zhang R., "Real-time energy storage management for renewable integration in microgrid: an off-line optimization approach.," *Smart Grid, IEEE Transactions on*, vol. 6, no. 1, 2015, pp. 124–134.

[89] A. Rong and R. Lahdelma, "An efficient linear programming model and optimization algorithm for trigeneration," *Applied Energy*, vol. 82, no. 1, 2005, pp. 40–63, cited By 91.

[90] N. V. Sahinidis, ," *Interfaces*, vol. 25, no. 5, 1995, pp. 215–217.

[91] T. Santoso, S. Ahmed, M. Goetschalckx, and A. Shapiro, "A stochastic programming approach for supply chain network design under uncertainty," *European Journal of Operational Research*, vol. 167, no. 1, 2005, pp. 96–115.

[92] Santoso T., Ahmed S., Goetschalckx M., Shapiro A., "A stochastic programming approach for supply chain network design under uncertainty.," *European Journal of Operational Research*, vol. 167, 2005, pp. 96–115.

[93] Schutz P., Tomasgard A., Ahmed S., "Supply chain design under uncertainty using sample average approximation and dual decomposition.," *European Journal of Operational Research*, vol. 199, 2009, pp. 409–419.

[94] T. Sels, C. Dragu, T. Van Craenenbroeck, and R. Belmans, "Electrical energy storage systems: existing systems versus newest systemsan overview," *International Conference Power Generation and Sustainable Development (AIM), Liège, Belgium, Oct*. Citeseer, 2001, pp. 8–9.

[95] W. Sheng, S. Peng, Y. Tang, X. Meng, D. Wang, Z. Wu, and W. Gu, "Stochastic multi-objective scheduling of a combined cooling, heating and power microgrid containing a fuel cell," *Journal of Renewable and Sustainable Energy*, vol. 7, no. 6, 2015, p. 063123.

[96] A. Shukla, "Combined Cooling, Heating, and Power (CCHP) or Trigeneration Technology: An Approach Toward Higher Energy Efficiency, Emission Reduction Potential and Policy," *Energy Sustainability Through Green Energy*, Springer, 2015, pp. 493–506.

[97] A. Smith, R. Luck, and P. J. Mago, "Analysis of a combined cooling, heating, and power system model under different operating strategies with input and model data uncertainty," *Energy and Buildings*, vol. 42, no. 11, 2010, pp. 2231 – 2240.

[98] M. D. Somma, B. Yan, N. Bianco, G. Graditi, P. Luh, L. Mongibello, and V. Naso, "Operation optimization of a distributed energy system considering energy costs and exergy efficiency," *Energy Conversion and Management*, vol. 103, 2015, pp. 739 – 751.

[99] SRP, "Residential price plans.," Available from: http://www.srpnet.com/menu/electricres/priceplans.aspx, 2015.

[100] Stadler M., Cardoso G., Mashayekh S., Forget T., DeForest N., Agarwal A., Schonbein A., "Value streams in microgrids: A literature review.," *Applied Energy*, vol. 162, 2016, pp. 980–989.

[101] Su W., Wang J., Roh J., "Stochastic energy scheduling in microgrids with intermittent renewable energy resources.," *Smart Grid, IEEE Transactions on*, vol. 5, no. 4, 2014, pp. 1876–1883.

[102] M. Sudhakaran and S. Slochanal, "Integrating genetic algorithms and tabu search for combined heat and power economic dispatch," 2003, vol. 1, pp. 67–71, cited By 7.

[103] C. Swamy and D. B. Shmoys, "The sample average approximation method for 2-stage stochastic optimization," *Unpublished manuscript*, 2004.

[104] Tenfen D., Finardi E. C., "A mixed integer linear programming model for the energy management problem of microgrids.," *Electric Power Systems Research*, vol. 122, 2015, pp. 19–28.

[105] S. Trukhanov, L. Ntaimo, and A. Schaefer, "Adaptive multicut aggregation for two-stage stochastic linear programs with recourse," *European Journal of Operational Research*, vol. 206, no. 2, 2010, pp. 395 – 406.

[106] Tsikalakis A.G., Hatziargyriou N.D., "Centralized Control for Optimizing Microgrids Operation.," *IEEE Transactions on Energy Conversion*, vol. 23, no. 1, 2008, pp. 241 – 248.

[107] U.S. EIA., "Annual Energy Outlook 2015 with Projections to 2040.," Available from: http://www.eia.gov/forecasts/aeo/pdf/0383(2015).pdf, 2015.

[108] B. Verweij, S. Ahmed, A. J. Kleywegt, G. Nemhauser, and A. Shapiro, "The sample average approximation method applied to stochastic routing problems: a computational study," *Computational Optimization and Applications*, vol. 24, no. 2-3, 2003, pp. 289–333.

[109] Verweij B., Ahmed S., Kleywegt A.J., Nemhauser G., Shapiro A., "The sample average approximation method applied to stochastic routing problems: A computational study.," *Computational Optimization and Applications*, vol. 24, 2003, pp. 289–333.

[110] Victoria G., "Lessons to be learned from Haiti's tsunami.," Available from: http://news.bbc.co.uk/2/hi/science/nature/8536561.stm, 2010.

[111] L. Wang and C. Singh, "Stochastic combined heat and power dispatch based on multi-objective particle swarm optimization," *International Journal of Electrical Power and Energy Systems*, vol. 30, no. 3, 2008, pp. 226–234, cited By 64.

[112] Wang J., Shahidehpour M., Li Z., "Security-constrained unit commitment with volatile wind power generation.," *IEEE Transactions on Power Systems*, vol. 23, no. 3, 2008, pp. 1319–1327.

[113] Wang Q., Guan Y., Wang J., "A chance-constrained two-stage stochastic program for unit commitment with uncertain wind power output.," *IEEE Transactions on Power Systems*, vol. 27, no. 1, 2012, pp. 206–215.

[114] Wang W., Ahmed S., "Sample average approximation of expected value constrained stochastic programs.," *Operations Research Letters*, vol. 36, no. 5, 2008, pp. 515–519.

[115] D. Wu and R. Wang, "Combined cooling, heating and power: a review," *progress in energy and combustion science*, vol. 32, no. 5, 2006, pp. 459–495.

[116] J. yi Wu, J. long Wang, and S. Li, "Multi-objective optimal operation strategy study of micro-CCHP system," *Energy*, vol. 48, no. 1, 2012, pp. 472 – 483, 6th Dubrovnik Conference on Sustainable Development of Energy Water and Environmental Systems, {SDEWES} 2011.

[117] F. You and I. E. Grossmann, "Multicut Benders decomposition algorithm for process supply chain planning under uncertainty," *Annals of Operations Research*, vol. 210, no. 1, 2013, pp. 191–211.

[118] A. Zakariazadeh, S. Jadid, and P. Siano, "Smart microgrid energy and reserve scheduling with demand response using stochastic optimization," *International Journal of Electrical Power & Energy Systems*, vol. 63, 2014, pp. 523–533.

[119] J. Zhang, H. Cho, and A. Knizley, "Evaluation of financial incentives for combined heat and power (CHP) systems in U.S. regions," *Renewable and Sustainable Energy Reviews*, vol. 59, 2016, pp. 738 – 762.

[120] Zhao C., Wang Q., Wang J., Guan Y., "Optimal unit sizing of cogeneration systems in consideration of uncertain energy demands as continuous random variables.," *Energy Conversion and Management*, vol. 43, no. 912, 2002, pp. 1349 –1361.

[121] Zhao C., Wang Q., Wang J., Guan Y., "Expected value and chance constrained stochastic unit commitment ensuring wind power utilization.," *IEEE Transactions on Power Systems*, vol. 29, no. 6, 2014, pp. 2696–2705.

[122] Z. Zhou, P. Liu, Z. Li, E. N. Pistikopoulos, and M. C. Georgiadis, "Impacts of equipment off-design characteristics on the optimal design and operation of combined cooling, heating and power systems," *Computers Chemical Engineering*, vol. 48, 2013, pp. 40 – 47.

[123] Z. Zhou, J. Zhang, P. Liu, Z. Li, M. C. Georgiadis, and E. N. Pistikopoulos, "A two-stage stochastic programming model for the optimal design of distributed energy systems," *Applied Energy*, vol. 103, 2013, pp. 135 – 144.

[124] Zhu H., Xu J. I., Wang X., *2009 4th IEEE Conference on Industrial Electronics and Applications.*, chapter Active power output calculation of wind farms connected to power grids based on fuzzy chanceconstrained programming, 2009, pp. 2141–2144.

[125] Y. Zoka, A. Sugimoto, N. Yorino, K. Kawahara, and J. Kubokawa, "An economic evaluation for an autonomous independent network of distributed energy resources," *Electric Power Systems Research*, vol. 77, no. 7, 2007, pp. 831 – 838.